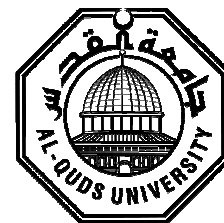


**Deanship of Graduate Studies
Al-Quds University**



**Design and Synthesis of Pyrimidine-Based Allosteric
Inhibitors of Bcr-Abl for Treatment of Leukemia**

Maha Nasri Awwad-Khoury

MSc. Thesis

Jerusalem-Palestine

1434-2013

Design and Synthesis of Pyrimidine-Based Allosteric Inhibitors of Bcr-Abl for Treatment of Leukemia

Prepared By:
Maha Nasri Awwad-Khoury

BSc. General Chemistry Jordan University

Supervisor:
Dr. Yousef Najajreh

A thesis submitted in partial fulfillment of the requirements
for the degree of Master of Applied and Industrial Technology
Department of Science and Technology - Al-Quds University

1434/2013

Al-Quds University
Deanship of Graduate Studies
Applied and Industrial Technology
Department of Science and Technology

Thesis Approval

**Design and Synthesis of Pyrimidine-Based Allosteric Inhibitors of Bcr-Abl
for Treatment of Leukemia**

Prepared By: Maha Nasri Awwad- Khoury

Registration No: 20612036

Supervisor: Dr. Yousef Najajreh

Master thesis submitted and accepted, Date:

The names and signatures of the examining committee members are as follows:

1-Head of Committee: Dr. Yousef Najajreh

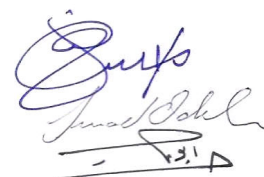
Signature:

2-Internal Examiner: Dr. Imad odeh

Signature:

3-External Examiner: Dr. Hijazi Abu Ali

Signature:

The image shows three handwritten signatures in blue ink. The first signature is 'Yousef Najajreh', the second is 'Imad Odeh', and the third is 'Hijazi Abu Ali'. The signatures are written in a cursive style.

Jerusalem – Palestine

1434/2013

Declaration:

I certify that this thesis submitted for the degree of Master in Applied and Industrial Technology is the result of my own research, except where otherwise acknowledged, and this (or any part of the same) has not been submitted for a higher degree to any other university or institution.

Signed:

Maha Nasri Awwad-Khoury

Date:

Acknowledgments:

At the end of my thesis, I would like to extend my appreciation especially to the following:

Thank God for the wisdom and perseverance that he has been bestowed upon me during this research project, and indeed, throughout my life: "I can do everything through him who gives me strength." (Philippians 4: 13).

I would kindly like to thank people at Al-Quds University for giving me the opportunity to achieve the MSc. degree.

I would like to express my gratitude to my supervisor Dr. Yousef Najajreh whose expertise, understanding, insightful comments and patience, added considerably to my graduate experience during this work.

Special thanks for the Faculty of Pharmacy for letting me use their lab, and for the group at the Anticancer Drugs Research Lab for their help and experimental assistance, working with you has been a real pleasure to me.

I would also like to thank my family for the support they provided me through my entire life and in particular, I must acknowledge my mom and my husband Wasim, without whose love and support, I would not have finished this thesis.

Finally, I would like to thank everyone who helped me and encouraged me throughout this research.

Abstract:

Leukemia disease like chronic myelogenous leukemia (CML) and acute lymphoblastic leukemia (ALL) is believed to be induced by a reciprocal translocation between the long arms of chromosomes 9 and 22, t(9:22), ending with a characteristic philadelphia chromosome generating a chimeric Bcr-Abl gene. Recognizing Bcr-Abl as the major leukemogenesis key player in 80% CML and 20% ALL initiated several trials to develop selective Bcr-Abl inhibitors as means for treating leukemia. The vast majority of known Bcr-Abl kinase inhibitors are ATP competitors that bind to the kinase domain. Despite the profound success in employing ATP competitors as potent anti-leukemogenic agents, resistance due to kinase domain mutant emerged as main limiting factors hindering patient cure. Among tens clinically relevant mutants the ‘gatekeeper’ T315I confers complete resistance to Abl kinase inhibitors. Recently, the discovery of two lead compounds GNF-2 and GNF-5 as selective non-ATP competitive inhibitors constitutes a new potential approach to the treatment of CML, these compounds were demonstrated to possess cellular activity against Bcr-Abl transformed cells by targeting the myristate binding site, also it was proved that these compounds can act cooperatively with an ATP-competitive inhibitor to suppress many mutations at the Bcr-Abl kinase domain especially the recalcitrant ‘‘T315I’’ gatekeeper mutant.

In the present work we focused on the regulatory myristoyl binding pocket as the postulated GNF-2 /-5 binding site. Accordingly, three groups of compounds have been designed, synthesized, purified using chromatography techniques, characterized by (¹H-NMR, ¹³C-NMR, FT-IR and ESIMS) spectroscopy and tested for their biological activity against Ba/F3 harboring native and T315I Bcr-Abl.

Our results demonstrated that MYJ-1 (**20**), MYJ-2 (**16**) and MYJ-17 (**29**) exhibited limited activities against Ba/F3 P185 tyrosine kinase and that MYJ-16 (**28**) showed improved activity that is concentration dependent compared to GNF-2 (**8**). Compound **28** showed comparable activity against clonogenicity of Ba/F3 harboring native and T315I Bcr-Abl constructs at concentration of 25 μM. It was shown that compound **28** was more active in inhibiting

proliferation of ALL cell lines Sup-B15 at lower concentrations compared to MYJ-18 (**30**) and MYJ-19 (**31**).

This work demonstrates that a variety of structures can effectively inhibit Bcr-Abl by presumably targeting myristate binding pocket and provides new leads for developing drugs to treat Bcr-Abl driven leukemia.

Table of Contents:

List of Abbreviations.....	xi
List of Figures.....	xiv
List of Schemes.....	xvi
List of Tables.....	xvii
List of Appendices.....	xviii
Chapter One: Introduction	1
1. Introduction.....	2
1.1 Protein Kinases and their role in Cancer	2
1.2 Tyrosine Kinases (TKs).....	5
1.3 Modes of activation of c-Abl tyrosine kinase.....	6
1.4 Chronic myelogenous leukemia (CML).....	7
1.5 Signaling pathways activated by Bcr-Abl.....	8
1.6 Therapeutic approaches targeting Bcr-Abl kinase for the treatment of CML.....	10
1.6.1 ATP-competitive inhibitors of Bcr-Abl.....	10
1.6.2 Second Generation ATP-Competitive Bcr-Abl Inhibitors.....	12
1.6.2.1 Nilotinib (AMN107).....	12
1.6.2.2 Dasatinib (BMS-345825).....	13
1.6.3 Third generation ATP-Competitive Bcr-Abl Inhibitors (Drugleads).....	14
1.6.3.1 Bosutinib (SKI-606).....	14
1.6.3.2 Ponatinib (AP24534).....	14
1.6.3.3 Bafetinib (INNO-406).....	14

1.6.4 Non-ATP-competitive inhibitors of Bcr-Abl.....	16
1.6.4.1 Substrate binding inhibitors.....	16
1.6.4.2 Allosteric binding inhibitors.....	16
1.7 Objectives.....	21
1.8 Research Questions.....	21
1.9 Significance of Proposed Research.....	22
Chapter Two: Experimental part	23
2. Experimental part.....	24
2.1 Materials.....	24
2.2 Instrumentation.....	24
2.2.1 Nuclear magnetic resonance (¹ H-, ¹³ C-, COSY & HMBC NMR).....	24
2.2.2 Fourier transform infrared spectroscopy (FTIR).....	25
2.2.3 Electrospray ionization mass spectrometry (ESIMS).....	25
2.3 Synthetic Chemistry.....	25
2.3.1 Synthesis of GNF-2 and GNF-5 analogues.....	25
2.3.1.1 Synthesis of (6-chloro-pyrimidin-4-yl)-(4-trifluoromethoxy-phenyl)-amine (13).....	25
2.3.1.2 Synthesis of [6-(4-phenyl-piperazin-1-yl)-pyrimidin-4-yl]-(4-trifluoromethoxy-phenyl)-amine {MYJ-1 (20)}.....	25
2.3.1.3 Synthesis of 4-[6-(4-trifluoromethoxyphenylamino)-pyrimidin-4-yl]-piperazine-1-carboxylic acid <i>tert</i> -butyl ester {MYJ-2 (16)}.....	26
2.3.1.4 Synthesis of (6-piperazin-1-yl-pyrimidin-4-yl)-(4-trifluoromethoxy-phenyl)-amine acidic salt (18).....	26
2.3.1.5 Preparation of aromatic acyl halides.....	27
2.3.1.5.1 Benzoyl chloride (21).....	27
2.3.1.5.2 3, 4-Dimethoxybenzoyl chloride (22).....	27
2.3.1.5.3 4-Trifluoromethylbenzoyl chloride (23).....	28
2.3.1.5.4 4-Ethylbenzoyl chloride (24).....	28
2.3.1.5.5 4-Phenylbenzoyl chloride (25).....	28

2.3.1.5.6 1-Naphthoyl chloride (54).....	28
2.3.1.6 Synthesis of (3,4-dimethoxy-phenyl)-{4-[6-(4-trifluoromethoxy-phenylamino)-pyrimidin-4-yl]-piperazin-1-yl}-methanone {MYJ-16 (28)}.....	28
2.3.1.7 Synthesis of 1-(2,3-dihydro-benzo[1,4]dioxin-6-yl)-2-{4-[6-(4-trifluoromethoxy-phenylamino)-pyrimidin-4-yl]-piperazin-1-yl}-ethanone {MYJ-17 (29)}.....	30
2.3.1.8 Synthesis of phenyl-{4-[6-(4-trifluoromethoxy-phenylamino)-pyrimidin-4-yl]-piperazin-1-yl}-methanone {MYJ-18 (30)}.....	31
2.3.1.9 Synthesis of {4-[6-(4-trifluoromethoxy-phenylamino)-pyrimidin-4-yl]-piperazin-1-yl}-(4-trifluoromethyl-phenyl)-methanone {MYJ-19 (31)}.....	32
2.3.1.10 Synthesis of [6-(4-methanesulfonyl-piperazin-1-yl)-pyrimidin-4-yl]-(4-trifluoromethoxy-phenyl)-amine {MYJ-20 (32)}.....	32
2.3.1.11 Synthesis of biphenyl-4-yl-{4-[6-(4-trifluoromethoxy-phenylamino)-pyrimidin-4-yl]-piperazin-1-yl}-methanone {MYJ-21 (33)}.....	33
2.3.1.12 Synthesis of (4-ethyl-phenyl)-{4-[6-(4-trifluoromethoxy-phenylamino)-pyrimidin-4-yl]-piperazin-1-yl}-methanone {MYJ-23 (35)}.....	33
2.3.1.13 Synthesis of naphthalen-1-yl-{4-[6-(4-trifluoromethoxy-phenylamino)-pyrimidin-4-yl]-piperazin-1-yl}-methanone {MYJ-25 (57)}.....	34
2.3.1.14 Synthesis of {6-[4-(toluene-4-sulfonyl)-piperazin-1-yl]-pyrimidin-4-yl}-(4-trifluoromethoxy-phenyl)-amine {MYJ-26 (56)}.....	35
2.3.1.15 Synthesis of (6-chloro-pyrimidin-4-yl)-(4-fluoro-phenyl)-amine (14)..	35
2.3.1.16 Synthesis of (6-piperazin-1-yl-pyrimidin-4-yl)-(4-fluoro-phenyl)-amine acidic salt (19).....	36
2.3.1.17 Synthesis of (3,4-dimethoxy-phenyl)-{4-[6-(4-fluoro-phenylamino)-pyrimidin-4-yl]-piperazin-1-yl}-methanone {MYJ-22 (34)}.....	36
2.3.2 Synthesis of piperazine symmetrical analogues.....	37
2.3.2.1 Synthesis of 1,4-Piperazine, bis {(6-Pyrimidin)-(4-trifluoromethoxy-phenyl)-amine} {MYJ-24 (38)}.....	37
2.3.3 Synthesis of pyridyl-/pyrimidyl -piperazinyl derivatives.....	38
2.3.3.1 2-Bromo-1-(2, 3-dihydro-benzo [1, 4] dioxin-6-yl)-ethanone (26)	38

derivatives.....	
2.3.3.1.1 1-(2,3-Dihydro-benzo[1,4]dioxin-6-yl)-2-[4-(5-trifluoromethyl-pyridin-2-yl)-piperazin-1-yl]-ethanone {MYJ-7 (45)}.	38
2.3.3.1.2 1-(2,3-Dihydro-benzo[1,4]dioxin-6-yl)-2-(4-pyridin-2-yl-piperazin-1-yl)-ethanone {MYJ-10 (48)}.....	39
2.3.3.1.3 1-(2,3-Dihydro-benzo[1,4]dioxin-6-yl)-2-(4-pyridin-4-yl-piperazin-1-yl)-ethanone {MYJ-13 (51)}.....	39
2.3.3.1.4 1-(2,3-Dihydro-benzo[1,4]dioxin-6-yl)-2-(4-pyrimidin-2-yl-piperazin-1-yl)-ethanone {MYJ-15 (53)}.....	39
2.3.3.2 Benzofuran-2- carboxylic acid (43) derivatives.....	40
2.3.3.2.1 Benzofuran-2-yl-[4-(5-trifluoromethyl-pyridin-2-yl)-piperazin-1-yl]-methanone {MYJ-8 (46)}.....	40
2.3.3.2.2 Benzofuran-2-yl-(4-pyridin-2-yl-piperazin-1-yl)-methanone {MYJ-9 (47)}.....	40
2.3.3.2.3 Benzofuran-2-yl-(4-phenyl-piperazin-1-yl)-methanone {MYJ-12 (50)}.....	41
2.3.3.3 6-Methoxy-Benzofuran-2- carboxylic acid (44) derivatives.....	41
2.3.3.3.1 (6-Methoxybenzofuran-2-yl)-[4-(5-trifluoromethylpyridin-2-yl)-piperazin-1-yl]-methanone {MYJ-11 (49)}.....	41
2.3.3.3.2 (6-Methoxybenzofuran-2-yl) - (4-pyrimidin-2-yl)piperazin-1-yl)-methanone {MYJ-14 (52)}.....	42
Chapter Three: Results and Discussion	43
3. Results and Discussion.....	44
3.1 Chemical synthesis of compounds.....	44
3.1.1 GNF-2 and GNF-5 analogues.....	44
3.1.1.1 Synthesis of (6-piperazin-1-yl-pyrimidin-4-yl)-(4-trifluoromethoxyphenyl)-ammonium.hydrochloride (18) and (6-piperazin-1-ylpyrimidin-4-yl)-(4-fluorophenyl)-ammonium.hydrochloride (19).....	45
3.1.1.2 Synthesis of GNF-2/ GNF-5 analogues (MYJ-16 -MYJ-23 (28-35) and MYJ-25 & MYJ-26 (57& 56)).....	46

3.1.1.3 Synthesis of aromatic acyl halides.....	47
3.1.1.4 Synthesis of [6-(4-phenyl-piperazin-1-yl)-pyrimidin-4-yl]-(4-trifluoromethoxy-phenyl)-amine MYJ-1 (20).....	48
3.1.2 Piperazine symmetrical analogues.....	49
3.1.2.1 Synthesis of 1,4-Piperazine, bis {(6-Pyrimidin)-(4-trifluoromethoxy-phenyl)-amine} MYJ-24 (38).....	49
3.1.3 Pyridyl-/Pyrimidyl -piperazinyl derivatives.....	50
3.1.3.1 Synthesis of benzofuran-2-carboxylic acid (43), 6-methoxybenzofuran-2-carboxylic acid (44) derivatives.....	50
3.1.3.2 Synthesis of 1-(2,3-dihydrobenzo[b][1,4]dioxin-6-yl)ethanone (26) derivatives.....	50
3.2 Biological evaluation of novel allosteric inhibitors of Bcr-Abl.....	51
3.2.1 <i>In-vitro</i> assessment of cellular auto-phosphorylation Activity in Ba/F3 Bcr-Abl cells.....	51
3.2.2 Inhibition of cellular auto-phosphorylation of the native Bcr-Abl.....	52
3.2.3 Inhibition of cellular auto-phosphorylation of the native and T315I mutated Bcr-Abl form by MYJ-16 (28).....	56
3.2.4 Clonigenicity Inhibition.....	58
3.2.5 Evaluation of the effect of MYJ's compounds on the inhibition of proliferation of ALL cell lines Sup-B15.....	60
3.2.6 Bcr-Abl Structure-Activity Relationships (SAR) of MYJ compounds.....	63
3.2.6.1 GNF-2 and GNF-5 subclass.....	63
3.2.6.2 Piperazine symmetrical analogues subclass.....	64
3.2.6.3 Pyridyl-/Pyrimidyl-piperazinyl subclass.....	64
Chapter Four: Conclusion	65
4. Conclusion.....	66
Chapter Five: References	68
5. References.....	69
Chapter Six: Appendices	74
6. Appendices.....	75

List of Abbreviations:

TKs	Tyrosine kinases
CML	Chronic myelogenous leukemia
ALL	Acute lymphoblastic leukemia
Bcr	Breakpoint cluster region
c-Abl	Abelson leukemia virus kinase
Bcr-Abl	Breakpoint cluster region-Abelson kinase
Ph+CML	Philadelphia chromosome-positive chronic myelogenous leukemia
Ph+ALL	Philadelphia chromosome positive Acute Lymphoblastic Leukemia
MBP	Myristoyl binding pocket
P-loop	Phosphate -binding loop
SH3	Src Homology 3
SH2	Src Homology 2
GIST	Gastrointestinal stromal tumours
HES	Hypereosinophilic syndrome
NSCLC	Non-small-cell lung cancers
RCC	Renal cell carcinoma
HCC	Hepatocellular carcinoma
STS	Soft tissue sarcoma
MTC	Medullary thyroid cancer
c-Kit	Proto-oncogene tyrosine-protein kinase Kit
PDGFR	Platelet-derived growth-factor receptor
DDR1	Discoidin domain receptor tyrosine kinase 1
EGFR	Epidermal growth-factor receptor
HER-4	Receptor tyrosine-protein kinase erbB-4
Raf	Proto-oncogene serine/threonine-protein kinase
VEGFR	Vascular endothelial growth-factor receptor
HER-2	Human epidermal growth factor receptor-2
Flt3	FL tyrosine kinase 3
Src	Cellular sarcoma

MAP	Mitogen activated protein kinase
PI₃K	Phosphatidylinositol-3-kinase
BRAF	V-raf murine sarcoma viral oncogene homolog B1
RET	Rearranged during transfection proto-oncogene
ALK	Anaplastic lymphoma kinase
ROS1	C-ros oncogene1 receptor tyrosine kinase
BOC-pz	Piperazine-1-carboxylic acid <i>tert</i> -butyl ester
DCC	N,N'-Dicyclohexylcarbodiimide
NHS	N-hydroxysuccinimide
Na₂SO₄	Sodium sulfate
DIPEA	Diisopropylethylamine
CDI	1,1'-Carbonyldiimidazole
DMF	N,N-Dimethylformamide
Eth.Ac.	Ethyl acetate
DCM	Dichloromethane
K₂CO₃	Potassium carbonate
CaCl₂	Calcium chloride
KBr	Potassium bromide
TEA	Triethylamine
MeOH	Methanol
EtOH	Ethanol
CHCl₃	Chloroform
HCl	Hydrochloric acid
TMS	Tetramethylsilane
D₂O	Deuterium oxide
CDCl₃	Chloroform-d
DMSO-d₆	Deuterated dimethyl sulfoxide (d ₆)
TLC	Thin layer chromatography
¹H-NMR	Proton nuclear magnetic resonance
¹³C-NMR	Carbon nuclear magnetic resonance
COSY	¹ H- ¹ H Correlation spectroscopy

HMBC	Heteronuclear multiple-bond correlation spectroscopy
FTIR	Fourier transform infrared spectroscopy
ESIMS	Electrospray ionization mass spectrometry
HXMS	Hydrogen exchange mass spectrometry
SAR	Structure-Activity Relationships
r.t.	Room temperature

List of Figures:

Figure No:	Details	Page
Figure 1.1	The domain structure of the enzymes Abl 1a and 1b	6
Figure 1.2	(a) The order of domains in the polypeptide chains of c-Abl and diagram of its assembled, autoinhibited state, (b) Modes of Activation for c-Abl: unlatching, unclamping, and switching	7
Figure 1.3	(a) Locations of the breakpoints in the c-Abl and Bcr genes and structure of the chimeric Bcr-Abl mRNA transcripts derived from the various breaks, (b) Domain structure of c-Src, c-Abl 1b, and Bcr-Abl. Potential tyrosine phosphorylation sites are indicated with red circles and the residue number	8
Figure 1.4	Cellular outcomes of activated pathways by Bcr-Abl	9
Figure 1.5	Imatinib development	10
Figure 1.6	Structural features of the Abl kinase domain important for activity and inhibitor binding	11
Figure 1.7	A range of Bcr-Abl kinase domain mutations identified including mutations in each of the three functional regions of Bcr-Abl, the p-loop region, the catalytic domain and the activation domain	12
Figure 1.8	The chemical structures of (1) Imatinib, (2) Nilotinib, (3) Dasatinib, (4) Bosutinib, (5) Ponatinib, (6) Bafetinib, (7) ON012380, (8) GNF-2 and (9) GNF-5	13
Figure 1.9	GNF-2, Imatinib and ON012380 binding to different binding sites in the kinase domain	17
Figure 1.10	(a) Schematic representation of the mechanism of action of Bcr-Abl/ c-Abl myristate pocket binders. The SH3, SH2 and kinase domains are shown in yellow, green and blue, respectively. The myristoyl group that is attached to the N-terminus of c-Abl binds to a deep hydrophobic pocket in the kinase domain and induces bending of the C-terminal α I'-helix (shown in dark red). Next to the schematic representations, a blow-up shows the myristate pocket from the crystal structures of the Abl kinase domain alone and in complex with myristate, GNF-2, (b) Binding conformation of GNF-2 (cyan) in the myristate binding site of Abl (side chains from helix α E are green, α F orange, α I dark orange, α I' red). Hydrogen bonds to a water molecule (red sphere) are indicated by dashed yellow lines	18
Figure	(a) Effect of various concentrations of GNF-2, imatinib, or combinations of both on the number of emerging Ba/F3 Bcr-Abl -	20

1.11	resistant clones, (b) IC ₅₀ for inhibition of wild-type, E505K and T315I Abl kinase activity by GNF-5, nilotinib or a combination of the two at an ATP concentration of 20 μM	
Figure 2.1	Chemical structure of 28	29
Figure 3.1	Rational of synthesizing the GNF-2/-5 analogues	45
Figure 3.2	Auto-phosphorylation inhibition of STAT5α and p185, p210 Bcr-Abl by GNF-2	52
Figure 3.3	Auto-phosphorylation inhibition of p185 Bcr-Abl by MYJ's compounds compared by GNF-2	56
Figure 3.4	Inhibition of Bcr-Abl cellular auto-phosphorylation and T315I mutated Bcr-Abl by MYJ-16 (28) compound. (a) Percentage of Bcr-Abl auto-phosphorylation (violet) and T315I mutated Bcr-Abl inhibition (purple), (b) Western blot of inhibition of Bcr-Abl auto-phosphorylation by MYJ-16 (28) for cells carrying native and T315I mutated Bcr-Abl forms.	57
Figure 3.5	Clonogenicity Inhibition of Ba/F3 cells carrying the native and T315I mutated Bcr-Abl constructs by Imatinib, GNF-2 (8) and MYJ-16 (28) compound using different concentrations	59
Figure 3.6	Inhibition of ALL cell lines Sup-B15 by the MYJ-16 (28), MYJ-18 (30) and MYJ-19 (31) compounds	62

List of Schemes:

Scheme No.	Details	Page
Scheme 1	Representative procedure for the synthesis of salts 18 and 19	46
Scheme 2	Representative procedure for the synthesis of GNF-2/-5 analogues	47
Scheme 3	Representative procedure for the synthesis of aromatic fatty acids halide: 22, 23, 24, 25, and 54	48
Scheme 4	Representative procedure for the synthesis of piperazine symmetrical analogues	49
Scheme 5	Representative procedure for the synthesis of Pyridyl-/Pyrimidyl - piperazinyl derivatives	51

List of Tables:

Table No.	Details	Page
Table 1.1	List of 14 kinase inhibitors approved to date for various cancer indications within the U.S. since 2001	3
Table 1.2	ATP-competitive inhibitors of Bcr-Abl summary	15
Table 2.1	NMR data on compound 28	30
Table 3.1	The percentage values of the Ba/F3 P185-tyrosine inhibition by the MYJ's compounds	53
Table 3.2	The percentage values of inhibition of ALL cell lines Sup-B15 by the MYJ's compounds comparing to GNF-2	61

List of Appendices:

Appendix No.	Details	Page
Appendix 6.1	Nuclear magnetic resonance (^1H -, ^{13}C -, COSY & HMBC NMR) of compound MYJ-16 (28)	75
Appendix 6.2	Electrospray ionization mass spectrometry (ESIMS) of compounds MYJ-15 (53), MYJ-16 (28), MYJ-18 (30), MYJ-19 (31) and MYJ-20 (32)	79
Appendix 6.3	Fourier transform infrared spectroscopy (FTIR) of compounds MYJ-11 (49), MYJ-16 (28), MYJ-18 (30), MYJ-20 (32), MYJ-22 (34) and MYJ-24 (38)	84

Chapter One

Introduction

1. Introduction:

1.1 Protein Kinases and their role in Cancer:

Protein kinases are class of cellular enzymes that contain an ATP-dependent catalytic activity results in the covalent attachment of a phosphate group to serine, threonine or tyrosine residues in specific peptide sequences of substrate proteins. There are an estimated 518 protein kinases encoded by the human genome, which are divided into two main groups on the basis of structural relatedness ^[1-3].

Those predicted 518 protein kinases are involved in mediating important events in normal cells such as: proliferation, cell cycle, metabolism, survival, apoptosis, DNA damage repair, cell motility and response to the microenvironment ^[4].

Several biochemical and genetic studies have revealed essential roles for many of the 518 human protein kinases in a broad range of diseases, where aberrant signals transduction processes have been identified. Therefore selective inhibition of distinct members of that target family offers novel opportunities for drug discovery and development for numerous diseases, including various cancer types, inflammatory, cardiovascular, metabolic, neurodegenerative, and even viral and bacterial diseases ^[5].

Kinases such as cellular sarcoma (c-Src) kinase, Abelson Leukemia Virus (c-Abl) kinase, mitogen activated protein (MAP) kinase, phosphatidylinositol-3-kinase (PI₃K), and the epidermal growth factor receptor (EGFR) are commonly activated in cancer cells. They play a central role in the growth and proliferation of tumor cells, hence making them a legitimate target for new anti-cancer drugs ^[6-8].

The benefit of using kinase inhibitors as anti-cancer drugs stems from the fact that they would be more specific than traditional chemotherapeutic agents, effectively targeting active tumor cells without affecting the rapid growth of healthy cells found in the bone marrow and gastrointestinal tract as example. The traditional chemotherapeutic agents typically inhibit the growth of all rapidly dividing cells, including non-tumor cells, which is why they cause a multitude of unwanted side effects. Another benefit of using kinase inhibitors is their good tolerability and oral bioavailability compared to the traditional cytotoxic agents currently in use.

Nevertheless, kinases are also involved in the growth of healthy cells and finding an agent that selectively inhibits tumor kinases with high efficacy is not an easy task. The main challenge stems from the lack of sufficient research to identify the kinases that are pathologically activated in a particular disease setting; also drug resistance is a significant challenge that faces the field, until such information becomes available it would be difficult to find a selective and efficacious kinase inhibitor ^[8, 9]. To date, more than 14 kinase inhibitors have received US Food and Drug Administration approval as cancer treatments, see Table 1.1 below ^[10-12].

Table 1.1: List of 14 kinase inhibitors approved to date for various cancer indications within the U.S. since 2001:

U.S. brand name	Year approved	Generic name	U.S. FDA-approved indications	Company	Target kinases
Gleevec	2001	Imatinib mesylate	CML, GIST, HES	Novartis	Bcr-Abl, c-Abl, c-Kit, PDGFR, DDR1
Iressa	2003	Gefitinib	NSCLC	AstraZeneca	EGFR, HER-4
Tarceva	2004	Erlotinib	NSCLC, pancreatic cancers	Genentech, OSIP, Roche	EGFR
Nexavar	2005	Sorafenib tosylate	HCC, RCC	Bayer and Onyx	Raf, VEGFR, c-Kit, PDGFR
Sutent	2006	Sunitinib malate	GIST, RCC	Pfizer	c-Kit, VEGFR, PDGFR, FLT3
Sprycel	2006	Dasatinib	CML (especially imatinib-resistant)	Bristol-Myers Squibb	Bcr-Abl, c-Abl, c-Kit, PDGFR, Src
Tasigna	2007	Nilotinib	CML (imatinib resistant and intolerant)	Novartis	Bcr-Abl, c-Abl, c-Kit, PDGFR, Src, Ephthrin
Tykerb	2007	Lapatinib	breast cancer	GlaxoSmithKline	EGFR, HER-2

Table 1.1, cont.:

Votrient	2009	Pazopanib	Advanced RCC, STS	GlaxoSmithKline	VEGFR-1, -2, and -3, PDGFR , c-Kit
Caprelsa	2011	Vandetanib	Unresectable, locally advanced, or metastatic MTC	AstraZeneca	VEGFR, EGFR
Zelboraf	2011	Vemurafenib	Unresectable or metastatic melanoma carrying the mutant BRAFV600E	Roche	BRAF
Xalkori	2011	Crizotinib	Locally advanced or metastatic NSCLC	Pfizer	ALK, ROS1
Bosulif	2012	Bosutinib	chronic, accelerated, or blast phase Ph+CML with resistance	Pfizer	Src, Bcr-Abl, c-Abl
Iclusig	2012	Ponatinib	CML with T3151 mutation, Ph ⁺ ALL	Ariad Pharmaceuticals	Bcr-Abl, FLT3, RET, c-Kit , members of the EGFR, PDGFR and VEGFR families of kinases.

Abbreviations: CML, chronic myeloid leukemia; GIST, gastrointestinal stromal tumours; HES, hypereosinophilic syndrome; NSCLC, non-small-cell lung cancers; RCC, renal cell carcinoma; HCC, hepatocellular carcinoma; STS, soft tissue sarcoma; MTC, medullary thyroid cancer; Ph+CML, Philadelphia chromosome-positive [chronic myelogenous leukemia](#); Ph+ALL, Philadelphia chromosome positive Acute Lymphoblastic Leukemia. Bcr-Abl, breakpoint cluster region-Abelson kinase; c-Abl, Abelson Leukemia Virus kinase; c-Kit, Proto-oncogene tyrosine-protein kinase Kit; PDGFR, platelet-derived growth-factor receptor; DDR1, discoidin domain receptor tyrosine kinase 1; EGFR, epidermal growth-factor receptor; HER-4, Receptor tyrosine-protein kinase erbB-4; Raf, proto-oncogene serine/threonine-protein kinase; VEGFR, vascular endothelial growth-factor receptor; HER-2, human epidermal growth factor receptor-2; Flt3, FL tyrosine kinase 3; Src, Proto-oncogene tyrosine-protein kinase; BRAF, v-raf murine sarcoma viral oncogene homolog B1; RET, rearranged during transfection proto-oncogene; ALK, [anaplastic lymphoma kinase](#); ROS1, [c-ros oncogene1 receptor tyrosine kinase](#).

1.2 Tyrosine Kinases (TKs):

Tyrosine kinases are a family of tightly regulated phosphotransferase enzymes which transfer phosphate groups from high energy donors, such as ATP, to substrates bearing a tyrosine residue. In the human genome, 90 tyrosine kinases have been identified, and are divided into two groups, receptor and nonreceptor^[13, 14].

There are 58 known receptor kinases which are subdivided into 20 subfamilies. Examples of such kinases include the epidermal growth factor receptor (EGFR), platelet-derived growth factor receptor (PDGFR), vascular endothelial growth factor (VEGF) receptor and c-kit/stem cell factor receptor. All the receptor kinases function in a similar fashion by transducing signals from both outside and inside the cell and serving as relay points for signaling pathways inside the cell. On the other hand, the 32 remaining tyrosine kinases are cytoplasmic non-receptor type which lack a transmembrane segment and generally function downstream of the receptor tyrosine kinases. Examples of such non-receptor kinases include the breakpoint cluster region-Abelson kinase (Bcr-Abl) fusion protein and c-Src^[15, 16].

Tyrosine kinases play a critical role in the signaling cascades; their strict regulation of activity controls the most fundamental processes of cells, such as, cell proliferation, migration, differentiation, metabolism and programmed cell death.

Recent advances showed a primary role of tyrosine kinases in the pathophysiology of cancer. Though their activity is tightly regulated in normal cells, they may acquire transforming functions due to mutations, overexpression or other reasons, leading to malignancy. The central role that tyrosine kinases, receptor and nonreceptor alike, play in tumorigenesis makes them primary targets for future cancer therapies. Examples of such kinases include Abl, Src, EGFR, PDGFR and VEGFR families^[17-19].

One such kinase is the Abelson Leukemia Virus kinase (c-Abl) which is a nonreceptor tyrosine kinase. Human cells express two spliced variants of this kinase; one is myristoylated at the N-terminal (Abl-1b) while the other is not (Abl-1a). The c-Abl kinase is approximately ~1150 residues long with a unique ~80 residue N-terminal cap thought to be important for autoinhibition of c-Abl. Following the N-terminal cap, there are Src Homology 3 (SH3), Src Homology 2 (SH2) and tyrosine kinase domains (Figure 1.1). The C-terminal half of c-Abl

contains nuclear localization and export signals, binding elements for the SH3 domains as well as DNA binding and actin binding domains ^[20-23].

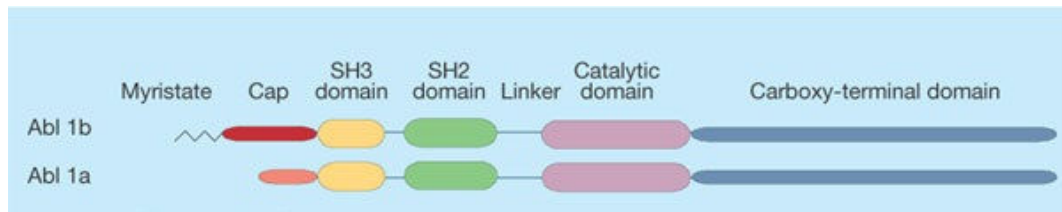


Figure 1.1: The domain structure of the enzymes Abl 1a and 1b ^[16].

1.3 Modes of activation of c- Abl tyrosine kinase:

The c-Abl tyrosine kinase is composed of a two-lobe enzymatic domain (catalytic site), with a smaller lobe containing an α -helix (C-helix) polypeptide segment and a larger lobe containing the “activation loop” polypeptide segment which is stabilized in its active form by phosphorylation. The aforementioned catalytic site lies in a cleft between the smaller amino terminal and the carboxy terminal and can open or close the active site by adopting a range of relative orientations ^[23]. The kinase control-machinery is composed of three critical components: the “switch”, the “clamp” and the “latch”. The “switch” is the “activation loop” which lies in the larger C-lobe while the “clamp” is an assembly of the SH2 and SH3 domains abutting both the C-lobe and the smaller N-lobe respectively (Figure 1.2; **(a)**). The SH2 domain is connected to the kinase via an adapter element which runs through the ligand-binding groove of the SH3 domain. Finally, the “latch” is the short C-terminal tail of the larger C-lobe ^[24-26].

Switching the kinase on begins with the “latch” which releases the “cap” that extends from the SH3 domain abutting the N-terminal and which is anchored by a myristoyl group to the C-lobe. Activation of the kinase is finally achieved by phosphorylation of a tyrosine in the “activation loop” after the SH2 and SH3 ligands (regulatory apparatus) are unclamped (Figure 1.2; **(b)**) ^[27, 28].

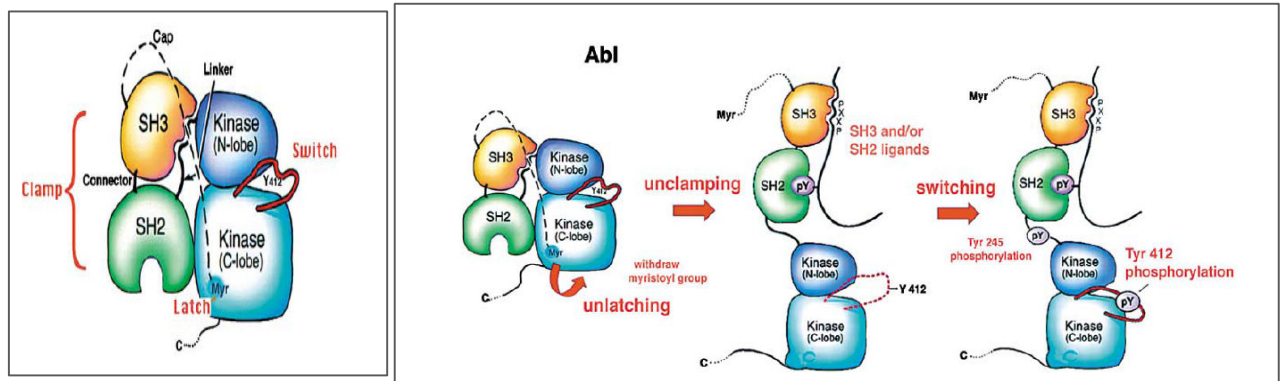


Figure 1.2: (a) The order of domains in the polypeptide chains of c-Abl and diagram of its assembled, autoinhibited state ^[26], (b) Modes of Activation for c-Abl: unlatching, unclamping, and switching ^[26].

1.4 Chronic myelogenous leukemia (CML):

Chronic myelogenous leukemia (CML) is a malignant myeloproliferative disorder of haematopoietic stem cells, characterized by the increased and unregulated growth of myeloid cells in the bone marrow and the accumulation of these cells in the blood. It accounts for 15–20% of all cases of leukemia with an annual incidence of 1–2 cases per 100,000 individuals per year. Clinically, the disease progresses through three distinct phases, the first chronic or stable phase which is characterized by increased number of myeloid precursors and mature cells that leave the bone marrow prematurely but retain their ability to differentiate normally. Within a period of 4–6 years, the disease transforms to the second accelerated phase which is characterized by the presence of primitive blast cells in the bone marrow and peripheral blood, and finally the disease advances to the fatal ‘blast-crisis’ phase, characterized by over 30% undifferentiated blasts in the bone marrow and peripheral blood, where median survival is 18 weeks nearly ^[29-31].

The majority of CML patients are diagnosed by the presence of Philadelphia chromosome (Ph), which results from a reciprocal translocation between the long arms of chromosomes 9 and 22, t(9:22), which generates a chimeric Bcr-Abl gene, formed by juxtaposition of the c-Abl oncogene on chromosome 9 with sequences from the breakpoint cluster region (Bcr) on chromosome 22.

There are multiple points along the Bcr-Abl genes at which a break can produce a chimeric fusion protein. For instance, the fusion of c-Abl proto-oncogene between the first and second exons will result in the p210 Bcr-Abl fusion genes which transcribe either a b2a2 or b3a2 mRNA, the product of which is a 210 kDa cytoplasmic fusion protein sufficient for the malignant transformation and phenotypic abnormalities seen in the vast majority of CML patients. Additionally, half of (Ph) positive Acute Lymphoblastic Leukemia (ALL) adults reportedly carry the p210 fusion genes while the other half bears the p185 Bcr-Abl (also called p190) product which results from fusion of the same sequences of c-Abl with a proximal site in Bcr (exon 1). The p185 Bcr-Abl product is also found in up to 80% of Ph-positive children suffering with ALL (Figure 1.3) [32-35].

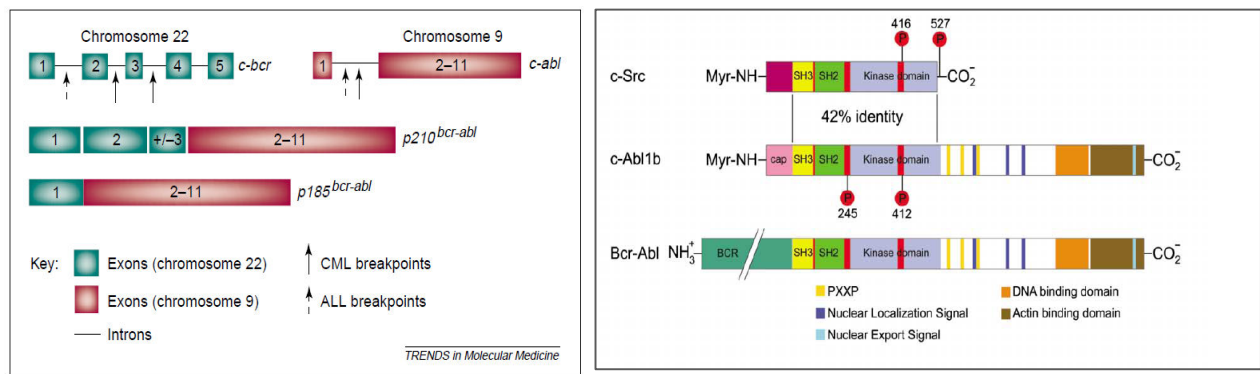


Figure 1.3: (a) Locations of the breakpoints in the c-Abl and Bcr genes and structure of the chimeric Bcr-Abl mRNA transcripts derived from the various breaks [31], (b) Domain structure of c-Src, c-Abl 1b, and Bcr-Abl. Potential tyrosine phosphorylation sites are indicated with red circles and the residue number [21].

1.5 Signaling pathways activated by Bcr-Abl:

In contrast to ABL which normally exists in an inactive conformation, Bcr-Abl oncogene encodes a chimeric Bcr-Abl protein that exhibits deregulated aberrant Abl tyrosine kinase activity and is found exclusively in the cytoplasm of the cell, complexed with a number of cytoskeletal proteins.

This mutant kinase increased activity is due to two reasons:

- 1- The fusion protein retains most Abl coding sequences, but deletes the myristoylation site from the extreme N terminus of Abl, thus “unlocking” the closed, inactive conformation.

2- Sequences from Bcr also contribute to fusion protein activity, where most studies agree that the N-terminal Bcr dimerization domain, present in both fusion proteins, disrupts the autoinhibited “closed” conformation and promotes transautophosphorylation and kinase activation.

The constitutive tyrosine kinase activity of Bcr-Abl causes activation of a cascade of intracellular signaling pathways, in a kinase-dependent manner, leading to increased proliferation, increased resistance to apoptosis and an alteration of their adhesion properties, and thus the activation of such pathways may affect the expression of genes that confer the malignant phenotype.

Signal transduction pathways activated by p210 Bcr-Abl are: Ras/Raf/mitogen activated protein kinase (MAPK), phosphatidylinositol 3 kinase (PI3-kinase), STAT5/Janus kinase, and Myc (Figure 1.4) ^[36-40].

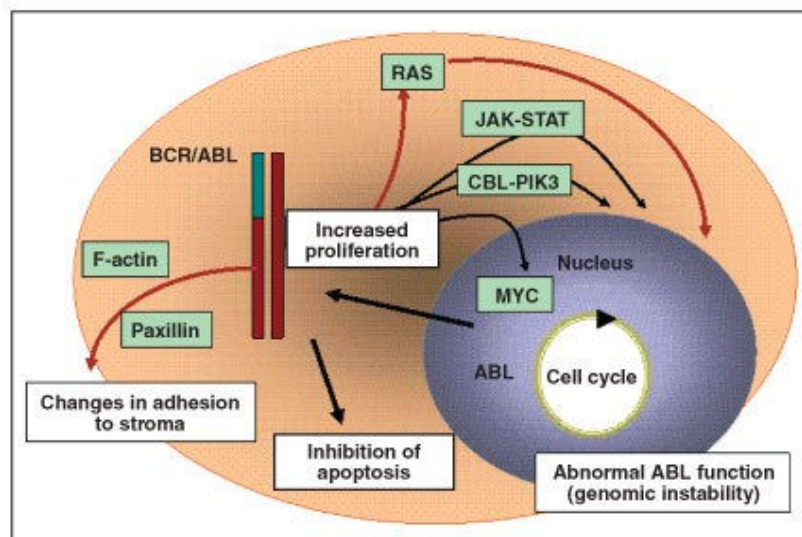


Figure 1.4: Cellular outcomes of activated pathways by Bcr-Abl ^[40].

Much of the knowledge regarding the function of this gene, the growing understanding of genetic alterations and the identification of the molecules that are part of the signaling cascade in CML cells, prompted searching for a specific inhibitor of the Bcr-Abl tyrosine kinase that would be effective and selective therapeutic agent for targeting various steps of the malignant transformation.

1.6 Therapeutic approaches targeting Bcr-Abl kinase for the treatment of CML:

1.6.1 ATP-competitive inhibitors of Bcr-Abl:

As CML arises from a single genetic lesion, a research goal has been to develop kinase-specific inhibitors, and after performing a high-throughput screening of chemical libraries searching for compounds with kinase inhibitory activity, a lead compound of the 2-phenylaminopyrimidine class was identified, Imatinib mesylate (also known as STI-571 and Gleevec) which is selective for two protein kinase receptors, the PDGFR and c-Kit, and a non-receptor TK, the Abl, where it behaves as an ATP-competitive inhibitor of it (Figure 1.5) [41-43].

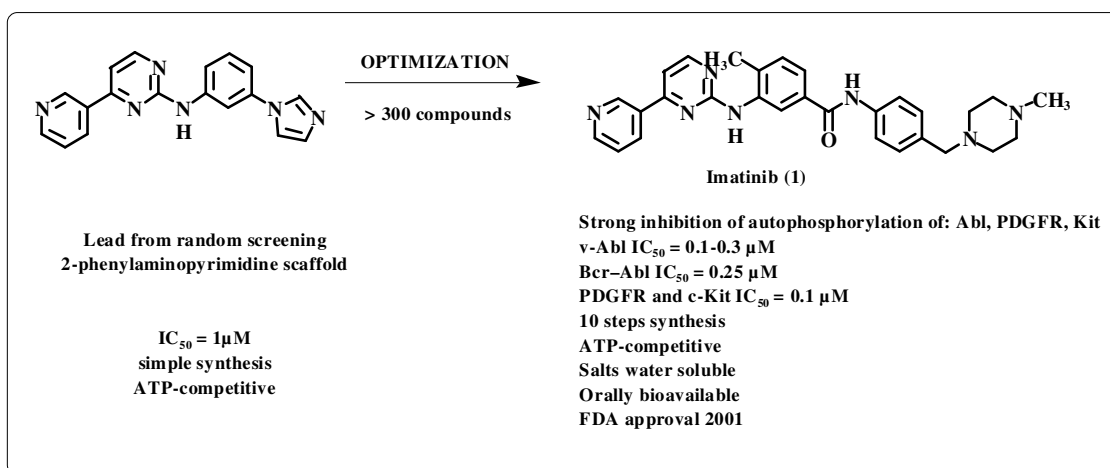


Figure 1.5: Imatinib development.

Clinically imatinib is very successful in treating Bcr-Abl positive leukemias, and thus considered as an effective and selective frontline therapy for chronic-phase CML, that binds to the catalytic cleft between the two N and C-lobes via six [hydrogen bond](#) interactions, thus stabilizing the kinase in an inactive conformation referred to as the 'DFG-out' conformation, in which the highly conserved aspartate-phenylalanine-glycine (DFG) triad is flipped out of its usual position in active kinase conformations with the activation loop in a closed position and P-loop ([phosphate](#)-binding loop) folding over the [ATP](#) binding site (Figure 1.6; (a)) [10, 12, 44, 45].

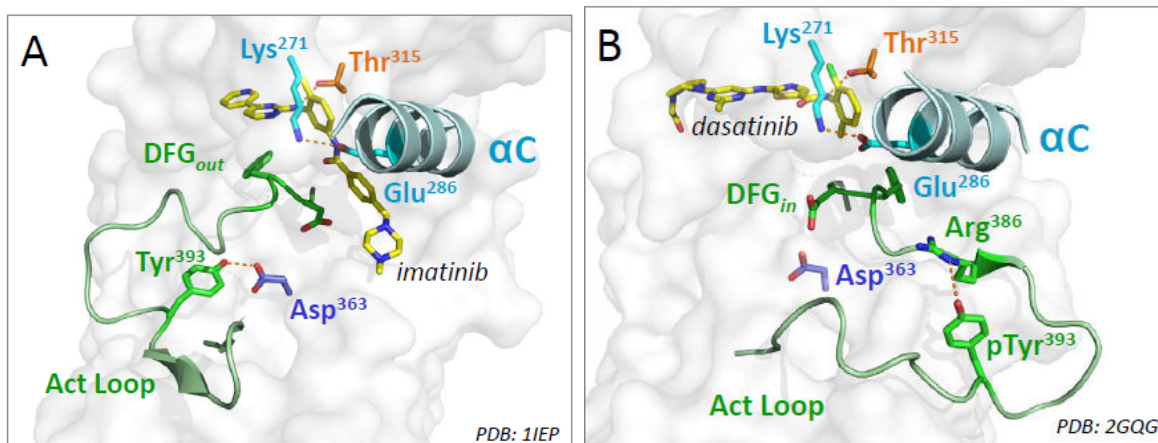


Figure 1.6: Structural features of the Abl kinase domain important for activity and inhibitor binding.

(a) Close-up view of the Abl kinase domain bound to imatinib, which stabilizes a down regulated conformation of the active site. Key structural elements of this off state include the inward rotation of the N-lobe α C-helix (cyan), which positions Glu286 for ion pairing with Lys271. The DFG motif (Asp381, Phe382, Gly383), which is located at the N-terminal end of the activation loop (Act Loop; green), is rotated away from the active site to accommodate imatinib binding (DFG-out). The activation loop tyrosine (numbered as Tyr393 in this structure) points into the active site and makes a hydrogen bond with the catalytic aspartate (Asp363; purple). Also shown is the side chain of the gatekeeper residue (Thr315; orange) which forms a critical hydrogen bond with imatinib^[45], (b) Close-up view of the Abl catalytic site in an active conformation with dasatinib bound (ligand carbon atoms in yellow). Note that the α C-helix and the Glu286 ion pair with Lys271 are positioned as per the inactive state in a, but the activation loop is completely reoriented. The phosphorylated activation loop tyrosine (pTyr393) is now paired with a nearby arginine residue (Arg386), releasing the catalytic aspartate and stabilizing the active conformation. The DFG motif is now flipped inward (DFG-in); this conformation is not compatible with imatinib binding due to steric clash. The gatekeeper threonine also makes an H-bond with dasatinib^[45].

However, accelerated or blast-crisis phase CML and Ph⁺ ALL patients often relapse due to drug resistance results from amplification or overexpression of the Bcr-Abl gene, or by the emergence of point mutations within the kinase domain of the Bcr-Abl protein, which frequencies appear to increase as the disease progresses^[10].

These point mutations either prevent the appropriate binding of imatinib (loss of response or acquired resistance) by disrupting hydrogen bonds between the drug and the Abl protein or leading to a steric clash or hindrance, which is the case with T315I (gatekeeper) that precludes imatinib from binding; or reduce the binding affinity of imatinib (lack of response or primary

resistance) by either preventing necessary conformational adjustments for imatinib binding, which is the case with Y253F/H and E255K/V, or stabilizing the active kinase conformation, from which imatinib is sterically excluded, which is likely the mechanism of resistance of M351T^[46-48]. Most mutations that confer resistance to imatinib are distributed throughout the Abl kinase domain. However, the most resistant ones are found in the P-loop at or near residues that are in direct contact with the drug (Figure 1.7)^[49, 50].

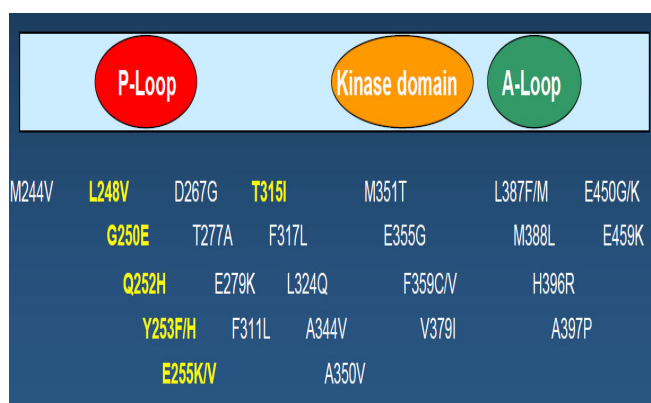


Figure 1.7: A range of Bcr-Abl kinase domain mutations identified including mutations in each of the three functional regions of Bcr-Abl, the p-loop region, the catalytic domain and the activation domain.

1.6.2 Second Generation ATP-Competitive Bcr-Abl Inhibitors:

Due to the resistance to Imatinib in blast-crisis phase CML, there is an urgency to develop novel compounds to prevent or overcome this resistance, the elucidation of the mechanisms of resistance has enabled the rational development of new ATP-competitive Bcr-Abl novel agents such as:

1.6.2.1 Nilotinib (AMN107): The substitution of the amide moiety in imatinib with an alternative binding group, led to the discovery of nilotinib (Figure 1.8; **(2)**). Like imatinib, nilotinib binds to the inactive conformation of the Abl tyrosine kinase by making four hydrogen bond interactions. Nilotinib is 10 to 30 times more potent than imatinib in inhibiting the proliferation and autophosphorylation of wild-type Bcr-Abl cell lines and is also significantly

active against 32/33 imatinib-resistant Bcr-Abl mutants, except the T315I mutant, which is situated in the middle of the ATP-binding cleft ^[51-53].

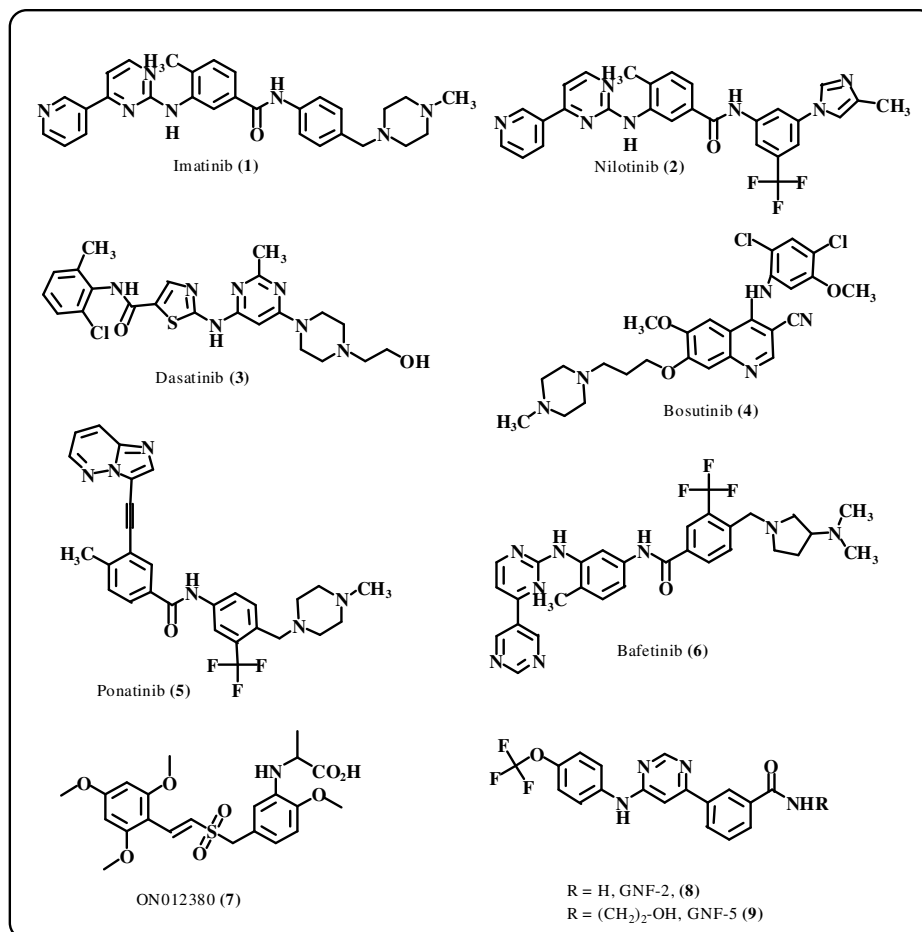


Figure 1.8: The chemical structures of (1) Imatinib, (2) Nilotinib, (3) Dasatinib, (4) Bosutinib (5) Ponatinib (6) Bafetinib (7) ON012380, (8) GNF-2, and (9) GNF-5.

1.6.2.2 Dasatinib (BMS-345825): A [thiazolylaminopyrimidine](#) core derivative which is a multi-target kinase inhibitor of Bcr-Abl and Src family kinases (Figure 1.8; (3)). Comparing with imatinib, dasatinib has an approximately 325-fold increased potency in proliferation assays of Bcr-Abl expressing cell lines and biochemical assays ^[54]. Unlike imatinib and most tyrosine kinase inhibitors (TKIs), dasatinib target the ATP binding site of the Abl kinase in its active conformation, in which the activation loop is phosphorylated (DFG-in) (Figure 1.6; (b)), but with less stringent conformational requirements, so it exhibits increased potency but reduced selectivity compared to imatinib. Also it can inhibit all Bcr-Abl kinase domain mutants except for T315I ^[9, 55, 56].

1.6.3 Third generation ATP-Competitive Bcr-Abl Inhibitors:

However, since the T315I mutation of Bcr-Abl is highly resistant to the first and second generations of TKIs and still unconquered, this approach needs to be extended to include more inhibitors of T315I Bcr-Abl to prevent it from becoming more prevalent. Some of more new drugs are in development, which are either refining current treatments or promising great improvements in efficacy, such as:

1.6.3.1 Bosutinib (SKI-606): Bosutinib inhibits Src, Abl and a wide range of both tyrosine and serine-threonine kinases (Figure 1.8; (4)). However, the T315I mutation was completely resistant to bosutinib ^[57-59].

1.6.3.2 Ponatinib (AP24534): Ponatinib has been proved as a potent drug and targets not just most of the known mutations on the Bcr-Abl TK but, most importantly of all, T315I. The reason was referred to the linearity of the linkage section of the molecule by which the drug appears to avoid steric hindrance with hydrophobic TK gatekeeper residues ^[60-63].

This agent is marketed as a second line therapy (Figure 1.8; (5)).

1.6.3.3 Bafetinib (INNO-406): Bafetinib is a multi-target kinase inhibitor of Bcr-Abl and Src family kinases Lck and Lyn; with unrivalled specificity, also it is effective against most of imatinib resistant mutations (not including T315I) and some dasatinib resistant mutations. Bafetinib has more affinity for Bcr-Abl than nilotinib (but less than dasatinib). However, this agent is in phase II clinical trials (Figure 1.8; (6)) ^[64-67].

Refer to Table 1.2.

Table 1.2: ATP-competitive inhibitors of Bcr-Abl summary:

Drug	H-bonds	H-bonding amino acids	Binding conformation	Discovery	Status
<u>Imatinib</u> (STI571)	6	Met-318, Thr-315, Glu-286, Asp-381, Ile-380, His-361	Inactive	Drug screening	Marketed as first line therapy
<u>Nilotinib</u> (AMN107)	4	Met-318, Thr-315, Glu-286, Asp-381	Inactive	Rational drug design	Marketed as second line therapy
<u>Dasatinib</u> (BMS-345825)	3	Met-318, Thr-315	Active	Rational drug design	Marketed as second line therapy
<u>Bosutinib</u> (SKI-606)	-	-	Inactive	Rational drug design	Marketed as second line therapy
<u>Ponatinib</u> (AP-24534)	5	Met-318, Asp-381, Glu-286, His-381, Ile-380	Inactive	Rational drug design	Marketed as second line therapy
<u>Bafetinib</u> (INNO-406)	6	Met-318, Thr-315, Glu-286, Asp-381, His-361, Ile-360	Inactive	Rational drug design	Phase II clinical trials

1.6.4 Non- ATP-competitive inhibitors of Bcr-Abl:

1.6.4.1 Substrate binding inhibitors:

Beside the ATP-binding site that has been traditionally targeted by medicinal chemists, the ligand binding site also was validated as targetable and a novel compound ON012380 was identified. The specific inhibitor of Bcr-Abl substrate binding ON012380, (amino-substituted (*E*)-2,6-dialkoxystyryl 4-substituted- benzylsulfone derivative (Figure 1.8; **(7)**), was proved to inhibit T315I- Bcr-Abl transformed leukemia cells through a distinct mechanism. However, this agent has not been tested in clinical studies yet (Figure 1.9) ^[68-70].

1.6.4.2 Allosteric binding inhibitors:

Allosteric inhibitors are the third class of compounds. These inhibitors bind at an allosteric site apart from the ATP catalytic active site where it modulates kinase activity in an allosteric manner involving a conformational change between active and inactive states of the protein. Inhibitors belonging to this category are characterized to exhibit the highest degree of kinase selectivity because they exploit binding sites and regulatory mechanisms that are unique to a particular kinase, also these inhibitors offer an alternative approach to inhibition of protein activities, particularly for proteins that undergo conformational changes as part of their activity cycle, and are regulated by autoinhibition ^[71].

Studies showed that the ATP-competitive inhibitors must bind with relatively higher affinity or be present at higher concentrations to effectively compete with the binding of naturally occurring substrates, whereas in contrast, a small molecule allosteric inhibitor may recognize a target site allowing effectiveness at substantially lower concentrations. Furthermore, enzyme active sites are highly conserved across large protein families (e.g., kinases, proteases), making the identification of inhibitors specific to a particular family member problematic because of cross-reactivity. In contrast, binding sites for potential allosteric inhibitors, involving sequences distant from the catalytic site, can vary significantly among the members of a protein family ^[72-74].

Abl possesses a deep hydrophobic pocket that can bind fatty acid chains such as myristoyl groups (a small hydrophobic chain of 14 carbons). Studies revealed that myristoylation of the N-

terminal region of wild-type Abl is involved in the regulation of the enzymatic activity by altering the protein conformation by inserting the myristate group into the hydrophobic pocket of the kinase domain (Myristoyl binding pocket-MBP). On the contrary, Bcr-Abl where N-terminal is replaced by the Bcr segment is not myristoylated and lacks this autoinhibitory mechanism. Hence it is believed that this Bcr-Abl translocation resulted in the absence of on control mechanism which rationalizes the idea of the strategy to develop inhibitors for the MBP “myristoyl mimics”. Such inhibitors if manage to bind to the MBP which located in the C lobe of the kinase more than 30 Å away from the active site in a selective manner, will induce the essential conformational changes to inhibit the kinase activity via binding to allosteric, non-ATP competitive mechanism, distant from the active site of the kinase (Figure 1.9) ^[75-77].

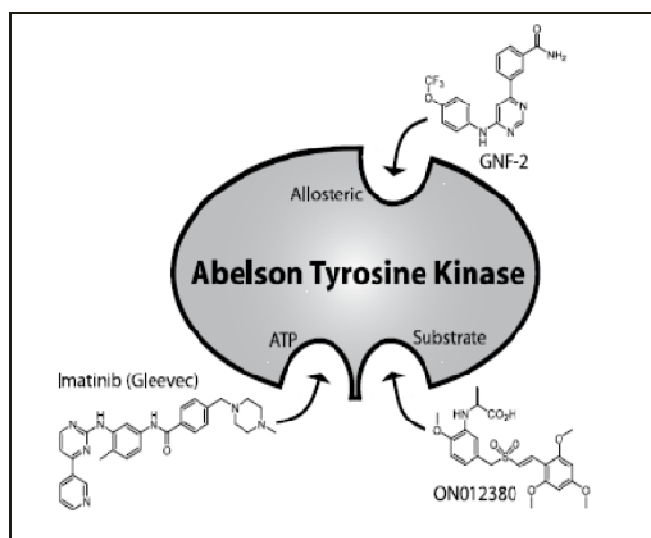


Figure 1.9: GNF-2, Imatinib and ON012380 binding to different binding sites in the kinase domain ^[75].

A recent cell based high-throughput screen identified novel 4,6-disubstituted pyrimidine derivatives with potent and selective inhibitory activity to Bcr-Abl. These compounds were proved to be not competitors with either the substrate or ATP, but the binding site of these inhibitors is the myristoyl pocket. This new class of Abl inhibitor could allow synergistic treatment with active-site inhibitors.

GNF-2 [3-(6-(4-(trifluoromethoxy) phenylamino) pyrimidin-4-yl) benzamide] (Figure 1.8; **(8)**), was discovered by Nathanael S. Gray and his colleagues and proved to be a potent and selective inhibitor of cellular proliferation. Using a differential cytotoxicity assay and screening a

combinatorial library of 50,000 heterocycles originally designed to target the ATP binding site GNF-2 identified as novel lead for MBP ligand.

GNF-2 specifically inhibited the proliferation, induced apoptosis and inhibited the autophosphorylation of the Bcr-Abl expressing cells with IC_{50} of 138 nM and did not show any cytotoxic effects on the nontransformed cells at concentrations up to $10 \mu\text{M}$ [78, 79].

Using solution NMR, X-ray crystallography, mutagenesis and hydrogen exchange mass spectrometry, it was shown that GNF-2 binds to the myristate-binding site of Abl located near the C-terminus of the kinase domain, where it seems to stabilize the inactive conformation of Bcr-Abl by inducing the bending of the kinase domain α -I helix (which is extended and clashes with the SH2 domain when the myristoyl pocket is not occupied) toward the C-lobe, allowing the SH2 domain to dock to the C-lobe. Subsequently, the SH3 domain can dock to the N-lobe, disrupting the catalytic machinery located in the ATP-binding site and holding the kinase in an inactive state (Figure 1.10 (a)) [80-82].

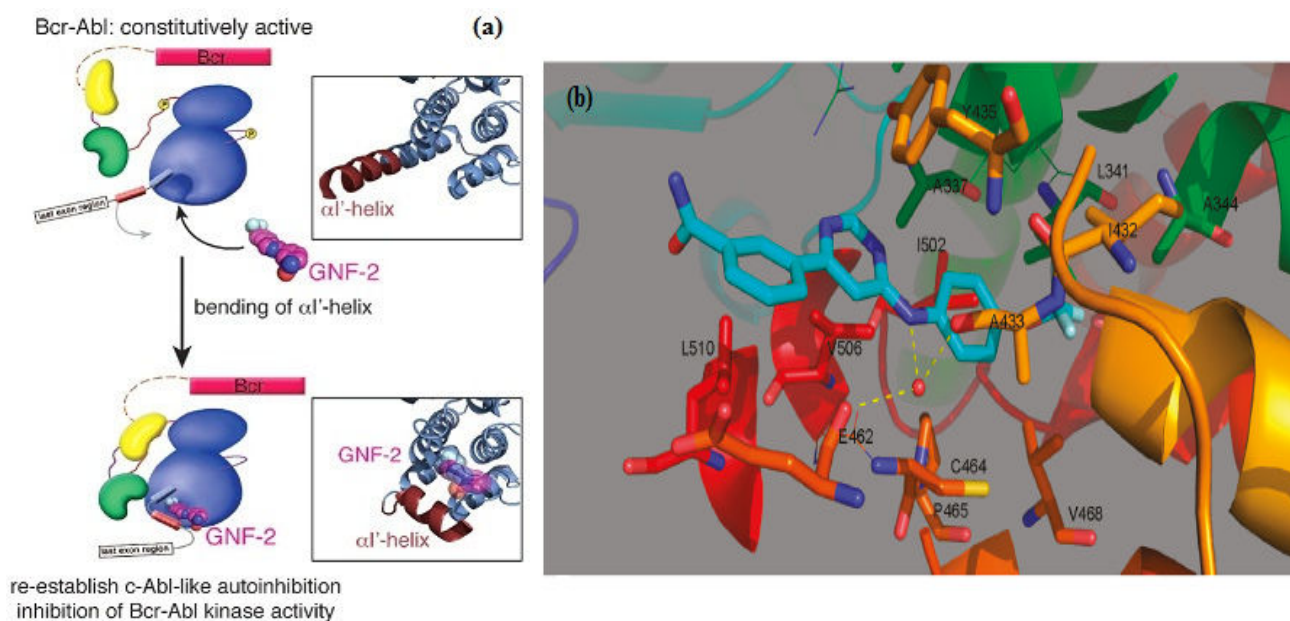


Figure 1.10:(a) Schematic representation of the mechanism of action of Bcr-Abl/c-Abl myristate pocket binders. The SH3, SH2 and kinase domains are shown in yellow, green and blue, respectively. The myristoyl group that is attached to the N-terminus of c-Abl binds to a deep hydrophobic pocket in the kinase domain and induces bending of the C-terminal α I'-helix (shown in dark red. Next to the schematic representations, a blow-up shows the myristate pocket from the crystal structures of the Abl kinase domain alone and in complex with myristate, GNF-2 [82], (b) Binding conformation of GNF-2 (cyan) in the myristate binding site of Abl (side chains from helix α E are green, α F orange, α I dark

orange, α I red). Hydrogen bonds to a water molecule (red sphere) are indicated by dashed yellow lines^[83].

The structure–activity relations done on GNF-2 showed that: The 4,6-pyrimidine substitution pattern is preferred over 2,4-substitution, and is strictly required to maintain cellular Bcr-Abl inhibitory activity by adopting the extended trans-conformation of the pyrimidine with the 4-trifluoromethoxyaniline pointed toward the bottom of the pocket.

The trifluoromethoxy group of GNF-2 can only be accommodated at the *para* position and it is an obligate; the aniline NH is required for the formation of a water-mediated hydrogen bond to the backbone carbonyls of A433 and E462; water-mediated hydrogen bonds between the carboxamide of GNF-2 which is pointed out toward the solvent exposed region and Abl confer enhanced inhibitory activity; and the extended compound conformation is required to fit the cylindrical binding cavity.

Residues making contact with GNF-2 at the base of the pocket are L341 and A344 from α E, I432 from α F, V468 from α H, F493 from α I, and I502 from α I'. The surface in the central part of the pocket is formed by A337 from α E, C464 and P465 from the start of α H, A433 from α F, and V506 from α I'.

Interactions at the mouth of the pocket are Y435 from α F, E462 from the loop before α H, and L510 at the end of α I', which are few and caused by the flexibility and slightly weaker electron density of the benzamide part of GNF-2, and this clarifies the diverse range of functionalities that can be incorporated into this position (Figure 1.10 (b)).

In addition, the compound did not exert inhibitory effect against other 40 kinases using cellular assays and 80 kinases using biochemical assays indicating the selective effect of GNF-2^[83, 84].

GNF-2 could inhibit the phosphorylation of Bcr–Abl in all mutants except the three myristate-site mutations (E505K, P465S and C464Y) that ablated the binding of Bcr–Abl to GNF-2 mainly for steric hindrance reason, and the ‘gatekeeper’ T315I mutation.

Fortunately, it was reported recently that GNF-2 suppresses Imatinib-resistant Bcr-Abl mutants in cooperative manner when co-administered with imatinib, where the number of resistant clones that emerged as a result of continuous exposure to 1 μ M imatinib was decreased by at least 90% when cells were treated for up to 21 days with 1 μ M imatinib combined with 5 or 10 μ M GNF-2 (Figure 1.11 (a))^[85, 86].

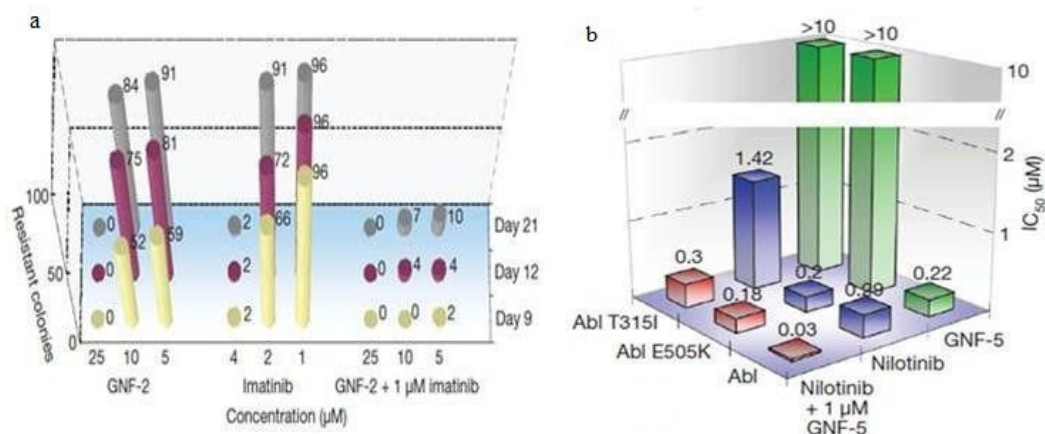


Figure 1.11: (a) Effect of various concentrations of GNF-2, imatinib, or combinations of both on the number of emerging Ba/F3 Bcr-Abl -resistant clones ^[84], **(b)** IC₅₀ for inhibition of wild-type, E505K and T315I Abl kinase activity by GNF-5, nilotinib or a combination of the two at an ATP concentration of 20 μM ^[84].

The N-hydroxyethyl carboxamide analogue of GNF-2, GNF-5 (Figure 1.8; **9**), is another example of this 4, 6-disubstituted pyrimidine series, with improved pharmacological profile. It was found that when GNF-5 is used in combination with the ATP-competitive inhibitors such as imatinib or nilotinib, it suppressed the emergence of resistance mutations *in-vitro*, displayed additive inhibitory activity in biochemical and cellular assays against T315I mutant Bcr-Abl and displayed *in-vivo* efficacy against this recalcitrant mutant and other mutants such E505K myristate mutant. Recently, Gray and his colleagues have shown that using a fixed GNF-5 concentration of 1 μM and an ATP concentration of 20 μM, will decrease the IC₅₀ values of nilotinib against T315I and wild-type enzyme by 4.7- and 9.6-fold, respectively, compared with those calculated in the absence of GNF-5 (Figure 1.11 **(b)**) ^[45, 84, 87].

The question is: How does binding in distant regions other than the ATP site influence kinase activity? How allosteric inhibitors can directly counteracts the effect of the mutation on the active-inactive kinase conformational equilibrium? And how these inhibitors could combine their effects?

One possible explanation is that GNF-2/5 binding to the myristate pocket stabilizes the inactive form of the T315I mutant and that this binding makes I315 no longer impeding ATP competitive inhibitors from accessing to the hydrophobic pocket.

Another recent research done by Gray and his colleagues using Hydrogen exchange (HX) mass spectrometry (MS) to study the conformational effects that result from binding of dasatinib and

GNF-5, both individually and in combination, to wild-type Abl core and a T315I mutant version of Abl core shows that, GNF-5 binding alters the dynamics properties of the ATP site in both wild type and T315I forms of Abl. GNF-5 restores the conformational changes that are seen when dasatinib binds to wild-type Abl. Residues located at positions 325–343 in the ATP site were most influenced by GNF-5 binding and the T315I mutation did not alter the ability of GNF-5 to elicit such changes.

These results show that allosteric interactions play a significant role in the Abl kinase downregulation and that combining allosteric and ATP-competitive inhibitors can provide a mechanism by which synergistic interactions between these two sites could occur and overcome resistance to either agent alone ^[88-90].

1.7 Objectives:

The major objective of this research is to explore the possibility of designing and synthesis of novel selective MBP inhibitors that will exert activity against Bcr-Abl expressing cells. Additional goal of the study will be to look for compounds that inhibit Imatinib resistant Bcr-Abl mutants.

Specific goals are:

- A) Design series of novel MBP inhibitors based on GNF-2 and GNF-5 scaffolds.
- B) Synthesize, purify, and characterize those analogues.
- C) Assess for the ability of newly synthesized compounds to interfere in the auto-phosphorylation Bcr-Abl and inhibit proliferation of Bcr-Abl transformed leukemia cells.
- D) Evaluate the ability of those new compounds to overcome the resistance emerging due to mutations at the Bcr-Abl kinase domain with special attention to the T315I gate-keeper mutation.

1.8 Research Questions:

Allosteric kinase inhibitors hold promise for revealing unique features of kinases that may not be apparent using conventional ATP-competitive inhibitors. Recent works demonstrated promising

lead compounds such as GNF-2/GNF-5 and derivatives that bind selectively to the MBP and inhibit cellular Bcr-Abl activity. The ability of these compounds to synergize with ATP-competitive inhibitors to inhibit the growth of cells transformed with Bcr-Abl mutants when combined with preventing or delaying the emergence of resistance is perceived as should encourage this new therapeutic modality to be our promising target. Hence the research questions of the proposal in hand will be:

Synthetic Question:

Would it be possible to synthesize GNF-2 and GNF-5 analogues based on 4,6-diaminopyrimidine derivatives that bind in higher affinity and improved selectivity to MBP in Bcr-Abl?

Structure-Activity Question:

Is it possible to explore 4,6-diaminopyrimidine scaffold to come up with new non-ATP competitors that inhibit Bcr-Abl via binding to MBP?

Would it be possible to overcome resistance rising due to mutations in the kinase domain by targeting the MBP in Bcr-Abl?

1.9 Significance of Proposed Research:

This research proposal constitutes a new potential approach to the treatment of CML and, if successful, could become complementary to the current methods of treatment mostly based on exploiting ATP-competitive inhibitors. It is hoped that such research would come out with novel molecular entities useful for studying several biomolecular systems in which myristoyl binding pocket is involved. It would be of value to define to what extent Abl and Bcr-Abl could be effectively inhibited by MBP binders that are remote from the active site of the kinases. Such effort will have implications to studies and plans for inhibitor development in other kinase studies.

Chapter Two

Experimental part

2. Experimental part:

2.1 Materials:

Chemicals: 4,6-dichloropyrimidine, *p*-trifluoromethoxyaniline, 4-fluoroaniline, 3,4-dimethoxybenzoic acid, 4-ethylbenzoic acid, 1-naphthoic acid, benzoyl chloride, oxalyl chloride, methyl sulfonyl chloride (mesyl chloride), *P*-toluene sulfonyl chloride (Tosyl chloride), 4-trifluoromethylbenzoic acid, biphenyl-4-carboxylic acid, benzofuran-2-carboxylic acid, 6-methoxybenzofuran-2-carboxylic acid, piperazine, phenyl-piperazine, piperazine-1-carboxylic acid *tert*-butyl ester (BOC-pz), 2-(1-piperazinyl) pyrimidine, 1-(4-pyridyl)piperazine, 1-(pyridin-2-yl)-piperazine, 1-(5-trifluoromethyl-pyridin-2-yl)-piperazine, 2-bromo-1-(2,3-dihydrobenzo{1,4}dioxin-6-yl)-ethanone, dicyclohexylcarbodiimide (DCC), *N*-hydroxysuccinimide (NHS), sodium sulfate (Na₂SO₄), diisopropylethylamine (DIPEA), potassium carbonate (K₂CO₃), calcium chloride (CaCl₂), potassium bromide (KBr), dimethylformamide (DMF), dichloromethane (DCM), ethyl acetate (EA), triethylamine (TEA), methanol (MeOH), ethanol (EtOH), hexane, isopropanol, chloroform (CHCl₃) and hydrochloric acid (HCl) were purchased from ACROS Chemicals Ltd, and were used without further purification.

Silica gel (Silica gel 60 (0.040-0.063 mm)), thin layer chromatography (TLC) (TLC Silica gel 60 F254) sheets were all purchased from Merck Ltd.

Deuterated solvents: D₂O, CDCl₃, DMSO-d₆ were purchased from ACROS Chemicals Ltd.

Commercially available starting materials including aromatic carboxylic acids [3,4-dimethoxybenzoic acid (**58**), 4-trifluoromethylbenzoic acid (**59**), 4-ethylbenzoic acid (**60**), 4-phenylbenzoic acid (**61**) and 1-naphthoic acid (**62**)] were all purchased and used with no further purification.

2.2 Instrumentation:

2.2.1 Nuclear magnetic resonance (¹H-, ¹³C-, COSY & HMBC NMR): Data were collected using Varian Unity Inova 500 MHz spectrometer equipped with a 5-mm switchable probe and data were processed using the VNMR software.

¹H-NMR chemical shifts are reported in parts per million (ppm, δ) downfield from tetramethylsilane (TMS). Spin multiplicities are described as s (singlet), brs (broad singlet), t (triplet), q (quartet), and m (multiplet).

2.2.2 Fourier transform infrared spectroscopy (FTIR): All infrared spectra were obtained from a KBr matrix (4000–400 cm^{-1}) using a Perkin-Elmer spectrum 100, FT-IR spectrometer.

2.2.3 Electrospray ionization mass spectrometry (ESIMS): Was performed using a Thermo Quest Finnigan LCQ-Duo in the positive ion mode.

Elution was in a mixture of 49:49:2 water/methanol/acetic acid at a flow rate of 15 $\mu\text{L}/\text{minute}$.

2.3 Synthetic Chemistry:

2.3.1 Synthesis of GNF-2 and GNF-5 analogues:

2.3.1.1 Synthesis of (6-chloro-pyrimidin-4-yl)-(4-trifluoromethoxy-phenyl)-amine (13):

In a 25 ml round bottom flask (1.0 g, 6.7 mmol) of 4,6-dichloropyrimidine (**10**) and (1.19 g, 6.7 mmol) of *p*-trifluoromethoxyaniline (**11**) were dissolved in 15 ml ethanol and 2 ml DIPEA (diisopropylethylamine), then the mixture was refluxed for 2 h and the reaction progress was followed using TLC (CHCl_3). When the reaction was completed ethanol was evaporated, and the crude product was purified by column chromatography using CHCl_3 to give 1.55 g of white fluffy powder. TLC (CHCl_3), $R_f = 5.8/8.2 = 0.71$; yield: 1.55 g (80%); ¹H-NMR 300 MHz (CDCl_3 , δ (ppm) 6.60-6.70 (s, 1H), 6.90-7.00 (s, 1N-H amide), 7.30-7.35 (d, 2H), 7.35-7.45 (d, 2H), 8.45-8.55 (s, 1H).

2.3.1.2 Synthesis of [6-(4-phenyl-piperazin-1-yl)-pyrimidin-4-yl]-(4-trifluoromethoxy-phenyl)-amine {MYJ-1 (20)}:

In a 25 ml round bottom flask (0.5 g, 1.7 mmol) of (6-chloro-pyrimidin-4-yl)(4-trifluoromethoxy-phenyl)-amine (**13**) and (0.28 g, 0.26 ml, 1.7 mmol) of phenylpiperazine (**36**)

and (0.24 g, 1.7 mmol) of K_2CO_3 were dissolved in 10 ml DMF, the reaction mixture was refluxed at 100 °C for 12 h and the completion of the reaction was indicated by TLC ($CHCl_3$).

When the reaction was completed the DMF was evaporated to dryness, and the crude product was purified by column chromatography using $CHCl_3$:hexane (50:50; v:v) to give 0.37 g brownish powder. TLC ($CHCl_3$), $R_f = 5.1/7.8 = 0.65$; yield: 0.37g (52%); 1H -NMR 300 MHz ($CDCl_3$, δ (ppm) 3.20-3.30 (m, 4H), 3.55-3.75 (m, 4H), 5.80-5.90 (d, 1H), 6.85-6.95 (m, 4H), 7.20-7.30 (m, 5H), 7.24 (s, 1H amine), 8.25-8.35 (s, 1H); FT-IR (KBr) (cm^{-1}): 3310.5 (N-H) stretching, 3072.9 Ar-H (C-H stretch), 2925.5, 2817.1 CH_2 , CH_3 (C-H stretch), 1601.2, 1575.8 & 1496.8 (C=C) aromatic & (C=N) stretching, 1440.5, 1409.1, 1382.8 & 1332.8 (C-H) bending, 873.5, 690.2, 661.3 & 562.3 Ar-H ($H_2C=CH_2$ bending).

2.3.1.3 Synthesis of 4-[6-(4-trifluoromethoxyphenylamino)-pyrimidin-4-yl]-piperazine-1-carboxylic acid *tert*-butyl ester {MYJ-2 (16)}:

In a 25 ml round bottom flask (0.5 g, 1.7 mmol) of (6-chloro-pyrimidin-4-yl)(4-trifluoromethoxy-phenyl)-amine (**13**) and (0.32 g, 1.7 mmol) of piperazine-1-carboxylic acid *tert*-butyl ester (**15**) and (0.24 g, 1.7 mmol) of K_2CO_3 were dissolved in 10 ml DMF, the reaction mixture was refluxed at 100 °C for 12 h and the completion of the reaction was indicated by TLC ($CHCl_3$). When the reaction was completed the DMF was evaporated to dryness the crude product was purified by column chromatography using $CHCl_3$:hexane (50: 50; v:v) to give 0.44 g yellowish powder. TLC ($CHCl_3$), $R_f = 4.6/7.9 = 0.58$; yield: 0.44 g (58%); 1H -NMR 300 MHz ($CDCl_3$, δ ppm) 1.40-1.50 (s, 9H), 3.45-3.55 (dd, 8H), 5.80-5.85 (s, 1H), 7.20-7.30 (d, 2H), 7.25-7.35 (d, 2H), 7.50-7.70 (s, 1H), 8.20-8.30 (s, 1 N-H amine); FT-IR (KBr) (cm^{-1}): 3341 (N-H) stretching, 1590.4 (C=O), 1365.5 (C-H) bending, 792.1, 661.4 Ar-H ($H_2C=CH_2$ bending).

2.3.1.4 Synthesis of (6-piperazin-1-yl-pyrimidin-4-yl)-(4-trifluoromethoxy-phenyl)-amine acidic salt (18):

In a 25 ml round bottom flask (0.5 g, 1.7 mmol) of (6-chloro-pyrimidin-4-yl)-(4-trifluoromethoxy-phenyl)-amine (**13**) and (0.32 g, 1.7 mmol) of piperazine-1-carboxylic acid *tert*-butyl ester (**15**) and (0.24 g, 1.7 mmol) of K_2CO_3 were dissolved in 10 ml DMF, the reaction

mixture was refluxed at 100 °C for 12 h and the completion of the reaction was indicated by TLC (CHCl₃). When the reaction was completed the DMF was evaporated to dryness the crude product was purified by column chromatography using CHCl₃:hexane (50:50; v:v) to give 0.44 g yellowish powder.

The obtained pure powder {MYJ-2 (**16**)}, was then dissolved in (15 ml) EtOH and acidified by 0.5 ml conc HCl and stirred for 1 h. Then the mixture was allowed to cool in ice-bath overnight, and the precipitate was filtered off. The precipitate was washed with additional 10 ml ethanol and filtrates were collected and evaporated to dryness to give a white precipitate of corresponding (6-piperazin-1-yl-pyrimidin-4-yl)-(4-trifluoromethoxy-phenyl)-amine hydrochloride salt (**18**). TLC (EA: MeOH (90:10; v:v)), R_f = 1.5/7.9 = 0.19; yield: 0.39 g (75%); ¹H-NMR 300 MHz (DMSO-d₆), δ (ppm), 3.15-3.20 (s, 4H), 3.85-3.90 (s, 4H), 6.10 (s, 1H), 7.30-7.40 (dd, 2H), 7.55-7.65 (dd, 2H), 8.40-8.45 (s, 1H), 9.50-9.80 (s, 1H amine), 10.35-10.75 (s, 1H amine).

2.3.1.5 Preparation of aromatic acyl halides:

Under calcium chloride tube, aromatic fatty acid was dissolved in dry DCM (20 ml) and cooled in ice-bath to -5 °C. While stirring at r.t, two equivalents of oxalyl chloride were added. Gas bubbles were evolved to indicate the release of gaseous CO₂ and HCl. The progress of the reaction was followed by TLC (CHCl₃ or EA). When the reaction was over, the volatiles were removed to dryness under reduced pressure leaving the desired product.

2.3.1.5.1 Benzoyl chloride (21):

TLC (CHCl₃), R_f = 6.8/8.0 = 0.85; commercially available; ¹H-NMR (CDCl₃, δ ppm): 7.45-7.50 (m, 2H), 7.55-7.60 (m, 1H), 7.95-7.80 (d, 2H).

2.3.1.5.2 3, 4-Dimethoxybenzoyl chloride (22):

TLC (EA), R_f = 4.9/7.8 = 0.63; yellowish solid; yield: 1.057 g (96%); ¹H-NMR (CDCl₃, δ ppm): 3.75 (q, 6H), 6.77 (d, 1H), 7.48 (d, 1H), 7.49 (d, 1H).

2.3.1.5.3 4-Trifluoromethylbenzoyl chloride (23):

TLC (EA), $R_f = 3.4/7.8 = 0.44$; yellowish solid; yield: 0.213 g (97%); $^1\text{H-NMR}$ (CDCl_3 , δ ppm): 7.65 (d, 2H), 8.01 (d, 2H).

2.3.1.5.4 4-Ethylbenzoyl chloride (24):

TLC (CHCl_3), $R_f = 6.6/8.0 = 0.83$; yellowish liquid; yield: 0.321 g (95%); $^1\text{H-NMR}$ (CDCl_3 , δ ppm): 1.24 (t, 3H), 2.59 (q, 2H), 7.33 (d, 2H), 8.02 (d, 2H).

2.3.1.5.5 4-Phenylbenzoyl chloride (25):

TLC (CHCl_3), $R_f = 6.7/8.0 = 0.84$; yellowish-white solid; yield: 1.057 g (96%); $^1\text{H-NMR}$ (CDCl_3 , δ ppm): 7.22 (d, 1H), 7.29 (d, 2H), 7.50 (d, 2H), 7.66 (d, 2H), 8.12 (d, 2H).

2.3.1.5.6 1-Naphthoyl chloride (54):

TLC (CHCl_3), $R_f = 6.5/7.9 = 0.82$; green-white solid; yield: 1.169 g (96%); $^1\text{H-NMR}$ (CDCl_3 , δ ppm): 7.50 (d, 1H), 7.57 (d, 1H), 7.65 (d, 1H), 7.86 (d, 1H), 8.04 (d, 1H), 8.51 (d, 1H), 8.74 (d, 1H).

2.3.1.6 Synthesis of (3,4-dimethoxy-phenyl)-{4-[6-(4-trifluoromethoxy-phenylamino)-pyrimidin-4-yl]-piperazin-1-yl}-methanone {MYJ-16 (28)}:

In a 25 ml round bottom flask (200 mg, 0.38 mmol) of (6-piperazin-1-yl-pyrimidin-4-yl)-(4-trifluoromethoxy-phenyl)-amine acidic salt (**18**), and 7.0 eq TEA (0.37 ml, 2.66 mmol) were dissolved in 10 ml DMF and cooled to 0 °C. (76.9 mg, 0.38 mmol) of 3,4-dimethoxy-benzoyl chloride (**22**) was then added to the reaction mixture and stirred for 48 h. The completion of the reaction was indicated by TLC (EA), when the reaction was completed the DMF was evaporated to dryness and crude product was extracted by EA against distilled basic water. The organic

phase was dried over Na₂SO₄ and the solvent was removed under reduced pressure. The desired product was purified by column chromatography using CHCl₃:hexane (70:30; v:v), to give 86.7 mg off-white powder.

TLC (EA), R_f = 4.6/8.4 = 0.55; yield: 0.087 g (44.9%); ¹H-NMR 300 MHz (DMSO-d₆), δ (ppm) 3.50-3.60 (s, 8H), 3.75-3.85 (d, 6H), 5.95-6.00 (s, 1H), 7.00-7.02 (d, 2H), 7.01-7.03 (s, 1H), 7.20-7.30 (d, 2H), 7.65-7.75 (d, 2H), 8.20-8.25 (s, 1H), 9.20-9.30 (s, 1 N-H amine); ¹³C{¹H}-NMR (DMSO-d₆, δ ppm), 169.92, 162.69, 161.38, 157.96, 150.55, 149.04, 142.87, 140.80, 128.40, 122.25, 120.86, 120.74, 111.71, 85.48, 56.21.

The ¹H-¹H correlation spectroscopy (COSY) NMR spectral revealed only two cross-peaks: H (3, 3')/H (4, 4') and H (4, 4')/H (3, 3').

HMBC spectrum showed many informative correlations, such as: δ_H 7.65-7.75 (2H, d, H-3, 3') to C(2), C(4), C(4') and C(5); δ_H 7.20-7.30 (2H, d, H-4, 4') to C(2), C(3), C(3') and C(5); δ_H 9.20-9.30 (1H, s, H-6) to C(4), C(4'), C(7) and C(8); δ_H 5.95-6.00 (1H, s, H-8) to C(6), C(7) and C(9); δ_H 8.20-8.25 (1H, s, H-10) to C(7) and C(9); δ_H 3.50-3.60 (8H, s, H-11, 11') to C(12) and C(12'); δ_H 3.50-3.60 (8H, s, H-12, 12') to C(11) and C(11'); δ_H 7.01-7.03 (1H, s, H-15) to C(13), C(14), C(16), C(17) and C(18); δ_H 7.00-7.02 (2H, d, H-18) to C(14), C(16), C(17) and C(19); δ_H 7.00-7.02 (2H, d, H-19) to C(14), C(15), C(17) and C(18) (Figure 2.1, Table 2.1).

FT-IR (KBr) (cm⁻¹): 3322.6 & 3197.4 (N-H) stretching, 3012.5 Ar-H (C-H stretch), 2965 & 2860.4 CH₂, CH₃ (C-H stretch), 1602 (C=O), 1510.5 (C=C) aromatic & (C=N) stretching, 1434, 1381.4, 1333.2 & 1301 (C-H) bending, 856.7, 701.5 & 653.1 Ar-H (H₂C=CH₂ bending).

MS (ESI) m/z calculated for C₂₄H₂₄F₃N₅O₄ 503.47, found 504.11 (M +H)⁺.

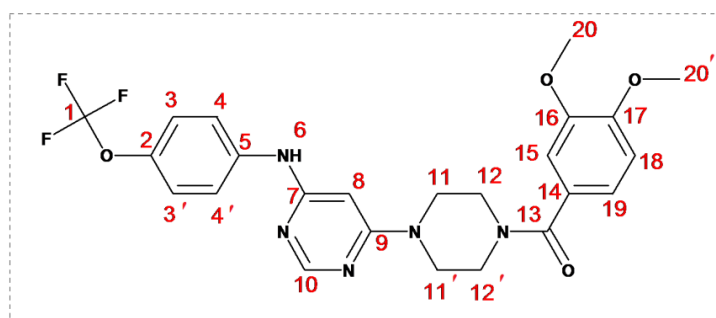


Figure 2.1: Chemical structure of **28**.

Table 2.1: NMR data of compound **28**:

Positions	¹ H-NMR (ppm)	¹³ C-NMR (ppm)	¹ H- ¹ H COSY	¹ H- ¹³ C HMBC
1	-	122.25 (C)	-	
2	-	140.80 (C)	-	
3, 3 ✓	7.65-7.75 (d, 2H)	120.86 (CH)	4, 4 ✓	C(2), C(4),C(4 ✓), C(5)
4, 4 ✓	7.20-7.30 (d, 2H)	120.86 (CH)	3, 3 ✓	C(2), C(3), C(3 ✓), C(5)
5	-	142.78 (C)	-	
6	9.20-9.30 (s, 1H)	-	-	C(4), C(4'), C(7), C(8)
7	-	161.38 (C)	-	
8	5.95-6.00 (s, 1H)	85.48 (CH)	-	C(6), C(7), C(9)
9	-	162.69 (C)	-	
10	8.20-8.25 (s, 1H)	157.96 (CH)	-	C(7), C(9)
11, 11 ✓	3.50-3.60 (s, 8H)	56.21 (CH ₂)	-	C(12), C(12 ✓)
12, 12 ✓	3.50-3.60 (s, 8H)	56.21 (CH ₂)	-	C(11), C(11 ✓)
13	-	169.92 (C)	-	
14	-	128.40 (C)	-	
15	7.01-7.03 (s, 1H)	111.71 (CH)	-	C(13), C(14), C(16), C(17), C(18)
16	-	150.55 (C)	-	
17	-	150.55 (C)	-	
18	7.00-7.02 (d, 2H)	111.71 (CH)	-	C(14), C(16), C(17), C(19)
19	7.00-7.02 (d, 2H)	120.74 (CH)	-	C(14), C(15), C(17), C(18)
20, 20 ✓	3.75-3.85 (d, 6H)	149.04 (CH ₃)	-	

2.3.1.7 Synthesis of 1-(2,3-dihydro-benzo[1,4]dioxin-6-yl)-2-{4-[6-(4-trifluoromethoxy-phenylamino)-pyrimidin-4-yl]-piperazin-1-yl}-ethanone {MYJ-17 (**29**)}

In a 25 ml round bottom flask (200 mg, 0.38 mmol) of (6-piperazin-1-yl-pyrimidin-4-yl)-(4-trifluoromethoxy-phenyl)-amine acidic salt (**18**), and 7.0 eq TEA (0.37 ml, 2.66 mmol) were dissolved in 10 ml DMF and cooled to 0 °C. (97.7 mg, 0.38 mmol) of 2-bromo-1-(2,3-dihydro-benzo[1,4]dioxin-6-yl)-ethanone (**26**) was then added to the reaction mixture and stirred for 6 h. The completion of the reaction was indicated by TLC (CHCl₃), when the reaction was completed

the DMF was evaporated to dryness and the crude product was extracted by CHCl_3 against distilled water. The organic phase was dried over Na_2SO_4 and the solvent was removed under reduced pressure. The desired product was purified by column chromatography using CHCl_3 :hexane (50:50; v:v) to give 80 mg of yellow to brown powder. TLC (CHCl_3), $R_f = 4.2/8.4 = 0.5$; yield: 0.08 g (41%); $^1\text{H-NMR}$ 300 MHz (DMSO-d_6), δ (ppm) 3.05-3.10 (s, 2H), 3.45 (t, 2H), 3.61 (t, 2H), 3.71 (t, 2H), 3.83 (t, 2H), 4.30-4.40 (dd, 4H), 5.85 (s, 1H), 6.95-7.00 (d, 1H), 7.10 (s, 1H amine), 7.20-7.25 (d, 2H), 7.28 (s, 1H), 7.35-7.40 (d, 2H), 7.50 (d, 1H), 8.25-8.30 (s, 1H); FT-IR (KBr) (cm^{-1}): 3359.9 (N-H) stretching, 2923.9 CH_2 , CH_3 (C-H stretch), 1588.4 (C=O), 1508.6 (C=C) aromatic & (C=N) stretching, 1379.3, 1260.2 (C-H) bending, 1103.6, 800 & 638.2 Ar-H ($\text{H}_2\text{C}=\text{CH}_2$ bending).

2.3.1.8 Synthesis of phenyl-{4-[6-(4-trifluoromethoxy-phenylamino)-pyrimidin-4-yl]-piperazin-1-yl}-methanone {MYJ-18 (30)}:

In a 25 ml round bottom flask (200 mg, 0.38 mmol) of (6-piperazin-1-yl-pyrimidin-4-yl)-(4-trifluoromethoxy-phenyl)-amine acidic salt (**18**), and 7.0 eq TEA (0.37 ml, 2.66 mmol) were dissolved in 10 ml DMF and cooled to 0 °C. (53.4 mg, 0.044 ml, 0.38 mmol) of benzoyl chloride (**21**) was then added to the reaction mixture and stirred for 48 h. The completion of the reaction was indicated by TLC (EA), when the reaction was completed the DMF was evaporated to dryness and crude product was extracted by EA against distilled basic water. The organic phase was dried over Na_2SO_4 and the solvent was removed under reduced pressure. The crude product was purified by column chromatography using CHCl_3 :hexane (50:50; v:v) to give compound **30** with a little impurity, which was followed by re-crystallization using isopropanol as solvent to afford 0.0884 g off-white powder of desired product. TLC (EA), $R_f = 4.2/7.5 = 0.56$; yield: 0.0884 g (52%); $^1\text{H-NMR}$ 300 MHz (CDCl_3) δ (ppm) 3.65-3.75 (d, 8H), 5.85-5.90 (s, 1H), 7.25 (d, 2H), 7.36 (d, 2H), 7.55-7.60 (t, 1H), 7.46 (m, 4H), 8.25-8.30 (s, 1H), 8.70-8.75 (s, 1H amine); FT-IR (KBr) (cm^{-1}): 3332.0 & 3231.1 (N-H) stretching, 2964.3 & 2853.9 CH_2 , CH_3 (C-H stretch), 1600.5 (C=O), 1509.0 (C=C) aromatic & (C=N) stretching, 1453.8 & 1361.6 (C-H) bending, 977.2, 926.0, 804.0 & 709.1 Ar-H ($\text{H}_2\text{C}=\text{CH}_2$ bending); MS (ESI) m/z calculated for $\text{C}_{22}\text{H}_{20}\text{F}_3\text{N}_5\text{O}_2$ 443.42, found 444.47 (M +H)⁺.

2.3.1.9 Synthesis of {4-[6-(4-trifluoromethoxy-phenylamino)-pyrimidin-4-yl]-piperazin-1-yl}-(4-trifluoromethyl-phenyl)-methanone {MYJ-19 (31)}:

In a 25 ml round bottom flask (200 mg, 0.38 mmol) of (6-piperazin-1-yl-pyrimidin-4-yl)-(4-trifluoromethoxy-phenyl)-amine acidic salt (**18**), and 7.0 eq TEA (0.37 ml, 2.66 mmol) were dissolved in 10 ml DMF and cooled to 0 °C. (79.3 mg, 0.38 mmol) of 4-trifluoromethylbenzoyl chloride (**23**) was then added to the reaction mixture and stirred for 6 h. The completion of the reaction was indicated by TLC (EA), when the reaction was completed the DMF was evaporated to dryness and crude product was extracted by EA against distilled water. The organic phase was dried over Na₂SO₄ and the solvent was removed under reduced pressure. The desired product was purified by column chromatography using CHCl₃:hexane (50:50; v:v) to give 0.128 g brownish powder. TLC (EA), R_f = 4.7/7.5 = 0.63; yield: 0.128 g (65%); ¹H-NMR 300 MHz (CDCl₃) δ (ppm) 3.65-3.70 (t, 8H), 5.85-5.90 (s, 1H), 7.10 (s, 1H amine), 7.23 (d, 2H), 7.35 (d, 2H), 7.56 (d, 2H), 7.72 (d, 2H), 8.25-8.30 (s, 1H); FT-IR (KBr) (cm⁻¹): 3238.5 & 3345.5 (N-H) stretching, 2852.7 CH₂, CH₃ (C-H stretch), 1629.7 (C=O), 1587, 1509 (C=C) aromatic & (C=N) stretching, 1440.5, 1408.3 & 1384 (C-H) bending, 1001.7, 847.7 & 765.8 Ar-H (H₂C=CH₂ bending); MS (ESI) m/z calculated for C₂₃H₁₉F₆N₅O₂ 511.42, found 512.16 (M +H)⁺.

2.3.1.10 Synthesis of [6-(4-methanesulfonyl-piperazin-1-yl)-pyrimidin-4-yl]-(4-trifluoromethoxy-phenyl)-amine {MYJ-20 (32)}:

In a 25 ml round bottom flask (200 mg, 0.38 mmol) of (6-piperazin-1-yl-pyrimidin-4-yl)-(4-trifluoromethoxy-phenyl)-amine acidic salt (**18**), and 7.0 eq TEA (0.37 ml, 2.66 mmol) were dissolved in 10 ml DMF and cooled to 0 °C. (43.9 mg, 0.38 mmol) of methyl sulfonyl chloride (mesyl chloride) (**27**) was then added to the reaction mixture and stirred for 24 h. The completion of the reaction was indicated by TLC (EA), when the reaction was completed the DMF was evaporated to dryness and crude product was extracted by EA against distilled water. The organic phase was dried over Na₂SO₄ and the solvent was removed under reduced pressure. The desired product was purified by column chromatography using CHCl₃ to give 0.144 g off-white to beige powder. TLC (EA), R_f = 4.7/7.6 = 0.62; yield: 0.144 g (91%); ¹H-NMR 300 MHz (DMSO-d₆), δ (ppm), 2.85-2.95 (s, 3H), 3.20-3.30 (t, 4H), 3.60-3.70 (t, 4H), 6.00-6.05 (s, 1H),

7.20-7.30 (d, 2H), 7.65-7.75 (d, 2H), 8.20-8.25 (s, 1H), 9.25-9.35 (s, 1 N-H amine); $^{13}\text{C}\{^1\text{H}\}$ -NMR ((DMSO- d_6 , δ ppm), 165.01, 145.11, 142.67, 125.06, 124.12, 123.99, 123.68, 122.59, 122.15, 88.51, 48.83, 47.78, 37.45; FT-IR (KBr) (cm^{-1}): 2964.7 Ar-H (C-H stretch), 1585, 1504.5 (C=C) aromatic & (C=N) stretching, 1457.8, 1360.9 (C-H) bending, 796, 694.3 & 634.9 Ar-H ($\text{H}_2\text{C}=\text{CH}_2$ bending); MS (ESI) m/z calculated for $\text{C}_{16}\text{H}_{18}\text{F}_3\text{N}_5\text{O}_3\text{S}$ 417.41, found 418.15 (M + H) $^+$.

2.3.1.11 Synthesis of biphenyl-4-yl-{4-[6-(4-trifluoromethoxy-phenylamino)-pyrimidin-4-yl]-piperazin-1-yl}-methanone {MYJ-21 (33)}:

In a 25 ml round bottom flask (200 mg, 0.38 mmol) of (6-piperazin-1-yl-pyrimidin-4-yl)-(4-trifluoromethoxy-phenyl)-amine acidic salt (**18**), and 7.0 eq TEA (0.37 ml, 2.66 mmol) were dissolved in 10 ml DMF and cooled to 0 °C. (83.1 mg, 0.38 mmol) of biphenyl-4-carbonyl chloride (**25**) was then added to the reaction mixture and stirred for 24 h. The completion of the reaction was indicated by TLC (EA), when the reaction was completed the DMF was evaporated to dryness and crude product was extracted by EA against distilled water. The organic phase was dried over Na_2SO_4 and the solvent was removed under reduced pressure. The desired product was purified by column chromatography using CHCl_3 to give 0.186 g of beige powder. TLC (EA), $R_f = 4.4/7.6 = 0.58$; yield: 0.186 g (93%); ^1H -NMR 300 MHz (DMSO- d_6), δ (ppm), 3.60-3.65 (d, 8H), 5.95-6.00 (s, 1H), 7.20-7.30 (d, 2H), 7.40-7.45 (t, 1H), 7.50-7.55 (t, 2H), 7.55-7.60 (d, 2H), 7.70-7.75 (m, 4H), 7.75-7.80 (d, 2H), 8.20-8.25 (s, 1H), 9.25-9.35 (s, 1 N-H amine); FT-IR (KBr) (cm^{-1}): 3330.5, 3230.7 (N-H) stretching, 2964.3 CH_2 , CH_3 (C-H stretch), 1617 (C=O), 1509 (C=C) aromatic & (C=N) stretching, 1425.6 & 1362.1 (C-H) bending, 977.5, 849.5 & 695.9 Ar-H ($\text{H}_2\text{C}=\text{CH}_2$ bending).

2.3.1.12 Synthesis of (4-ethyl-phenyl)-{4-[6-(4-trifluoromethoxy-phenylamino)-pyrimidin-4-yl]-piperazin-1-yl}-methanone {MYJ-23 (35)}:

In a 25 ml round bottom flask (200 mg, 0.38 mmol) of (6-piperazin-1-yl-pyrimidin-4-yl)-(4-trifluoromethoxy-phenyl)-amine acidic salt (**18**), and 7.0 eq TEA (0.37 ml, 2.66 mmol) were dissolved in 10 ml DMF and cooled to 0 °C. (64.1 mg, 0.056 ml, 0.38 mmol) of 4-ethylbenzoyl

chloride (**24**) was then added to the reaction mixture and stirred for 24 h. The completion of the reaction was indicated by TLC (EA), when the reaction was completed the DMF was evaporated to dryness and crude product was extracted by EA against distilled water. The organic phase was dried over Na₂SO₄ and the solvent was removed under reduced pressure. The desired product was purified by column chromatography using CHCl₃: EA (80:20; v:v) to give 0.172 g as off-white powder. TLC (EA), R_f = 4.6/7.7 = 0.6; yield: 0.172 g (95%); ¹H-NMR 300 MHz (DMSO-d₆), δ (ppm) 1.15 (t, 3H), 2.60-2.65 (q, 2H), 3.55 (s, 8H), 5.94 (s, 1H), 7.25-7.30 (dd, 4H), 7.30-7.35 (dd, 2H), 7.65-7.70 (dd, 2H), 8.20-8.25 (s, 1H), 9.30-9.35 (s, 1 N-H amine); FT-IR (KBr) (cm⁻¹): 3330.5 & 3231 (N-H) stretching, 2965.2 CH₂, CH₃ (C-H stretch), 1683.7, 1617.5 (C=O), 1508 (C=C) aromatic & (C=N) stretching, 1427, 1361.6 (C-H) bending, 693.9, 637.4, 606.8 & 509.9 Ar-H (H₂C=CH₂ bending).

2.3.1.13 Synthesis of naphthalen-1-yl-{4-[6-(4-trifluoromethoxy-phenylamino)-pyrimidin-4-yl]-piperazin-1-yl}-methanone {MYJ-25 (57)}:

In a 25 ml round bottom flask (200 mg, 0.38 mmol) of (6-piperazin-1-yl-pyrimidin-4-yl)-(4-trifluoromethoxy-phenyl)-amine acidic salt (**18**), and 7.0 eq TEA (0.37 ml, 2.66 mmol) were dissolved in 10 ml DMF and cooled to 0 °C. (73.1 mg, 0.38 mmol) of 1-naphthoyl chloride (**54**) was then added to the reaction mixture and stirred for 24 h. The completion of the reaction was indicated by TLC (EA), when the reaction was completed the DMF was evaporated to dryness and crude product was extracted by EA against distilled water. The organic phase was dried over Na₂SO₄ and the solvent was removed under reduced pressure. The desired product was purified by column chromatography using CHCl₃:EA (70:30; v:v), and finally afforded by recrystallization using isopropanol as eluent to give 0.122 g of brownish desired precipitate. TLC (EA), R_f = 4.8/7.8 = 0.62; yield: 0.122 g (64.9%); ¹H-NMR 300 MHz (DMSO-d₆), δ (ppm), 3.20-3.38 (t, 4H), 3.70-3.90 (t, 4H), 5.90-5.95 (s, 1H), 7.20-7.25 (dd, 2H), 7.45-7.55 (dd, 2H), 7.55-7.60 (dd, 2H), 7.65-7.70 (dd, 2H), 7.80 (m, 1H), 7.95-7.99 (d,1H), 7.99-8.10 (d,1H), 8.20-8.25 (s, 1H), 9.25-9.30 (s, 1 N-H amine); FT-IR (KBr) (cm⁻¹): 3328.3, 3236.8 & 3198 (N-H) stretching, 3133.1 Ar-H (C-H stretch), 3012.8, 2901.5 & 2855.2 CH₂, CH₃ (C-H stretch), 1805.7, 1633.5 & 1620.6 (C=O), 1589.9 & 1507.9 (C=C) aromatic & (C=N) stretching, 1412.7, 1393.3 & 1361.3 (C-H) bending, 949.6, 871.1 & 733.2 Ar-H (H₂C=CH₂ bending).

2.3.1.14 Synthesis of {6-[4-(toluene-4-sulfonyl)-piperazin-1-yl]-pyrimidin-4-yl}-(4-trifluoromethoxy-phenyl)-amine {MYJ-26 (56)}:

In a 25 ml round bottom flask (200 mg, 0.38 mmol) of (6-piperazin-1-yl-pyrimidin-4-yl)-(4-trifluoromethoxy-phenyl)-amine acidic salt (**18**), and 7.0 eq TEA (0.37 ml, 2.66 mmol) were dissolved in 10 ml DMF and cooled to 0 °C. (72.4 mg, 0.38 mmol) of P-toluene sulfonyl chloride (tosyl chloride) (**55**) was then added to the reaction mixture and stirred for 24 h. The completion of the reaction was indicated by TLC (EA), when the reaction was completed the DMF was evaporated to dryness and crude product was extracted by EA against distilled water. The organic phase was dried over Na₂SO₄ and the solvent was removed under reduced pressure. The desired product was finally obtained by re-crystallization using isopropanol as solvent to give 0.150 g of brownish solid. TLC (EA), R_f = 5.1/8.0 = 0.64; yield: 0.150 g (80.2%); ¹H-NMR 300 MHz (DMSO-d₆), δ (ppm), 2.90-2.95 (t, 4H), 3.55-3.60 (t, 4H), 5.90-5.95 (s, 1H), 7.20-7.25 (d, 2H), 7.40-7.45 (d, 2H), 7.60-7.65 (m, 5H), 8.15-8.20 (s, 1H), 9.25-9.35 (s, 1 N-H amine); FT-IR (KBr) (cm⁻¹): 3375, 3231 & 3192 (N-H) stretching, 3125 Ar-H (C-H stretch), 2968, 2846 & 2738.4 CH₂, CH₃ (C-H stretch), 1625, 1592 & 1510.1 (C=C) aromatic & (C=N) stretching, 1446, 1428 & 1328.8 (C-H) bending, 917.3, 897.2, 706.4 & 668.4 Ar-H (H₂C=CH₂ bending).

2.3.1.15 Synthesis of (6-chloro-pyrimidin-4-yl)-(4-fluoro-phenyl)-amine (**14**):

In a 25 ml round bottom flask (1.0 g, 6.7 mmol) of 4,6-dichloropyrimidine (**10**) and (0.64 ml, 6.7 mmol) of 4-fluoroaniline (**12**) were dissolved in 15 ml ethanol and 2 ml DIPEA (diisopropylethylamine), then the mixture was refluxed for 2 h and the reaction progress was followed using TLC (CHCl₃). When the reaction was completed ethanol was evaporated under reduced pressure, and the crude solid was washed with additional 10 ml ethanol and evaporated to dryness using suction filtration to give a white solid of corresponding amine. TLC (CHCl₃), R_f = 5.9/8.1 = 0.73; yield: 1.27 g (85%); ¹H-NMR 300 MHz (DMSO-d₆), δ (ppm) 6.75-6.80 (s, 1H), 7.20 (dd, 2H), 7.63 (dd, 2H), 8.45-8.50 (s, 1H), 9.90-9.95 (s, 1H amine).

2.3.1.16 Synthesis of (6-piperazin-1-yl-pyrimidin-4-yl)-(4-fluoro-phenyl)-amine acidic salt (19):

In a 25 ml round bottom flask (0.5 g, 2.24 mmol) of (6-chloro-pyrimidin-4-yl)-(4-fluoro-phenyl)-amine (14) and (0.42 g, 2.24 mmol) of piperazine-1-carboxylic acid *tert*-butyl ester (15) and (0.31 g, 2.24 mmol) of K₂CO₃ were dissolved in 10 ml DMF, the reaction mixture was refluxed at 100 °C for 12 h and the completion of the reaction was indicated by TLC (CHCl₃).

When the reaction was completed the DMF was evaporated to dryness and the crude product was purified by column chromatography using CHCl₃:hexane (50:50; v:v) to give 0.40 g of yellowish powder of 4-[6-(4-fluoro-phenylamino)-pyrimidin-4-yl]-piperazine-1-carboxylic acid *tert*-butyl ester (17).

The obtained pure powder was then dissolved in (15 ml) EtOH and acidified by 0.5 ml conc HCl and stirred for 1 h. The mixture was then allowed to cool in ice-bath overnight (refrigerator), and the precipitate was filtered off. The precipitate was washed with additional 10 ml ethanol and filtrates were collected and evaporated to dryness to give a white solid.

TLC (EA: MeOH (90:10; v:v)), R_f = 1.6/8.1 = 0.2; yield: 0.39 g (80%); ¹H-NMR 300 MHz (DMSO-d₆), δ (ppm) 3.15-3.20 (s, 4H), 3.85-3.90 (s, 4H), 6.10 (s, 1H), 7.25-7.30 (dd, 2H), 7.45-7.50 (dd, 2H), 8.40-8.45 (s, 1H), 9.50-9.80 (s, 1H amine), 10.35-10.75 (s, 1H amine).

2.3.1.17 Synthesis of (3,4-dimethoxy-phenyl)-{4-[6-(4-fluoro-phenylamino)-pyrimidin-4-yl]-piperazin-1-yl}-methanone {MYJ-22 (34)}:

In a 25 ml round bottom flask (200 mg, 0.44 mmol) (6-piperazin-1-yl-pyrimidin-4-yl)-(4-fluoro-phenyl)-amine acidic salt (19), and 7.0 eq TEA (0.43 ml, 3.07 mmol) were dissolved in 10 ml DMF and cooled to 0 °C. (88.3 mg, 0.44 mmol) of 3,4-dimethoxy-benzoyl chloride (22) was then added to the reaction mixture and stirred for 48 h. The completion of the reaction was indicated by TLC (EA), when the reaction was completed the DMF was evaporated to dryness and crude product was extracted by EA against distilled basic water. The organic phase was dried over Na₂SO₄ and the solvent was removed under reduced pressure. The desired product was purified by column chromatography using CHCl₃:EA (80:20; v:v), to give 87 mg brownish powder.

TLC (EA), $R_f = 2.0/7.6 = 0.26$; yield: 0.087 g (45%); $^1\text{H-NMR}$ 300 MHz (DMSO- d_6), δ (ppm) 3.50-3.60 (s, 8H), 3.75-3.80 (d, 6H), 5.85-5.90 (s, 1H), 6.95-7.00 (d, 3H), 7.05-7.10 (t, 2H), 7.50-7.55 (m, 2H), 8.15-8.20 (s, 1H), 9.10-9.15 (s, 1 N-H amine); FT-IR (KBr) (cm^{-1}): 3746.9, 3672.1 & 3650.1 (N-H) stretching, 2964.2 Ar-H (C-H stretch), 1594.7 (C=O), 1508 (C=C) aromatic & (C=N) stretching, 1432.8 (C-H) bending, 876.7, 702.2 & 616.4 Ar-H ($\text{H}_2\text{C}=\text{CH}_2$ bending).

2.3.2 Synthesis of piperazine symmetrical analogues:

2.3.2.1 Synthesis of 1,4-Piperazine, bis {(6-Pyrimidin)-(4-trifluoromethoxy-phenyl)-amine} {MYJ-24 (38)}:

In a 25 ml round bottom flask (100 mg, 1.16 mmol) of piperazine pure (**37**) and 2.0 eq (6-chloropyrimidin-4-yl)-(4-trifluoromethoxy-phenyl)-amine (**13**) (0.672 mg, 2.32 mmol) and (0.321 g, 2.32 mmol) of K_2CO_3 were dissolved in 10 ml DMF, the reaction mixture was refluxed at 100 °C for 12 h and the completion of the reaction was indicated by TLC (EA). When the reaction was completed the DMF was evaporated to dryness and crude product was extracted by EA against distilled water. The organic phase was dried over Na_2SO_4 and the solvent was removed under reduced pressure. The desired product was purified by column chromatography using CHCl_3 to give 309 mg brownish powder. TLC (EA), $R_f = 3.5/7.6 = 0.46$; yield: 0.309 g (45%); $^1\text{H-NMR}$ 300 MHz (DMSO- d_6), δ (ppm) 3.66 (s, 8H), 5.98 (s, 2H), 7.25 (d, 4H), 7.70 (d, 4H), 8.23 (s, 2H), 9.30 (s, 2H); $^{13}\text{C}\{^1\text{H}\}$ -NMR ((DMSO- d_6 , δ ppm), 164.99, 161.43, 158.82, 157.15, 140.66, 122.83, 120.47, 119.94, 86.05, 43.48, 41.06; FT-IR (KBr) (cm^{-1}): 3747, 3672.3 & 3650 (N-H) stretching, 2964.2 Ar-H (C-H stretch), 1584.5 (C=C) aromatic & (C=N) stretching, 1487, 1440.4 & 1356.4 (C-H) bending, 922.2, 672.9 & 605.6 Ar-H ($\text{H}_2\text{C}=\text{CH}_2$ bending).

2.3.3 Synthesis of pyridyl-/pyrimidyl -piperazinyl derivatives:

2.3.3.1 2-Bromo-1-(2, 3-dihydro-benzo [1, 4] dioxin-6-yl)-ethanone (26) derivatives:

General Procedure:

In a 25 ml round bottom flask, (0.5 g, 2.16 mmol) of the pyridyl-/pyrimidyl -piperazinyl derivative [1-(5-trifluoromethyl-pyridin-2-yl)-piperazine] (**39**) as example and (0.33 ml, 2.38 mmol) of dry triethylamine (TEA) were mixed in 10 ml EA and cooled to 0 °C. 1.0 eq of 2-bromo-1-(2,3-dihydro-benzo[1,4]dioxin-6-yl)-ethanone (**26**) (0.56 g, 2.16 mmol) was added and the reaction mixture was stirred at room temperature for the time needed to completion. The reaction progress was followed by TLC using (EA), or (EA:MeOH (90:10; v:v)). When the reaction was completed the mixture was partitioned between the aqueous and ethyl acetate phases (30 ml X 3). The organic fractions were collected and dried over anhydrous sodium sulfate. After filtering off the solids the volatiles were evaporated to dryness under reduced pressure. The powder was finally afforded by re-crystallization using ethanol as solvent to give the purified desired product.

2.3.3.1.1 1-(2,3-Dihydro-benzo[1,4]dioxin-6-yl)-2-[4-(5-trifluoromethyl-pyridin-2-yl)-piperazin-1-yl]-ethanone {MYJ-7 (**45**)}:

TLC (EA), $R_f = 5.7/8.4 = 0.68$; yellowish crystals; yield: 0.39 g (44.8%); $^1\text{H-NMR}$ 300 MHz (CDCl_3) δ (ppm) 2.65-2.75 (m, 4H), 3.70-3.75 (m, 4H), 3.75-3.80 (s, 1H), 4.25-4.30 (t, 4H), 6.60-6.65 (dd, 1H), 6.85-6.90 (dd, 1H), 7.53 (m, 1H), 7.55 (d, 1H), 7.59 (d, 1H), 8.35-8.40 (s, 1H); FT-IR (KBr) (cm^{-1}): 2898.3 Ar-H (C-H stretch), 1675.3, 1614.4 (C=O), 1509.4 (C=C) aromatic & (C=N) stretching, 1461, 1432.9 & 1388 (C-H) bending, 777.7, 744.5, 672, 624.7 & 558.8 Ar-H ($\text{H}_2\text{C}=\text{CH}_2$ bending).

2.3.3.1.2 1-(2,3-Dihydro-benzo[1,4]dioxin-6-yl)-2-(4-pyridin-2-yl-piperazin-1-yl)-ethanone {MYJ-10 (48)}:

TLC (EA), $R_f = 4.5/8.4 = 0.54$; yellowish crystals; yield: 0.45 g (43.3%); $^1\text{H-NMR}$ 300 MHz (CDCl_3) δ (ppm) 2.65-2.70 (t, 4H), 3.55-3.60 (t, 4H), 3.76 (s, 1H), 4.25-4.30 (dd, 4H), 6.59-6.64 (m, 2H), 6.88-6.90 (d, 1H), 7.50-7.55 (d, 1H), 7.55-7.60 (t, 2H), 8.15 (d, 1H). There are some more peaks in the NMR spectrum belonging to impurities; FT-IR (KBr) (cm^{-1}): 2994.7 Ar-H (C-H stretch), 2824 CH_2 , CH_3 (C-H stretch), 1678 (C=O), 1584 (C=C) aromatic & (C=N) stretching, 1480, 1435.5 & 1381.5 (C-H) bending, 936, 743.8, 604 & 560.5 Ar-H ($\text{H}_2\text{C}=\text{CH}_2$ bending).

2.3.3.1.3 1-(2,3-Dihydro-benzo[1,4]dioxin-6-yl)-2-(4-pyridin-4-yl-piperazin-1-yl)-ethanone {MYJ-13 (51)}:

TLC (EA:MeOH (90:10; v:v)), $R_f = 2.8/8.2 = 0.34$; yellowish crystals; yield: 0.55 g (52.9%); $^1\text{H-NMR}$ 300 MHz (CDCl_3) δ (ppm) 2.70-2.75 (t, 4H), 3.40 (t, 4H), 3.75-3.80 (s, 2H), 4.30 (m, 4H), 6.65-6.70 (d, 2H), 6.90-6.95 (d, 1H), 7.54-7.57 (d, 1H), 7.57-7.60 (s, 1H), 8.25-8.30 (d, 2H); FT-IR (KBr) (cm^{-1}): 3000 Ar-H (C-H stretch), 2941.5, 2887.7, 2850.6 & 2799.1 CH_2 , CH_3 (C-H stretch), 1692 (C=O), 1593.5, 1544.3 & 1506.5 (C=C) aromatic & (C=N) stretching, 1444.5, 1392.5 & 1375 (C-H) bending, 948.9, 671.2, 645.7, 602.1 & 553.2 Ar-H ($\text{H}_2\text{C}=\text{CH}_2$ bending).

2.3.3.1.4 1-(2,3-Dihydro-benzo[1,4]dioxin-6-yl)-2-(4-pyrimidin-2-yl-piperazin-1-yl)-ethanone {MYJ-15 (53)}:

TLC (EA:MeOH (90:10; v:v)), $R_f = 2.8/8.3 = 0.34$; yellowish crystals ; yield: 0.457 g (44.1%); $^1\text{H-NMR}$ 300 MHz (CDCl_3) δ (ppm) 2.65-2.70 (t, 4H), 3.75-3.80 (s, 2H), 3.85-3.90 (t, 4H), 4.30 (m, 4H), 6.45-6.50 (t, 1H), 6.90 (d, 1H), 7.55 (d, 1H), 7.58 (s, 1H), 8.30 (d, 2H); FT-IR (KBr) (cm^{-1}): 3121, 2992 Ar-H (C-H stretch), 2943.8, 2874.5 & 2824.6 CH_2 , CH_3 (C-H stretch), 1667 (C=O), 1584.5, 1546 (C=C) aromatic & (C=N) stretching, 1497.5, 1450, 1358 & 1309 (C-H) bending, 851, 751.5, 713.7, 577.2 & 518.2 Ar-H ($\text{H}_2\text{C}=\text{CH}_2$ bending); MS (ESI) m/z calculated for $\text{C}_{18}\text{H}_{20}\text{N}_4\text{O}_3$ 340.38, found 341.08 (M +H)⁺.

2.3.3.2 Benzofuran-2- carboxylic acid (43) derivatives:

General Procedure:

In a 25 ml round bottom flask, (0.2 g, 1.2 mmol) of benzofuran-2- carboxylic acid (**43**), (0.28 g, 1.36 mmol) DCC and (0.16 g, 1.36 mmol) NHS were mixed in 5-10 ml DMF. The reaction mixture was stirred at room temperature overnight. Then 1.0 eq (0.28 g, 1.2 mmol) of the pyridyl/pyrimidyl-piperazinyl derivative [1-(5-trifluoromethyl-pyridin-2-yl)-piperazine] (**39**) as example was added to the reaction mixture. The reaction progress was followed by TLC using (EA). When the reaction was completed DMF was evaporated under reduced pressure to dryness and the powder was finally afforded by re-crystallization using ethanol as solvent to give the purified desired product.

2.3.3.2.1 Benzofuran-2-yl-[4-(5-trifluoromethyl-pyridin-2-yl)-piperazin-1-yl]-methanone {MYJ-8 (46)}:

TLC (EA), $R_f = 6.7/8.3 = 0.81$; white crystals; yield: 0.203 g (43.9%); $^1\text{H-NMR}$ 300 MHz (CDCl_3) δ (ppm) 3.75-3.80 (t, 4H), 4.00 (s, 4H), 6.65-6.70 (d, 1H), 7.30-7.35 (t, 1H), 7.35-7.40 (t, 1H), 7.40-7.45(d, 1H), 7.50-7.55 (d, 1H), 7.66 (s, 1H), 7.69-7.70 (d, 1H); FT-IR (KBr) (cm^{-1}): 3003, 2943.6 Ar-H (C-H stretch), 2853.9 CH_2 , CH_3 (C-H stretch), 1613.5 (C=O), 1566.4, 1508.2 (C=C) aromatic & (C=N) stretching, 1477.2, 1463.1, 1444.7 & 1388.1 (C-H) bending, 950.2, 860, 832.8, 672.8 & 645 Ar-H ($\text{H}_2\text{C}=\text{CH}_2$ bending).

2.3.3.2.2 Benzofuran-2-yl-(4-pyridin-2-yl-piperazin-1-yl)-methanone {MYJ-9 (47)}:

TLC (EA), $R_f = 5.8/8.2 = 0.71$; white crystals; yield: 0.129 g (34.01%); $^1\text{H-NMR}$ 300 MHz (CDCl_3) δ (ppm) 3.65-3.70 (s, 4H), 3.95-3.40 (s, 4H), 6.65-6.70 (m, 2H), 7.30-7.35 (t, 1H), 7.35-7.40 (t, 1H), 7.40-7.45 (t, 1H), 7.50-7.55 (m, 2H), 7.65-7.70 (d, 1H), 8.22 (m, 1H); FT-IR (KBr) (cm^{-1}): 3004.1 Ar-H (C-H stretch), 2929.4, 2851 CH_2 , CH_3 (C-H stretch), 1614.4 (C=O), 1481.6 (C=C) aromatic & (C=N) stretching, 1439.3, 1382.1 & 1311.6 (C-H) bending, 979.4, 860.6, 834.2, 672.6 & 522.5 Ar-H ($\text{H}_2\text{C}=\text{CH}_2$ bending).

2.3.3.2.3 Benzofuran-2-yl-(4-phenyl-piperazin-1-yl)-methanone {MYJ-12 (50)}:

TLC (EA), $R_f = 6.7/8.3 = 0.81$; white to slightly yellowish crystals; yield: 0.313 g (82.8%); $^1\text{H-NMR}$ 300 MHz (CDCl_3) δ (ppm) 3.25-3.30 (t, 4H), 4.00-4.05 (s, 4H), 6.90-6.95 (m, 3H), 7.28 (s, 1H), 7.30-7.35 (t, 2H), 7.36 (t, 1H), 7.40-7.45 (t, 1H), 7.54 (d, 1H), 7.67 (d, 1H); FT-IR (KBr) (cm^{-1}): 3036.2 Ar-H (C-H stretch), 2929, 2852 CH_2 , CH_3 (C-H stretch), 1599.5 (C=O), 1439, 1346.7 & 1312 (C-H) bending, 968.3, 917, 865, 568.6, 538.4 & 518.4 Ar-H ($\text{H}_2\text{C}=\text{CH}_2$ bending).

2.3.3.3 6-Methoxy-Benzofuran-2- carboxylic acid (44) derivatives:

General Procedure:

In a 25 ml round bottom flask, (0.2 g, 1.04 mmol) of 6-methoxy-benzofuran-2-carboxylic acid (**44**), (0.24 g, 1.14 mmol) DCC and (0.13 g, 1.14 mmol) NHS were mixed in 5-10 ml DMF. The reaction mixture was stirred at room temperature overnight. Then 1.0 eq (0.24 g, 1.04 mmol) of the pyridyl/pyrimidyl-piperazinyl derivative [1-(5-trifluoromethyl-pyridin-2-yl)-piperazine] (**39**) as example was added to the reaction mixture. The reaction progress was followed by TLC using (EA). When the reaction was completed DMF was evaporated under reduced pressure to dryness and the powder was finally afforded by re-crystallization using ethanol as solvent to give the purified desired product.

2.3.3.3.1 (6-Methoxybenzofuran-2-yl)-[4-(5-trifluoromethylpyridin-2-yl)-piperazin-1-yl]-methanone {MYJ-11 (49)}:

TLC (EA), $R_f = 6.4/8.2 = 0.78$; slightly brownish crystals; yield: 0.275 g (65.2%); $^1\text{H-NMR}$ 300 MHz (CDCl_3) δ (ppm) 3.75-3.80 (t, 4H), 3.85-3.90 (d, 3H), 4.00 (s, 4H), 6.65-6.70 (d, 1H), 6.95 (d, 1H), 7.00-7.05 (s, 1H), 7.30-7.35 (d, 1H), 7.50-7.55 (d, 1H), 7.65-7.70 (d, 1H), 8.40-8.45 (s, 1H); FT-IR (KBr) (cm^{-1}): 3126.7 Ar-H (C-H stretch), 3034.7, 2925 & 2852.5 CH_2 , CH_3 (C-H stretch), 1588 (C=O), 1438, 1319.5 (C-H) bending, 967.7, 950.2, 837.7 & 537.7 Ar-H ($\text{H}_2\text{C}=\text{CH}_2$ bending).

2.3.3.3.2 (6-Methoxybenzofuran-2-yl) - (4-pyrimidin-2-ylpiperazin-1-yl)-methanone {MYJ-14 (52)}:

TLC (EA), $R_f = 4.9/8.3 = 0.59$; slightly brownish crystals; yield: 0.192 g (54.5%); $^1\text{H-NMR}$ 300 MHz (CDCl_3) δ (ppm) 3.85-3.90 (s, 3H), 3.90-3.95 (s, 8H), 6.55 (t, 1H), 6.90-6.95 (d, 1H), 7.00-7.05 (s, 1H), 7.25-7.30 (s, 1H), 7.50-7.55 (d, 1H), 8.30-8.35 (dd, 2H); FT-IR (KBr) (cm^{-1}): 3119.6 Ar-H (C-H stretch), 2929.5, 2851.4 CH_2 , CH_3 (C-H stretch), 1549.5 (C=O), 1500 (C=C) aromatic & (C=N) stretching, 1438.5, 1361.5 & 1311.9 (C-H) bending, 892.7, 777, 738.7, 678.3 & 529.4 Ar-H ($\text{H}_2\text{C}=\text{CH}_2$ bending).

Chapter Three

Results and Discussion

3. Results and Discussion:

The major challenge in developing kinase inhibitor is to achieve selective inhibition of kinase(s) associated with the disease (cancer). In contrast to ATP-binding site which is common to all kinases and is thus difficult to achieve selectivity, allosteric sites are likely to be selective and specific to individual kinases and by that it represents a promising strategy for the design of kinase inhibitors with improved selectivity and also utility in overcoming drug resistance.

In this research our efforts have been invested in synthesizing small molecules that act as allosteric inhibitors of Bcr-Abl through binding to the myristoyl binding pocket MBP.

All the compounds (including intermediates) planned to be prepared during the execution of the project in hand are designed, prepared, purified using chromatography techniques and characterized using physical methods that include nuclear magnetic resonance (^1H -, ^{13}C -, COSY and HMBC NMR), Fourier transform infrared spectroscopy (FTIR), Electrospray ionization mass spectrometry (ESIMS) and then tested for their biological activity and on the basis of the results new generations of compounds are designed, prepared and tested.

3.1 Chemical synthesis of compounds:

Three groups of compounds have been synthesized in the course of the proposed study:

3.1.1 GNF-2 and GNF-5 analogues:

With knowledge of the two known MBP selective inhibitors GNF-2 and -5 in hand, and knowing that the 4-trifluoromethoxyaniline at 6-position of the pyrimidine core is an obligate structural feature for achieving submicromolar potency as a cellular Bcr-Abl inhibitor and that the pyrimidine ring can be elaborated to include a variety of other heterocyclic ring systems ^[83], we aimed at exploring the possibility of introducing different structural moieties at the 4-position of the pyrimidine heterocyclic moiety. To that end we plan to replace the 3-benzamide moiety with piperazinyl-derivatives (see Figure 3.1 below).

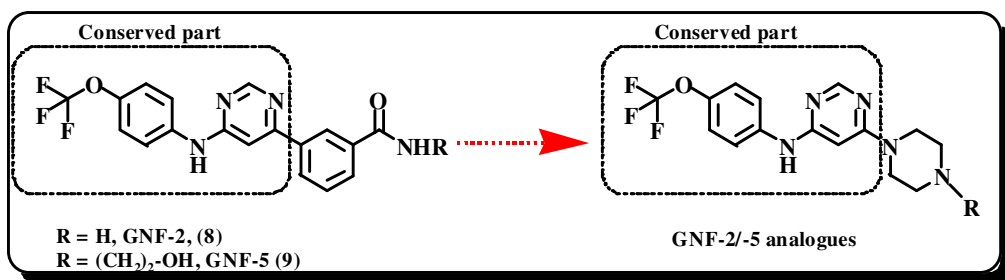


Figure 3.1: Rational of synthesizing the GNF-2/-5 analogues.

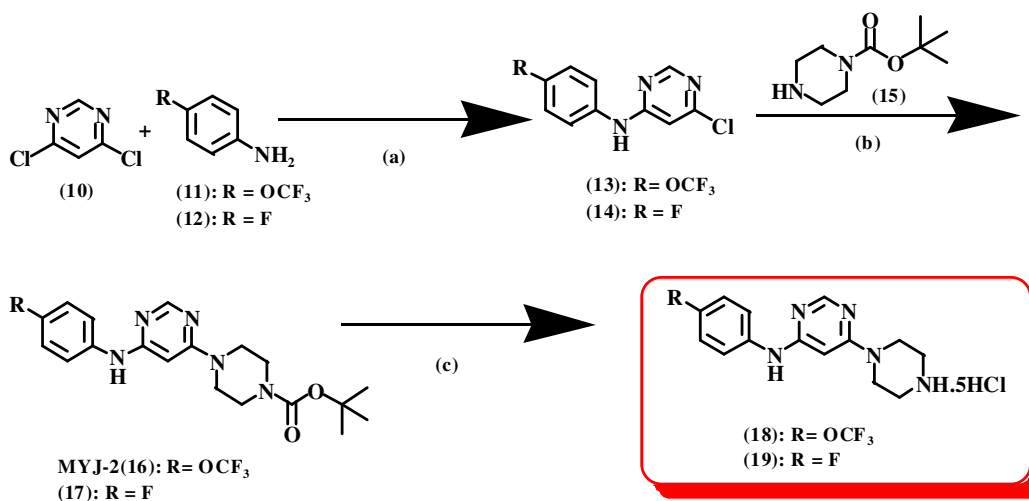
Several analogues including aromatic derivatives conjugated via an amide group [benzoyl (**21**) and dimethoxy benzoyl (**22**)], alkyl chain linker such as 1-(2,3-dihydrobenzo[b][1,4]dioxin-6-yl)ethanone (**26**), or via sulfonamide group [mesyl (**27**) and tosyl (**55**)] have been synthesized following the procedures depicted in Schemes 1 and 2 below.

3.1.1.1 Synthesis of (6-piperazin-1-yl-pyrimidin-4-yl)-(4-trifluoromethoxyphenyl)-ammonium.hydrochloride (**18**) and (6-piperazin-1-ylpyrimidin-4-yl)-(4-fluorophenyl)-ammonium.hydrochloride (**19**):

These precursors **18** and **19** were prepared starting from the commercially available 4,6-dichloropyrimidine (**10**) that was reacted with *p*-trifluoromethoxyaniline (**11**) or 4-fluoroaniline (**12**) under basic conditions using DIPEA to get the white fluffy amines **13** and **14** in 80% and 85% yields, respectively.

These corresponding 6-substituted pyrimidines **13** and **14** were then subjected to nucleophilic displacement of the chloro group by piperazine-1-carboxylic acid *tert*-butyl ester (BOC-piperazine) (**15**) under elevated temperature for 12 h. The BOC was then cleaved under acidic conditions to afford the amine free form of piperazinyipyrimidine as white salts **18** and **19** in 75% and 80% yields, respectively.

Scheme 1: Representative procedure for the synthesis of salts 18 and 19:



Reagents and conditions: **a)** DIPEA, reflux 2 h, column chromatography CHCl₃; **b)** K₂CO₃, reflux 12 h, column chromatography CHCl₃:hexane (50: 50; v:v); **c)** EtOH, HCl, stirring 1 h, cooling, filtration.

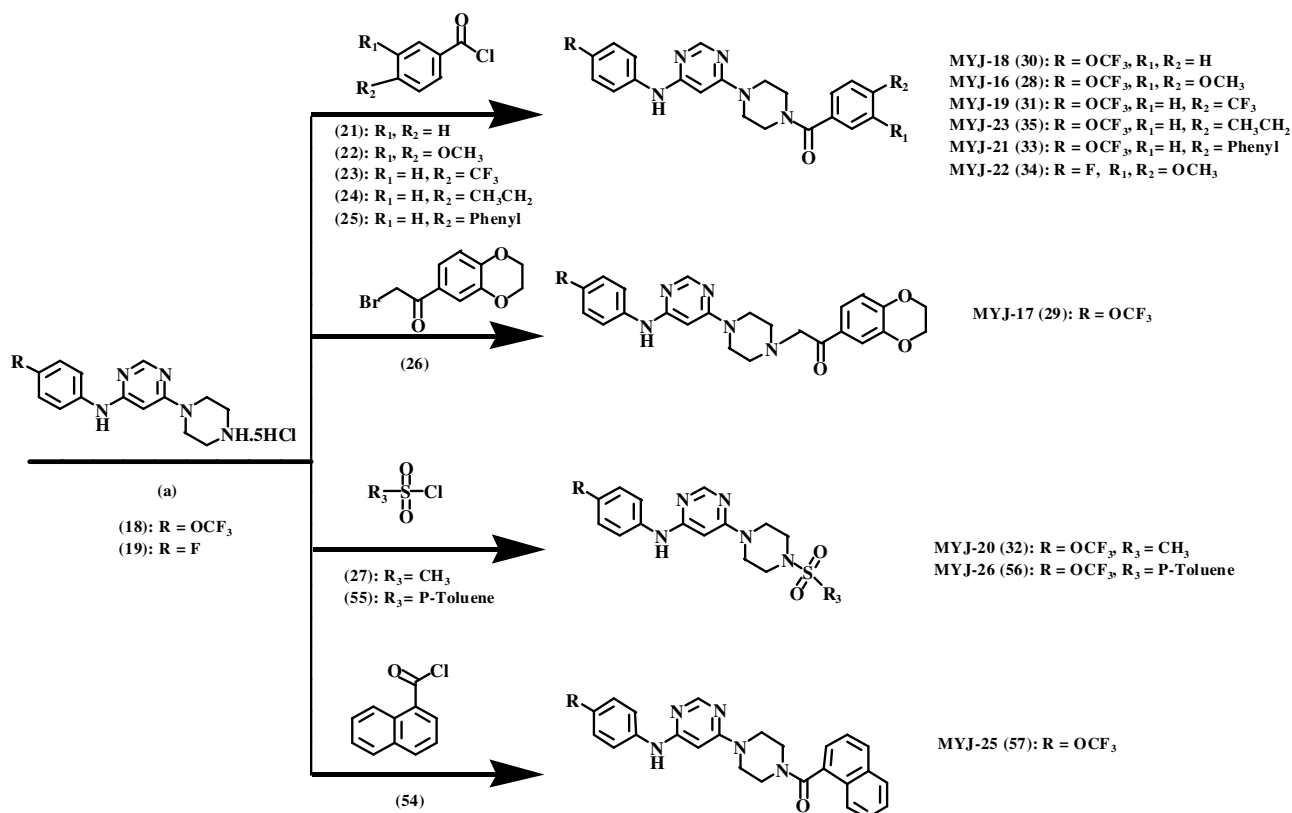
3.1.1.2 Synthesis of GNF-2/ GNF-5 analogues (MYJ-16 -MYJ-23 (28-35) and MYJ-25 & MYJ-26 (57 & 56)):

The synthesis of these target compounds was obtained by conjugating the terminal piperazinyl secondary amine in **18** or **19** with the corresponding acyl halide **21**, **22**, **23**, **24**, **25** or **54**, sulfonyl halide **27** or **55**, or 2-bromo-1-(2,3-dihydro-benzo[1,4]dioxin-6-yl)-ethanone (**26**) under basic conditions using TEA to afford the desired products **28-35** and **57& 56**.

Reactions were carried out in DMF at room temperature and the final products were purified using column chromatography to give **28**, **29**, **30**, **31**, **32**, **33**, **34**, **35**, **57** and **56** final products in 44.9%, 41.0%, 52.0%, 65.0%, 91.0%, 93.0%, 45.0%, 95.0%, 64.9% and 80.2% yields, respectively.

The final products were characterized by ¹H-NMR, ¹³C-NMR, FT-IR and ESIMS spectroscopy. To confirm the purity, the proton sequences, protons' spin-spin coupling and the proton-carbon correlations COSY and HMBC 2D-NMR were done further for **28** (Figure 2.1, Table 2.1).

Scheme 2: Representative procedure for the synthesis of GNF-2/-5 analogues:



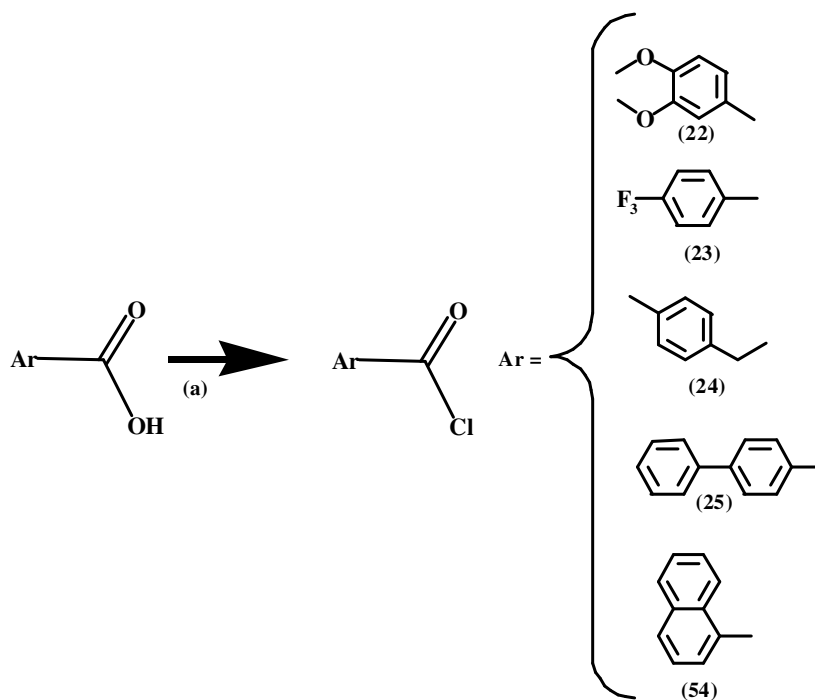
Reagents and conditions: a) TEA, stirring 6 h for **29** and **31**, 24 h for **32**, **33**, **35**, **57** & **56**, 48 h for **28**, **30** and **34** 8 at r.t, evaporation, extraction, column chromatography CHCl₃: hexane (50: 50; v:v) for **29**, **30** & **31**, CHCl₃: hexane (70: 30; v:v) for **28**, CHCl₃: Eth.Ac. (80: 20; v:v) for **34** & **35**, CHCl₃: Eth.Ac. (70: 30; v:v) for **57**, CHCl₃ for **32** & **33**, recrystallization from EtOH for **56**.

3.1.1.3 Synthesis of aromatic acyl halides:

The acyl halides were prepared by reaction of the corresponding carboxylic acid **58**, **59**, **60**, **61** or **62** with excess oxalyl chloride at room temperature and inert conditions. The reaction progress was followed by TLC using CHCl₃ for compounds **21**, **24**, **25** and **54** and EA for compounds **22** and **23**.

All acid chlorides were obtained in high yields 96% for **22**, **25** & **54**; 95% for **24**; 97% for **23** and characterized by ¹H-NMR. Acid chlorides were used without further purification.

Scheme 3: Representative procedure for the synthesis of aromatic fatty acids halide: **22**, **23**, **24**, **25**, and **54**:



Reagents and conditions: **a)** 2.0 eq oxalyl chloride, 20 ml dry DCM, stirring 24 h at r.t., evaporation.

3.1.1.4 Synthesis of [6-(4-phenyl-piperazin-1-yl)-pyrimidin-4-yl]-(4-trifluoromethoxy-phenyl)-amine MYJ-1 (**20**):

Compound **20** was prepared in the same manner described in Scheme 1, starting from the commercially available 4,6-dichloropyrimidine (**10**) which was reacted with *p*-trifluoromethoxyaniline (**11**) under basic conditions using DIPEA to get a white fluffy amine **13** in a high yield (80%).

Amine **13** was subjected to nucleophilic displacement of the chloro leaving group by phenylpiperazine (**36**) using potassium carbonate as a base under refluxing DMF.

The product was purified by column chromatography using CHCl_3 :hexane (50:50; v:v), obtained by 52.0% yield and characterized by $^1\text{H-NMR}$ and FT-IR spectroscopy.

3.1.2 Piperazine symmetrical analogues:

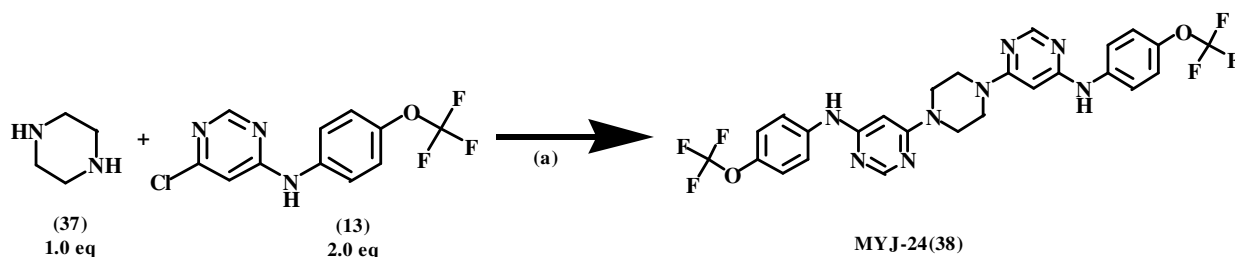
As we mentioned above, we investigated the consequences of replacing the 3-benzamide moiety with piperazinyl-derivatives. Considering that the lowest energy pose places GNF-2 in an extended trans conformation with the 4-trifluoromethoxyaniline pointed toward the bottom of the pocket^[83], we aimed to synthesize a symmetrical extended analogue by binding the 4-trifluoromethoxyaniline from both sides to the piperazine, which could noticeably enhance binding affinity toward the MBP.

Synthesis of 1,4-Piperazine, bis {(6-Pyrimidin)-(4-trifluoromethoxy-phenyl)-amine} MYJ-24 (38):

The synthesis of this final compound was a one step reaction, simply by reacting 1.0 equivalent of the commercially available piperazine (37) and 2.0 equivalents (6-chloropyrimidin-4-yl)-(4-trifluoromethoxyphenyl) amine (13) under basic condition and elevated temperature using DMF as solvent.

The completion of the reaction was indicated by TLC using EA and the product was purified by column chromatography using CHCl₃, obtained by 45.0% yield and characterized by ¹H-, ¹³C-NMR and FT-IR spectroscopy.

Scheme 4: Representative procedure for the synthesis of piperazine symmetrical analogues:



Reagents and conditions: a) K₂CO₃, reflux at 100 °C for 12 h, extraction, column chromatography using CHCl₃.

3.1.3 Pyridyl-/Pyrimidyl-piperazinyl derivatives:

Assisted by computational chemistry techniques several 2-, 4-pyridyl piperazinyl (**39**, **40** or **41**) and 2-pyrimidyl piperazinyl derivatives (**42**) were proposed as having binding affinity to the MBP.

To explore the diversity of the MBP inhibitors, derivatives including benzofuran-2-carboxylic acid (**43**), 6-methoxybenzofuran-2-carboxylic acid (**44**) and 1-(2,3-dihydrobenzo[b][1,4]dioxin-6-yl)ethanone (**26**) with variations in the position of the pyridine or pyrimidine amine were all examined.

To evaluate the effect of pyridine heterocycle on the activity, derivative of phenylpiperazine (**36**) was also synthesized and examined. For the synthesis of these compounds see general procedure depicted in Scheme 5 below.

3.1.3.1 Synthesis of benzofuran-2-carboxylic acid (**43**), 6-methoxybenzofuran-2-carboxylic acid (**44**) derivatives:

Compound **43** or **44** were coupled to 2- or 4-pyridylpiperazinyl (**39**, **40** or **41**) or 2-pyrimidylpiperazinyl (**42**) or phenyl piperazine (**36**), respectively to get the desired products in two steps. First; the desired carboxylic acid was mixed and stirred with the coupling agent DCC using NHS as coupling agent at room temperature overnight. Second; the resulting intermediate was coupled to the corresponded **39**, **40**, **41**; **42** or **36** to get the desired product which was afforded by re-crystallization using ethanol as solvent.

The resulted derivatives **46**, **47**, **49**, **50** and **52** were obtained as crystals in 43.9%, 34.01%, 65.2%, 82.8% and 54.5% yields, respectively.

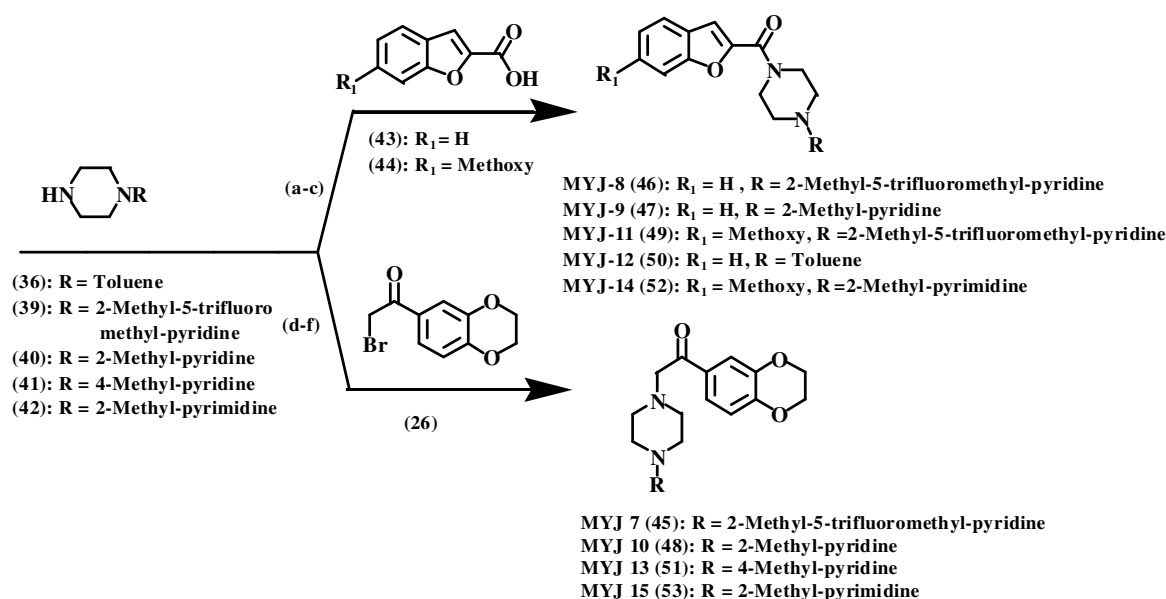
3.1.3.2 Synthesis of 1-(2,3-dihydrobenzo[b][1,4]dioxin-6-yl)ethanone (**26**) derivatives:

The commercially available compound **26** underwent nucleophilic substitution of the bromo leaving group by the corresponding pyridyl or pyrimidylpiperazinyl derivative **39**, **40**, **41** or **42** using TEA as a base at room temperature the time needed for completion.

The desired product was then purified by extraction, evaporation and re-crystallization using ethanol as solvent.

The resulting derivatives **45**, **48**, **51** and **53** were obtained as crystals in 44.8%, 43.3%, 52.9%, and 44.1% yields, respectively.

Scheme 5: Representative procedure for the synthesis of Pyridyl-/Pyrimidyl-piperazinyl derivatives:



Reagents and conditions: **a)** DCC, NHS, 24 h at r.t for **46**, **47**, **49**, **50** & **52**; **b)** evaporation; **c)** recrystallization by EtOH; **d)** TEA, stirring 12 h for **45**, 15 h for **48** and **51**, 24 h for **53** at r.t.; **e)** extraction, evaporation; **f)** recrystallization from EtOH.

3.2 Biological evaluation of novel allosteric inhibitors of Bcr-Abl:

3.2.1 *In-vitro* assessment of cellular auto-phosphorylation activity in Ba/F3 Bcr-Abl cells:

To evaluate the cellular auto-phosphorylation activity of the different compounds we utilized Ba/F3, murine B lymphocytes cells, transfected with Bcr-Abl gene. We noticed that responsiveness to allosteric inhibitors such as GNF-2 is a cell-type specific and also depends on

the size of Bcr-Abl. Figure 3.2 demonstrated that while activity of Imatinib, ATP competitor of Abl, was comparable against p185 and p210 Bcr-Abl, activity of GNF-2 was varied. GNF-2 was less effective in inhibiting cellular auto-phosphorylation of Ba/F3 transfected with p210 Bcr-Abl compared to p185 Bcr-Abl.

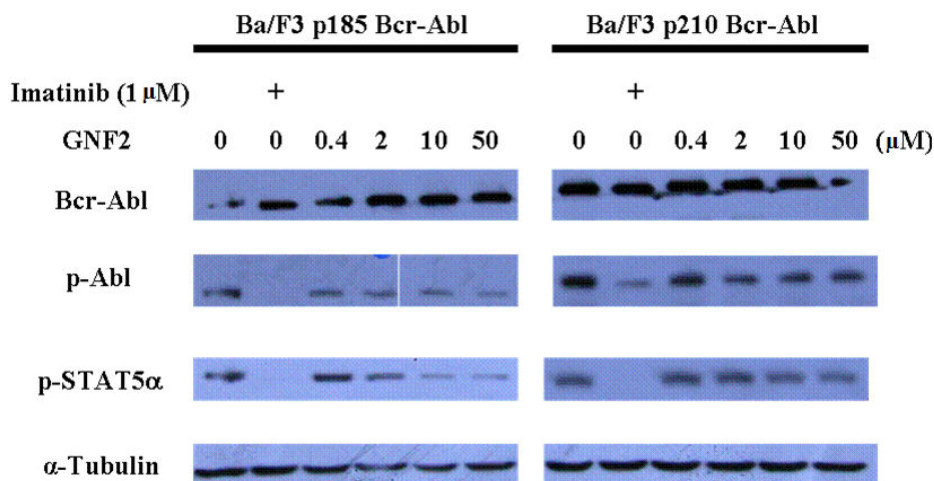


Figure 3.2: Auto-phosphorylation inhibition of STAT5α and p185, p210 Bcr-Abl by GNF-2.

3.2.2 Inhibition of cellular auto-phosphorylation of the native Bcr-Abl:

We screened our compounds for inhibitory activity of the p185 Bcr-Abl auto-phosphorylation function. Compounds were evaluated in duplicate in two or more concentrations. Bcr-Abl transfected cells were treated for one hour and viability of the cells were determined using Trypan blue exclusion assay and the lysates were used to evaluate cellular auto-phosphorylation as previously described. See Table 3.1 and Figure 3.3 below.

Results of tested compounds demonstrated that MYJ-1 (**20**), MYJ-2 (**16**) and MYJ-17 (**29**) exhibited some activities in the Ba/F3 Bcr-Abl cell lines at high concentrations, and that MYJ-16 (**28**) shows significant activity at different concentrations comparing to GNF-2 (**8**).

Table 3.1: The percentage values of the Ba/F3 P185-tyrosine inhibition by the MYJ's compounds:

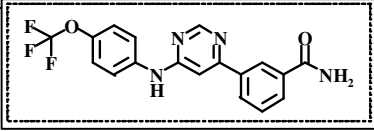
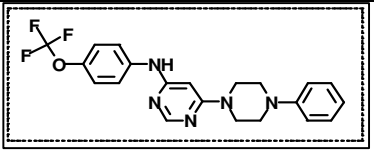
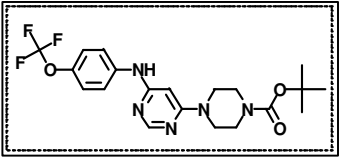
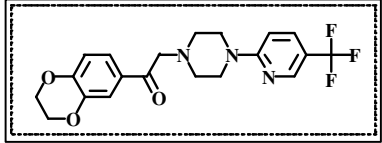
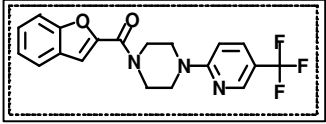
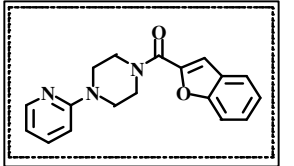
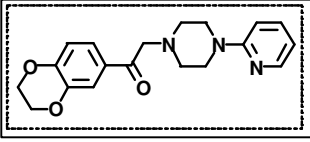
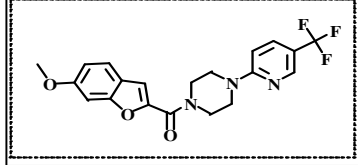
Compound No.	Compound Code	Structure	Concentrations	% pTyr Inhibition
8	GNF-2		50 μ M	57.53
			10 μ M	43.34
			2 μ M	39.64
20	MYJ-1		200 μ M	70.62
			20 μ M	43.81
			2 μ M	4.48
16	MYJ-2		200 μ M	69.33
			20 μ M	21.79
			2 μ M	4.52
45	MYJ-7		200 μ M	24.1
			50 μ M	9.59
46	MYJ-8		200 μ M	16.85
			50 μ M	11.93
47	MYJ-9		200 μ M	13.25
			50 μ M	6.67
48	MYJ-10		200 μ M	-2.58
			50 μ M	7.95
49	MYJ-11		200 μ M	32.64
			50 μ M	8.57

Table 3.1, cont.:

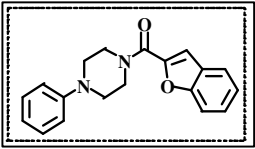
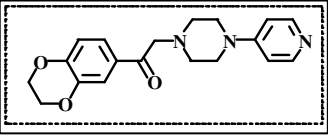
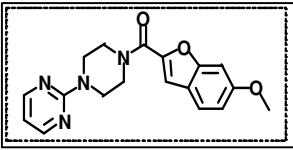
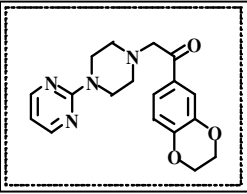
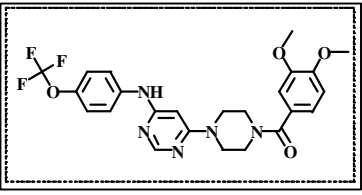
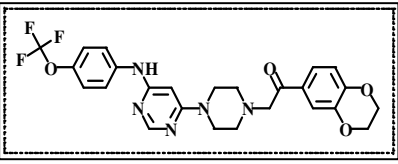
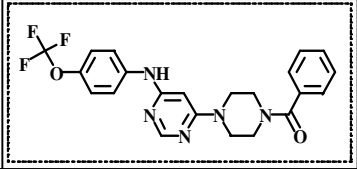
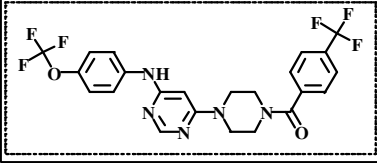
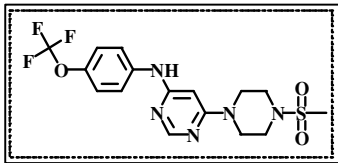
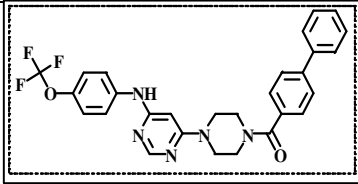
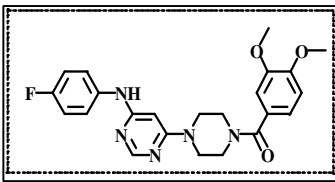
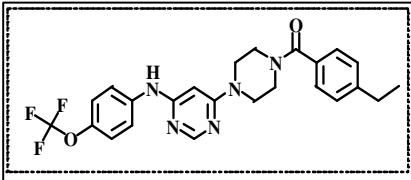
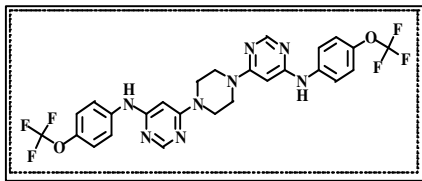
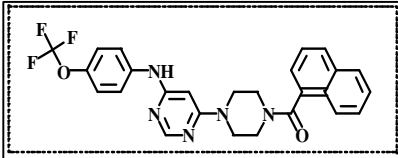
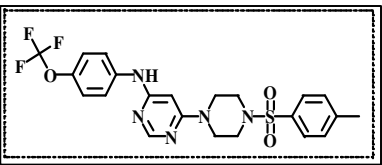
50	MYJ-12		200 μ M	-8.82
			50 μ M	-6.75
51	MYJ-13		200 μ M	15.47
			50 μ M	8.68
52	MYJ-14		200 μ M	15.13
			50 μ M	-3.93
53	MYJ-15		200 μ M	20.18
			50 μ M	-1.85
28	MYJ-16		200 μ M	95.58
			100 μ M	94.68
			50 μ M	75.36
			25 μ M	64.47
			10 μ M	52.35
			2 μ M	30.77
29	MYJ-17		200 μ M	58.15
			20 μ M	20.59
			2 μ M	-0.24
30	MYJ-18		----	ND
31	MYJ-19		----	ND

Table 3.1, cont.:

32	MYJ-20		---	ND
33	MYJ-21		---	ND
34	MYJ-22		---	ND
35	MYJ-23		---	ND
38	MYJ-24		---	ND
57	MYJ-25		---	ND
56	MYJ-26		---	ND

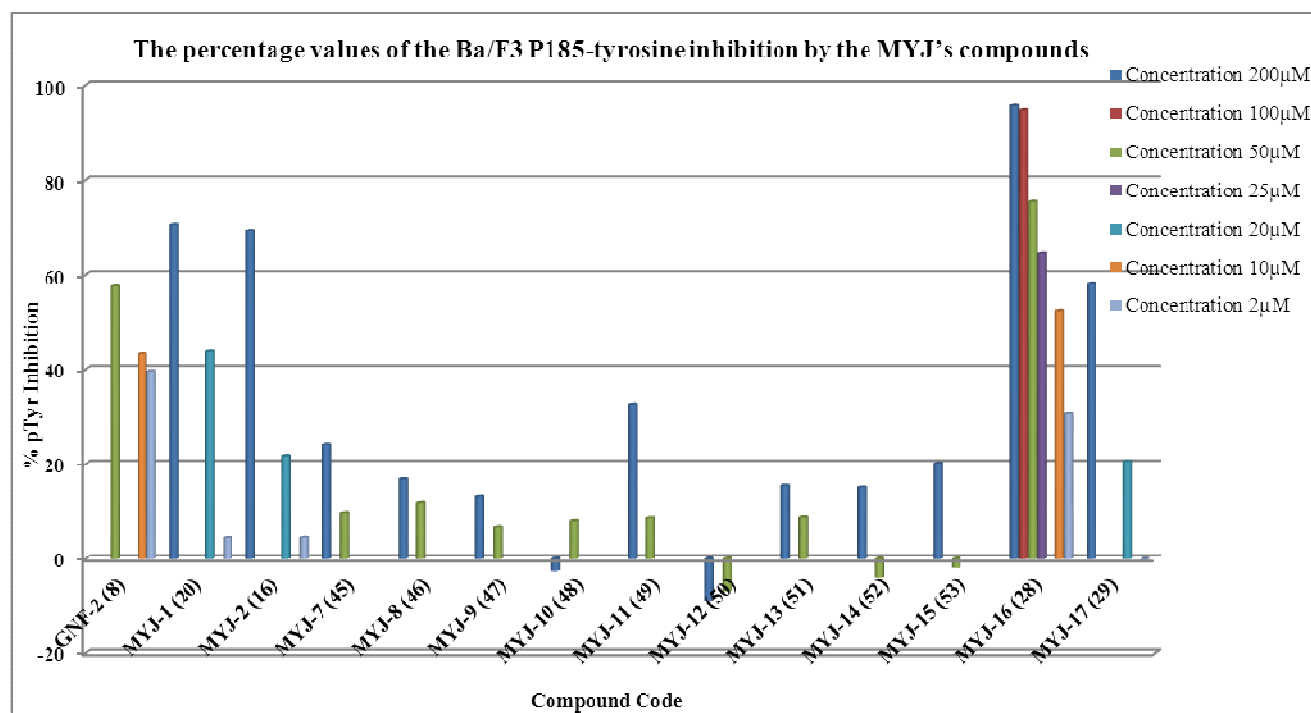


Figure 3.3: Auto-phosphorylation inhibition of p185 Bcr-Abl by MYJ's compounds compared by GNF-2.

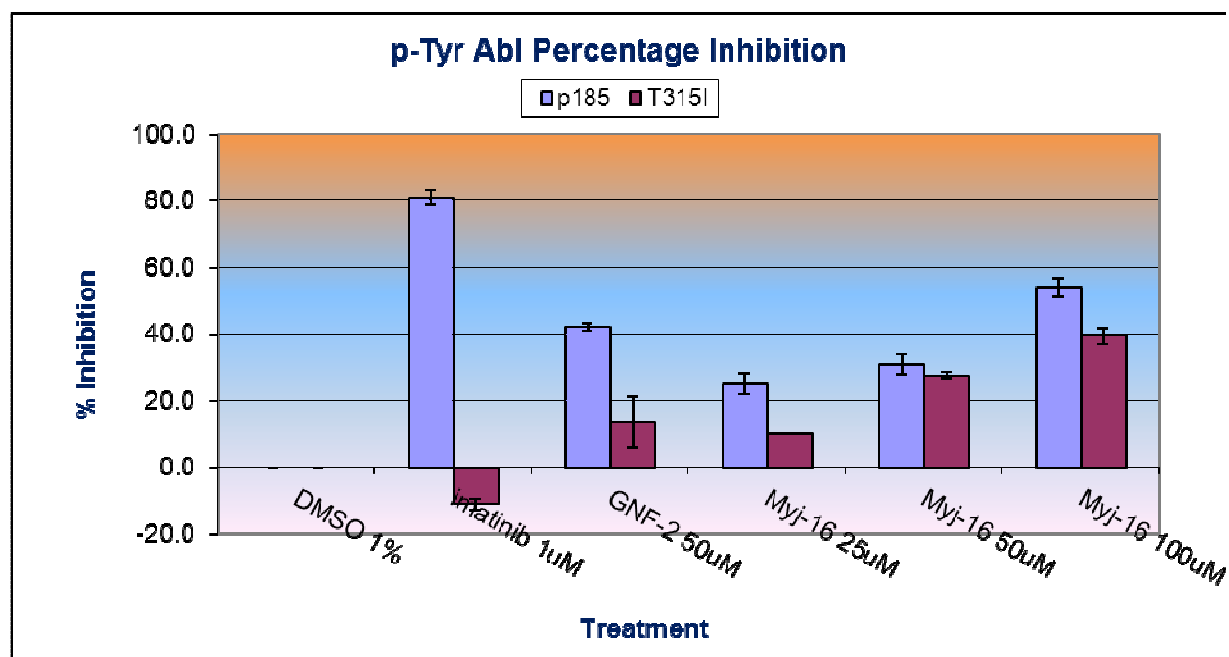
3.2.3 Inhibition of cellular auto-phosphorylation of the native and T315I mutated Bcr-Abl form by MYJ-16 (28):

Results shown in Figure 3.3 above demonstrated that MYJ-16 (28) was the most active compound in inhibiting auto-phosphorylation of native Bcr-Abl, thus it was also tested for its ability to affect auto-phosphorylation of T315I mutated Bcr-Abl form.

Results shown in Figure 3.4 illustrated that Imatinib at 1 µM and GNF-2 at 50 µM were active in inhibiting Bcr-Abl auto-phosphorylation in Ba/F3 cells carrying native Bcr-Abl, but failed to do so in cells carrying the T315I mutated Bcr-Abl.

In contrast Figure 3.4 (a) and (b) showed that treatment of Ba/F3 cells containing native and T315I mutated Bcr-Abl with MYJ-16 (28) caused gradual elimination of Bcr-Abl apparently by degradation mechanism. 28 exhibited a dose-dependent effect and exerted its effect in all Ba/F3 cells tested.

(a)



(b)

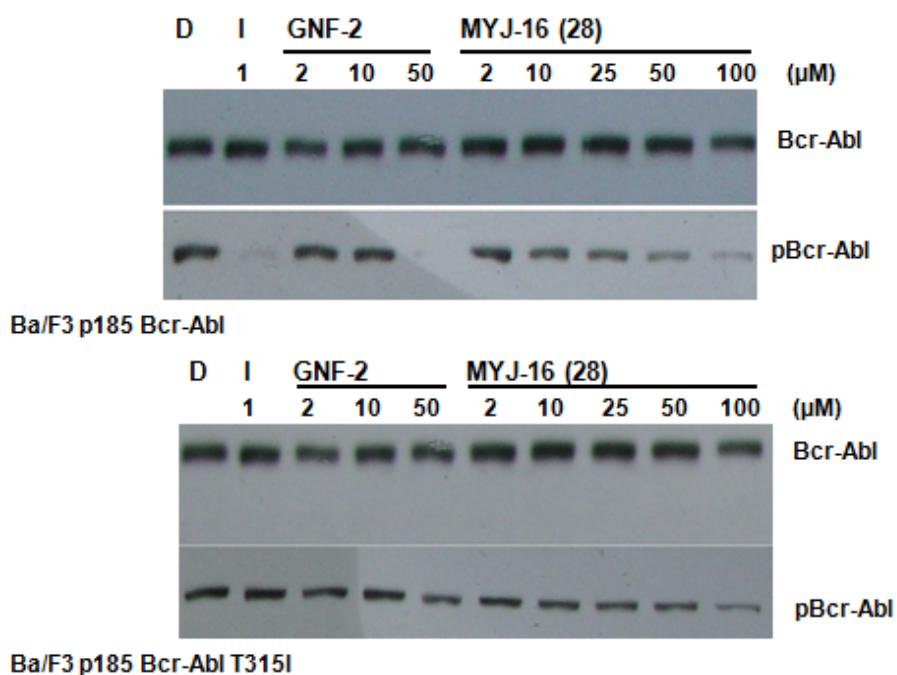


Figure 3.4: Inhibition of Bcr-Abl cellular auto-phosphorylation and T315I mutated Bcr-Abl by MYJ-16 (28) compound. (a) Percentage of Bcr-Abl auto-phosphorylation (violet) and T315I mutated Bcr-Abl inhibition (purple), (b) Western blot of inhibition of Bcr-Abl auto-phosphorylation by MYJ-16 (28) for cells carrying native and T315I mutated Bcr-Abl forms.

3.2.4 Clonogenicity Inhibition:

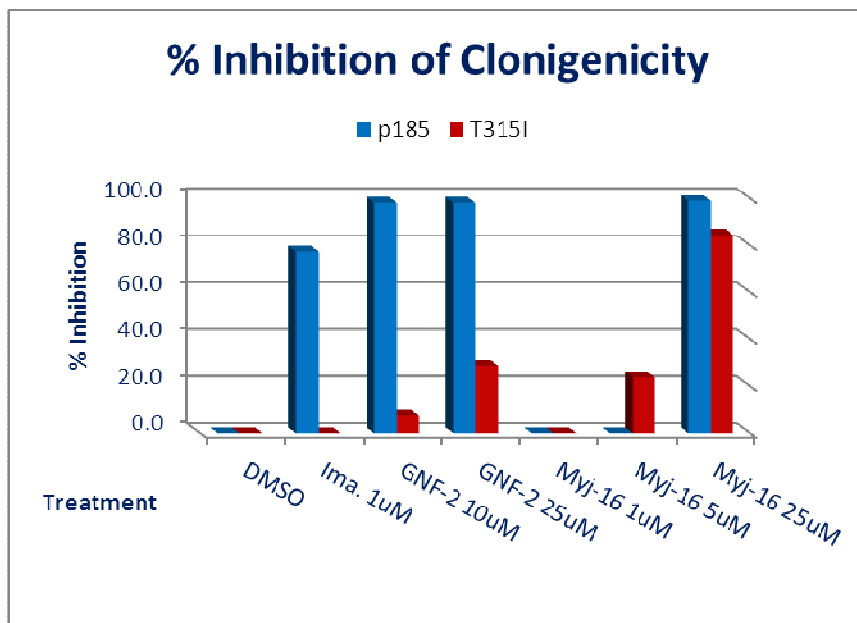
Anchorage-independent growth of cells is a typical characteristic of the tumorigenicity of cancer cells *in-vitro* [91]. Thus, we tested the ability of different compounds to affect clonogenicity of Ba/F3 harboring native and T315I Bcr-Abl constructs. Figure 3.5 showed that Imatinib at 1 μ M and GNF-2 at 10 μ M were active in inhibiting clonogenicity of Ba/F3 cells carrying native Bcr-Abl, but not T315I mutated Bcr-Abl. GNF-2 at higher concentration (25 μ M) also was active in inhibiting Ba/F3 cells carrying native Bcr-Abl, but T315I mutated Bcr-Abl form by about 27% only.

MYJ-16 (**28**) showed variable potency in inhibiting Ba/F3 cells carrying Bcr-Abl constructs. Interestingly, **28** at 25 μ M showed nearly comparable activity against clonogenicity of Ba/F3 harboring native or T315I Bcr-Abl constructs.

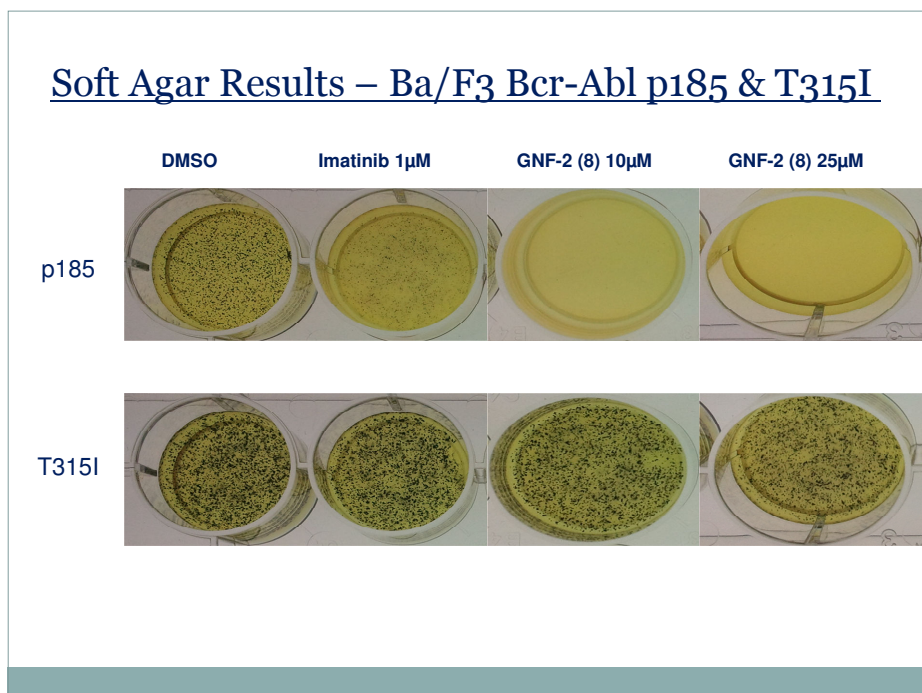
This result is probably a proof that **28** compound do indeed bind to the myristate pocket, and that it's binding in allosteric manner induces changes in the dynamics properties of the ATP site in both wild type and T315I forms of Bcr-Abl, which indicates that T315I mutation did not alter the ability of **28** to do changes in the ATP site that located approximately 30 Å from the MBP which is **28** site of interaction as we suppose.

And if so, it is very worthy to test **28** for the cellular inhibition of the T315I in combination with nilotinib or dasatinib or other ATP competitive inhibitor which could be very effective in suppressing T315I both *in-vitro* and *in-vivo* at lower concentrations.

(a)



(b)



(c)

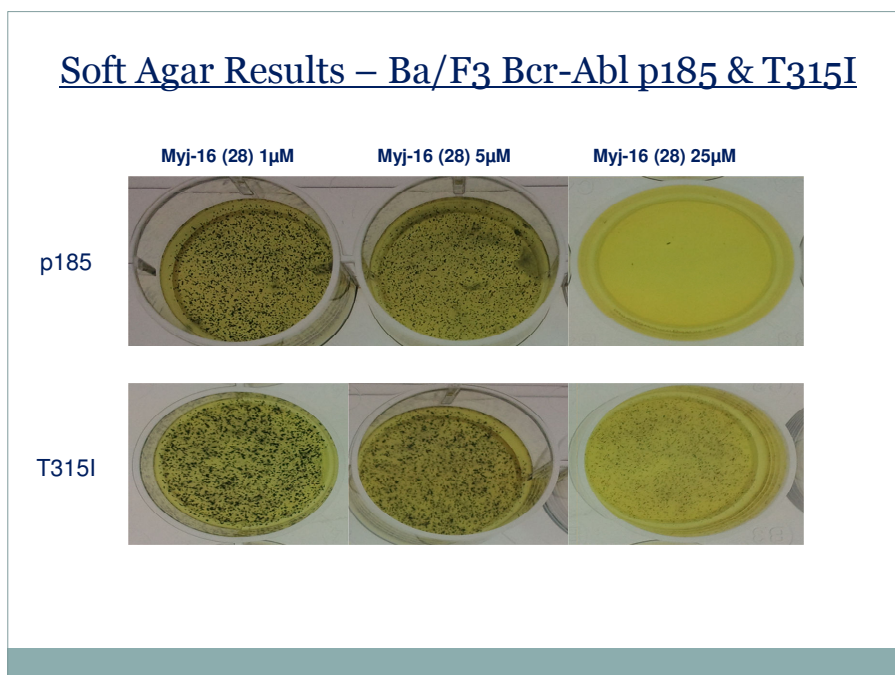


Figure 3.5: Clonogenicity Inhibition of Ba/F3 cells carrying the native and T315I mutated Bcr-Abl constructs by Imatinib, GNF-2 (**8**) and MYJ-16 (**28**) compound using different concentrations.

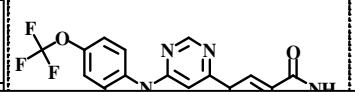
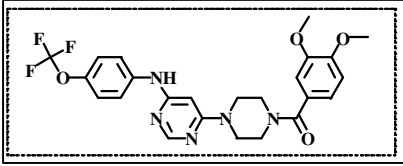
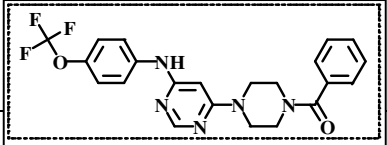
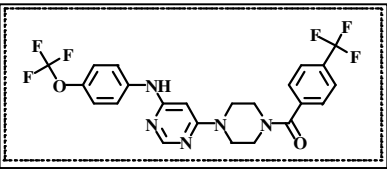
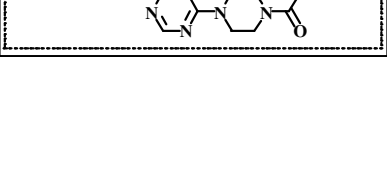
3.2.5 Evaluation of the effect of MYJ's compounds on the inhibition of proliferation of ALL cell lines Sup-B15:

The ability of few MYJ compounds (MYJ-16 (**28**), MYJ-18 (**30**) and MYJ-19 (**31**)) to inhibit proliferation of Sup-B15 ALL cell lines was evaluated. .

Table 3.2 and Figure 3.6 below showed that **28**, **30** & **31** compounds exhibited a dose-dependent effect to inhibit proliferation of ALL cell lines Sup-B15 comparing with GNF-2 (**8**).

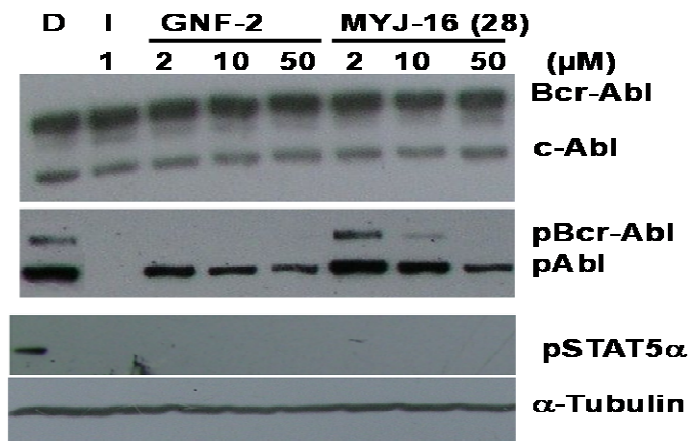
Compound **28** was more active in inhibiting proliferation of ALL cell lines Sup-B15 at lower concentrations comparing to **30** and **31**.

Table 3.2: The percentage values of inhibition of ALL cell lines Sup-B15 by the MYJ's compounds comparing to GNF-2:

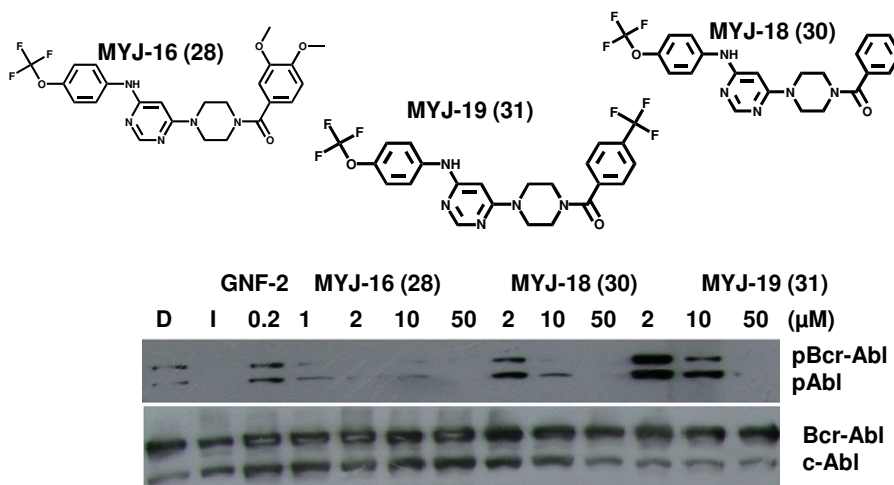
Compound No.	Compound Code		Concentrations	% pTyr Inhibition
8	GNF-2		1 μ M	48.94
			0.2 μ M	11.74
28	MYJ-16		200 μ M	95.61
			50 μ M	68.63
			10 μ M	64.14
			2 μ M	49.51
30	MYJ-18		50 μ M	67.36
			10 μ M	61.28
			2 μ M	43.84
31	MYJ-19		50 μ M	61.96
			10 μ M	42.25
			2 μ M	14.87

(a)

Sup B15



(b)



Need STAT5a and Tubulin

SupB15 ALL cells

Figure 3.6: Inhibition of ALL cell lines Sup-B15 by the MYJ-16 (28), MYJ-18 (30) and MYJ-19 (31) compounds.

3.2.4 Bcr-Abl Structure-Activity Relationships (SAR) of MYJ compounds:

We have presented a comprehensive exploration of Bcr-Abl targeted ligands that have binding affinity to the MBP. Three groups of compounds have been synthesized in this proposed study and evaluated for their potency to inhibit the auto-phosphorylation in Ba/F3 Bcr-Abl transfected cells carrying either the native or the T315I mutated form.

3.2.4.1 GNF-2 and GNF-5 subclass:

Depending on the two lead compounds GNF-2 and -5 that specifically inhibited Bcr-Abl in an allosteric manner, keeping the 4,6- pyrimidine substitution pattern with the trifluoromethoxyaniline group at *para* position, and adding several structural moieties at the 4-position of the pyrimidine ring using different piperazinyl-derivatives, 12 analogues have been synthesized, purified using chromatography techniques, characterized by ¹H-NMR, ¹³C-NMR, {COSY and HMBC 2D-NMR for MYJ-16 (**28**)}, FT-IR and ESIMS spectroscopy and investigated for having activity as cellular Bcr-Abl inhibitors.

Results of the tested compounds demonstrated that compounds containing phenyl piperazine such as MYJ-1 (**20**), piperazine-1-carboxylic acid *tert*-butyl ester such as MYJ-2 (**16**) or 2-bromo-1-(2,3-dihydro-benzo[1,4]dioxin-6-yl)-ethanone such as MYJ-17 (**29**) at the 4-position of the pyrimidine ring exhibit limited activity against Ba/F3 P185 kinase. And that compound MYJ-16 (**28**) having 3,4-dimethoxy-benzoyl at pyrimidine 4 position have shown impressive activity at different concentrations compared to GNF-2 (**8**).

Compound **28** showed nearly comparable activity against clonogenicity of Ba/F3 harboring native and T315I Bcr-Abl constructs at 25µM concentration and this result suggested that this myristate ligand can display a differential ability to synergize with ATP-competitive inhibitors to inhibit both wild-type and T315I Bcr-Abl mutant and also decrease the number of resistant clones that emerge as a response to continued exposure to a single agent.

Compound **28** was also more active in inhibiting proliferation of ALL cell lines Sup-B15 at lower concentrations comparing to MYJ-18 (**30**) and MYJ-19 (**31**) having benzoyl and 4-trifluoromethyl benzoyl, respectively at the pyrimidine 4 position that showed activity at higher concentrations.

The biological activity for the other analogues will be assessed against Bcr-Abl transfected cells in the near future.

3.2.4.2 Piperazine symmetrical analogues subclass:

By knowing that the 4-trifluoromethoxyaniline is a necessary part for achieving potency as a Bcr-Abl inhibitor, we envisaged that binding this ligand from both sides to the piperazine to have a symmetrical analogue would enhance the affinity and increase the number of hydrogen bonds with the MBP. To that end MYJ-24 (**38**) was synthesized and the biological activity will be assessed against Bcr-Abl transfected cells in the near future.

3.2.4.3 Pyridyl-/Pyrimidylpiperazinyl subclass:

According to computational chemistry techniques that showed that compounds sharing 2-, 4-pyridyl piperazinyl (**39**, **40** or **41**) and 2-pyrimidylpiperazinyl (**42**) scaffolds supposed to have binding affinity to the MBP, nine compounds were synthesized MYJ-7~MYJ-15 (**45-53**, respectively) and assessed for their ability to inhibit the auto-phosphorylation in Ba/F3 p185 Bcr-Abl transfected cells.

Results showed that none of these nine compounds exert any auto-phosphorylation inhibitory effect when compared to GNF-2 (**8**) or Imatinib at different concentrations.

Chapter Four

Conclusion

4. Conclusion:

Despite the impressive success of imatinib which revolutionized the treatment of CML, 5–10% clinical relapse due to drug resistance has been documented following long-term imatinib therapy in CML T315I. Second and third generations of tyrosine kinase inhibitors have been developed to obtain an increased potency and a broad range of activity against known imatinib-resistant mutants, but none was effective against the T315I recalcitrant mutant.

A new class of allosteric Bcr-Abl inhibitors appeared, and represented a promising new strategy for the design of kinase inhibitors with improved selectivity and utility in overcoming drug resistance, two promising lead compounds GNF-2 /-5 approved to inhibit wild-type Bcr-Abl and many clinically relevant imatinib resistant mutants.

These MBP inhibitors represent not only a safe and effective therapy for CML, but also a proof-of-principle that targeting a single protein can be an effective therapeutic strategy in certain types of cancers, also the ability of these compounds to synergize with ATP-competitive inhibitors to inhibit the growth of cells transformed with Bcr-Abl mutants made this new therapeutic modality a promising approach.

In our research we focused on the myristate pocket as the prime candidate for the GNF-2 /-5 binding site, and accordingly many analogues were designed, synthesized, purified using chromatography techniques, characterized by ¹H-NMR, ¹³C-NMR, FT-IR and ESIMS spectroscopy and tested for their biological activity against Ba/F3 harboring native and T315I Bcr-Abl. Results of tested compounds demonstrated that MYJ-1 (**20**), MYJ-2 (**16**) and MYJ-17 (**29**) exhibited some activities against Ba/F3 P185-tyrosine and that MYJ-16 (**28**) having 3,4-dimethoxy-benzoyl at pyrimidine 4 position shows impressive activity at different concentrations comparing to GNF-2 (**8**).

Compound **28** showed nearly comparable activity against clonogenicity of Ba/F3 harboring native and T315I Bcr-Abl constructs at 25 μM concentration and this result indicates that this myristate ligand which binds in allosteric manner can induce changes in the dynamics properties of the ATP site in both wild type and T315I forms of Bcr-Abl, which suggests that it can display a differential ability to synergize with ATP-competitive inhibitors to inhibit the growth of cells transformed with Bcr-Abl mutants and likely to prevent or delay the emergence of resistance mutations.

Compound **28** was also more active in inhibiting proliferation of ALL cell lines Sup-B15 at lower concentrations comparing to MYJ-18 (**30**) and MYJ-19 (**31**) that showed activity at higher concentrations.

This work demonstrates that a variety of structures can effectively inhibit Bcr-Abl by presumably targeting myristate binding pocket and provides new leads for developing drugs to treat Bcr-Abl driven leukemia.

Chapter Five

References

5. References:

1. Manning, G., et al., *The protein kinase complement of the human genome*. Science, 2002. **298**(5600): p. 1912-34.
2. Eck, M.J. and P.W. Manley, *The interplay of structural information and functional studies in kinase drug design: insights from BCR-Abl*. Curr Opin Cell Biol, 2009. **21**(2): p. 288-95.
3. Chahrour, O., D. Cairns, and Z. Omran, *Small molecule kinase inhibitors as anti-cancer therapeutics*. Mini Rev Med Chem. 2012. **12**(5): p. 399-411.
4. Dancey, J. and E.A. Sausville, *Issues and progress with protein kinase inhibitors for cancer treatment*. Nat Rev Drug Discov, 2003. **2**(4): p. 296-313.
5. Garske, A.L., et al., *Chemical genetic strategy for targeting protein kinases based on covalent complementarity*. Proc Natl Acad Sci U S A. 2011. **108**(37): p. 15046-52.
6. Fabian, M.A., et al., *A small molecule-kinase interaction map for clinical kinase inhibitors*. Nat Biotechnol, 2005. **23**(3): p. 329-36.
7. Badrinarayan, P. and G.N. Sastry, *Rational approaches towards lead optimization of kinase inhibitors: The issue of specificity*. Curr Pharm Des. 2012.
8. Arora, A. and E.M. Scholar, *Role of tyrosine kinase inhibitors in cancer therapy*. J Pharmacol Exp Ther, 2005. **315**(3): p. 971-9.
9. Gozalbes, R., et al., *Development and experimental validation of a docking strategy for the generation of kinase-targeted libraries*. J Med Chem, 2008. **51**(11): p. 3124-32.
10. Bikker, J.A., et al., *Kinase domain mutations in cancer: implications for small molecule drug design strategies*. J Med Chem, 2009. **52**(6): p. 1493-509.
11. Janne, P.A., N. Gray, and J. Settleman, *Factors underlying sensitivity of cancers to small-molecule kinase inhibitors*. Nat Rev Drug Discov, 2009. **8**(9): p. 709-23.
12. Zhang, J., P.L. Yang, and N.S. Gray, *Targeting cancer with small molecule kinase inhibitors*. Nat Rev Cancer, 2009. **9**(1): p. 28-39.
13. Lee, S., et al., *Determination of the substrate-docking site of protein tyrosine kinase C-terminal Src kinase*. Proc Natl Acad Sci U S A, 2003. **100**(25): p. 14707-12.
14. Tatosyan, A.G. and O.A. Mizenina, *Kinases of the Src family: structure and functions*. Biochemistry (Mosc), 2000. **65**(1): p. 49-58.
15. Boulikas, T., *The phosphorylation connection to cancer (review)*. Int J Oncol, 1995. **6**(1): p. 271-8.
16. Courtneidge, S.A., *Cancer: Escape from inhibition*. Nature, 2003. **422**(6934): p. 827-8.
17. Broekman, F., E. Giovannetti, and G.J. Peters, *Tyrosine kinase inhibitors: Multi-targeted or single-targeted?* World J Clin Oncol. 2011. **2**(2): p. 80-93.
18. Paul, M.K. and A.K. Mukhopadhyay, *Tyrosine kinase - Role and significance in Cancer*. Int J Med Sci, 2004. **1**(2): p. 101-115.
19. Vlahovic, G. and J. Crawford, *Activation of tyrosine kinases in cancer*. Oncologist, 2003. **8**(6): p. 531-8.
20. Colicelli, J., *ABL tyrosine kinases: evolution of function, regulation, and specificity*. Sci Signal. 2010. **3**(139): p. re6.
21. Nagar, B., et al., *Structural basis for the autoinhibition of c-Abl tyrosine kinase*. Cell, 2003. **112**(6): p. 859-71.
22. Van Etten, R.A., *c-Abl regulation: a tail of two lipids*. Curr Biol, 2003. **13**(15): p. R608-10.

23. Yang, J., et al., *Discovery and characterization of a cell-permeable, small-molecule c-Abl kinase activator that binds to the myristoyl binding site*. Chem Biol. 2011. **18**(2): p. 177-86.
24. Hantschel, O. and G. Superti-Furga, *Regulation of the c-Abl and Bcr-Abl tyrosine kinases*. Nat Rev Mol Cell Biol, 2004. **5**(1): p. 33-44.
25. Pluk, H., K. Dorey, and G. Superti-Furga, *Autoinhibition of c-Abl*. Cell, 2002. **108**(2): p. 247-59.
26. Harrison, S.C., *Variation on an Src-like theme*. Cell, 2003. **112**(6): p. 737-40.
27. Sirvent, A., C. Benistant, and S. Roche, *Cytoplasmic signalling by the c-Abl tyrosine kinase in normal and cancer cells*. Biol Cell, 2008. **100**(11): p. 617-31.
28. Chen, S., et al., *Abl N-terminal cap stabilization of SH3 domain dynamics*. Biochemistry, 2008. **47**(21): p. 5795-803.
29. Druker, B.J., *Imatinib as a Paradigm of Targeted Therapies*, in *Advances in Cancer Research*. 2004, Academic Press. p. 1-30.
30. Calabretta, B. and D. Perrotti, *The biology of CML blast crisis*. Blood, 2004. **103**(11): p. 4010-22.
31. Druker, B.J., *STI571 (Gleevec™) as a paradigm for cancer therapy*. Trends in Molecular Medicine, 2002. **8**(4): p. S14-S18.
32. Deininger, M.W., J.M. Goldman, and J.V. Melo, *The molecular biology of chronic myeloid leukemia*. Blood, 2000. **96**(10): p. 3343-56.
33. Kurzrock, R., et al., *Philadelphia chromosome-positive leukemias: from basic mechanisms to molecular therapeutics*. Ann Intern Med, 2003. **138**(10): p. 819-30.
34. Pérez-Caro, M. and I. Sánchez-García, *BCR-ABL and Human Cancer*, in *Apoptosis, Cell Signaling, and Human Diseases*, R. Srivastava, Editor. 2007, Humana Press. p. 3-34.
35. Telegeev, G.D., et al., *Influence of BCR/ABL fusion proteins on the course of Ph leukemias*. Acta Biochim Pol, 2004. **51**(3): p. 845-9.
36. Deininger, M.W., et al., *BCR-ABL tyrosine kinase activity regulates the expression of multiple genes implicated in the pathogenesis of chronic myeloid leukemia*. Cancer Res, 2000. **60**(7): p. 2049-55.
37. Salesse, S. and C.M. Verfaillie, *BCR/ABL: from molecular mechanisms of leukemia induction to treatment of chronic myelogenous leukemia*. Oncogene, 2002. **21**(56): p. 8547-59.
38. Zou, X. and K. Calame, *Signaling pathways activated by oncogenic forms of Abl tyrosine kinase*. J Biol Chem, 1999. **274**(26): p. 18141-4.
39. Neshat, M.S., et al., *The survival function of the Bcr-Abl oncogene is mediated by Bad-dependent and -independent pathways: roles for phosphatidylinositol 3-kinase and Raf*. Mol Cell Biol, 2000. **20**(4): p. 1179-86.
40. Jabbour, E., J. Cortes, and H. Kantarjian, *Optimal first-line treatment of chronic myeloid leukemia. How to use imatinib and what role for newer drugs?* Oncology (Williston Park), 2007. **21**(6): p. 653-62; discussion 663-4, 667-8.
41. Capdeville, R., et al., *Glivec (STI571, imatinib), a rationally developed, targeted anticancer drug*. Nat Rev Drug Discov, 2002. **1**(7): p. 493-502.
42. Deininger, M., *Imatinib – an overview*. 2009. Vol. 1. 2009.
43. Hantschel, O., U. Rix, and G. Superti-Furga, *Target spectrum of the BCR-ABL inhibitors imatinib, nilotinib and dasatinib*. Leuk Lymphoma, 2008. **49**(4): p. 615-9.

44. Liu, Y. and N.S. Gray, *Rational design of inhibitors that bind to inactive kinase conformations*. Nat Chem Biol, 2006. **2**(7): p. 358-64.
45. Panjarian, S., et al., *Structure and dynamic regulation of abl kinases*. J Biol Chem. 2013. **288**(8): p. 5443-50.
46. Deininger, M.W.N., *Novel agents for chronic myeloid leukemia: from imatinib to dasatinib and nilotinib: overcoming resistance*. Community Oncology, 2006. **3**(8): p. 519-523.
47. Hochhaus, A. and P. La Rosee, *Imatinib therapy in chronic myelogenous leukemia: strategies to avoid and overcome resistance*. Leukemia, 2004. **18**(8): p. 1321-31.
48. Weisberg, E., et al., *Second generation inhibitors of BCR-ABL for the treatment of imatinib-resistant chronic myeloid leukaemia*. Nat Rev Cancer, 2007. **7**(5): p. 345-56.
49. Branford, S., et al., *Detection of BCR-ABL mutations in patients with CML treated with imatinib is virtually always accompanied by clinical resistance, and mutations in the ATP phosphate-binding loop (P-loop) are associated with a poor prognosis*. Blood, 2003. **102**(1): p. 276-83.
50. Bixby, D. and M. Talpaz, *Mechanisms of resistance to tyrosine kinase inhibitors in chronic myeloid leukemia and recent therapeutic strategies to overcome resistance*. Hematology Am Soc Hematol Educ Program, 2009: p. 461-76.
51. Weisberg, E., et al., *AMN107 (nilotinib): a novel and selective inhibitor of BCR-ABL*. Br J Cancer, 2006. **94**(12): p. 1765-9.
52. Weisberg, E., et al., *Characterization of AMN107, a selective inhibitor of native and mutant Bcr-Abl*. Cancer Cell, 2005. **7**(2): p. 129-41.
53. Manley, P.W., S.W. Cowan-Jacob, and J. Mestan, *Advances in the structural biology, design and clinical development of Bcr-Abl kinase inhibitors for the treatment of chronic myeloid leukaemia*. Biochimica et Biophysica Acta (BBA) - Proteins and Proteomics, 2005. **1754**(1-2): p. 3-13.
54. Radi, M., et al., *Discovery and SAR of 1,3,4-thiadiazole derivatives as potent Abl tyrosine kinase inhibitors and cytodifferentiating agents*. Bioorg Med Chem Lett, 2008. **18**(3): p. 1207-11.
55. Lombardo, L.J., et al., *Discovery of N-(2-chloro-6-methyl-phenyl)-2-(6-(4-(2-hydroxyethyl)-piperazin-1-yl)-2-methylpyrimidin-4-ylamino)thiazole-5-carboxamide (BMS-354825), a dual Src/Abl kinase inhibitor with potent antitumor activity in preclinical assays*. J Med Chem, 2004. **47**(27): p. 6658-61.
56. Kantarjian, H., et al., *Dasatinib versus imatinib in newly diagnosed chronic-phase chronic myeloid leukemia*. N Engl J Med. 2010. **362**(24): p. 2260-70.
57. Cortes, J.E., et al., *Safety and efficacy of bosutinib (SKI-606) in chronic phase Philadelphia chromosome-positive chronic myeloid leukemia patients with resistance or intolerance to imatinib*. Blood. 2011. **118**(17): p. 4567-76.
58. Redaelli, S., et al., *Activity of bosutinib, dasatinib, and nilotinib against 18 imatinib-resistant BCR/ABL mutants*. J Clin Oncol, 2009. **27**(3): p. 469-71.
59. Boschelli, F., K. Arndt, and C. Gambacorti-Passerini, *Bosutinib: a review of preclinical studies in chronic myelogenous leukaemia*. Eur J Cancer. 2010. **46**(10): p. 1781-9.
60. Cortes, J.E., et al., *Ponatinib in refractory Philadelphia chromosome-positive leukemias*. N Engl J Med. 2012. **367**(22): p. 2075-88.
61. Maru, Y., *Molecular biology of chronic myeloid leukemia*. Cancer Sci. 2012. **103**(9): p. 1601-10.

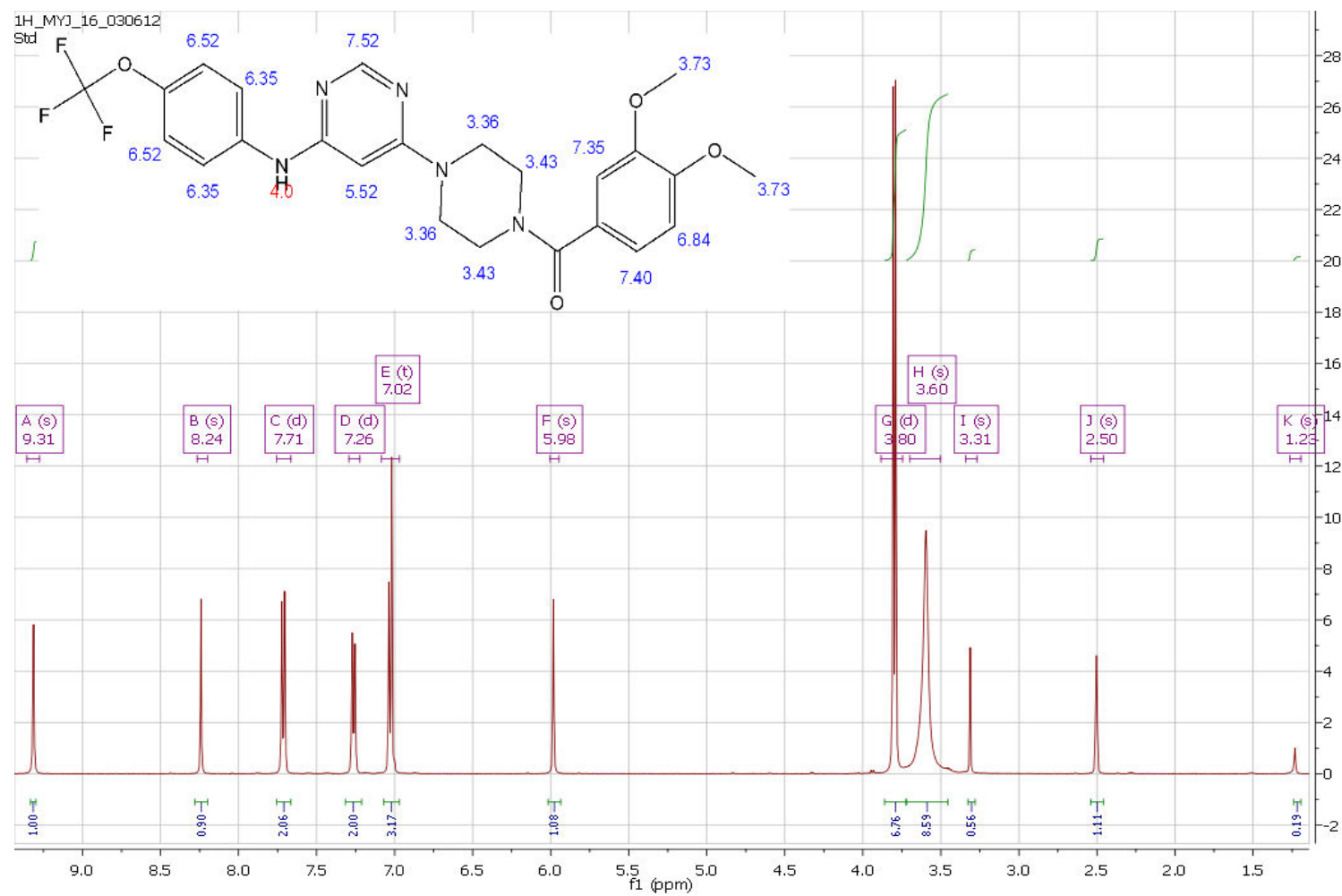
62. Melo, J.V. and C. Chuah, *Novel agents in CML therapy: tyrosine kinase inhibitors and beyond*. Hematology Am Soc Hematol Educ Program, 2008; p. 427-35.
63. Santos, F.P. and A. Quintas-Cardama, *New drugs for chronic myelogenous leukemia*. Curr Hematol Malig Rep. 2011. **6**(2): p. 96-103.
64. Santos, F.P., et al., *Bafetinib, a dual Bcr-Abl/Lyn tyrosine kinase inhibitor for the potential treatment of leukemia*. Curr Opin Investig Drugs. 2010. **11**(12): p. 1450-65.
65. Kantarjian, H., et al., *Phase 1 study of INNO-406, a dual Abl/Lyn kinase inhibitor, in Philadelphia chromosome-positive leukemias after imatinib resistance or intolerance*. Cancer. 2010. **116**(11): p. 2665-72.
66. Yokota, A., et al., *INNO-406, a novel BCR-ABL/Lyn dual tyrosine kinase inhibitor, suppresses the growth of Ph+ leukemia cells in the central nervous system, and cyclosporine A augments its in vivo activity*. Blood, 2007. **109**(1): p. 306-14.
67. Deguchi, Y., et al., *Comparison of imatinib, dasatinib, nilotinib and INNO-406 in imatinib-resistant cell lines*. Leuk Res, 2008. **32**(6): p. 980-3.
68. Gumireddy, K., et al., *A non-ATP-competitive inhibitor of BCR-ABL overrides imatinib resistance*. Proc Natl Acad Sci U S A, 2005. **102**(6): p. 1992-7.
69. Wu, J., et al., *ON012380, a putative BCR-ABL kinase inhibitor with a unique mechanism of action in imatinib-resistant cells*. Leukemia. 2010. **24**(4): p. 869-72.
70. Kimura, S., *[Novel anti-CML agents beyond imatinib]*. Rinsho Ketsueki, 2007. **48**(6): p. 475-84.
71. Li, B., et al., *Creating chemical diversity to target protein kinases*. Comb Chem High Throughput Screen, 2004. **7**(5): p. 453-72.
72. Fabbro, D., et al., *Inhibitors of the Abl kinase directed at either the ATP- or myristate-binding site*. Biochim Biophys Acta. 2010. **1804**(3): p. 454-62.
73. Lamba, V. and I. Ghosh, *New directions in targeting protein kinases: focusing upon true allosteric and bivalent inhibitors*. Curr Pharm Des. 2012. **18**(20): p. 2936-45.
74. Mian, A.A., et al., *Oligomerization inhibition, combined with allosteric inhibition, abrogates the transformation potential of T315I-positive BCR/ABL*. Leukemia, 2009. **23**(12): p. 2242-7.
75. Lavis, L.D., *The Chemistry of Abelson Tyrosine Kinase Inhibitors*. June 3, 2006.
76. Mian, A.A., et al., *p185(BCR/ABL) has a lower sensitivity than p210(BCR/ABL) to the allosteric inhibitor GNF-2 in Philadelphia chromosome-positive acute lymphatic leukemia*. Haematologica. 2012. **97**(2): p. 251-7.
77. Hantschel, O., et al., *A myristoyl/phosphotyrosine switch regulates c-Abl*. Cell, 2003. **112**(6): p. 845-57.
78. Adrian, F.J., et al., *Allosteric inhibitors of Bcr-abl-dependent cell proliferation*. Nat Chem Biol, 2006. **2**(2): p. 95-102.
79. Ron Geyer, T.Z., Asha Lakshmikuttyamma, David P. Sheridan, John F. DeCoteau, *GNF-2, An Allosteric BCR-ABL Inhibitor, Identifies a Novel Myristoylation-Mediated Mechanism Regulating the Ability of BCR-ABL to Activate HCK and IGF-1 Signaling* Conference Auditorium C (Ernest N. Morial Convention Center) 2009.
80. Hassan, A.Q., S.V. Sharma, and M. Warmuth, *Allosteric inhibition of BCR-ABL*. Cell Cycle. 2010. **9**(18): p. 3710-4.
81. Jahnke, W., et al., *Binding or bending: distinction of allosteric Abl kinase agonists from antagonists by an NMR-based conformational assay*. J Am Chem Soc. 2010. **132**(20): p. 7043-8.

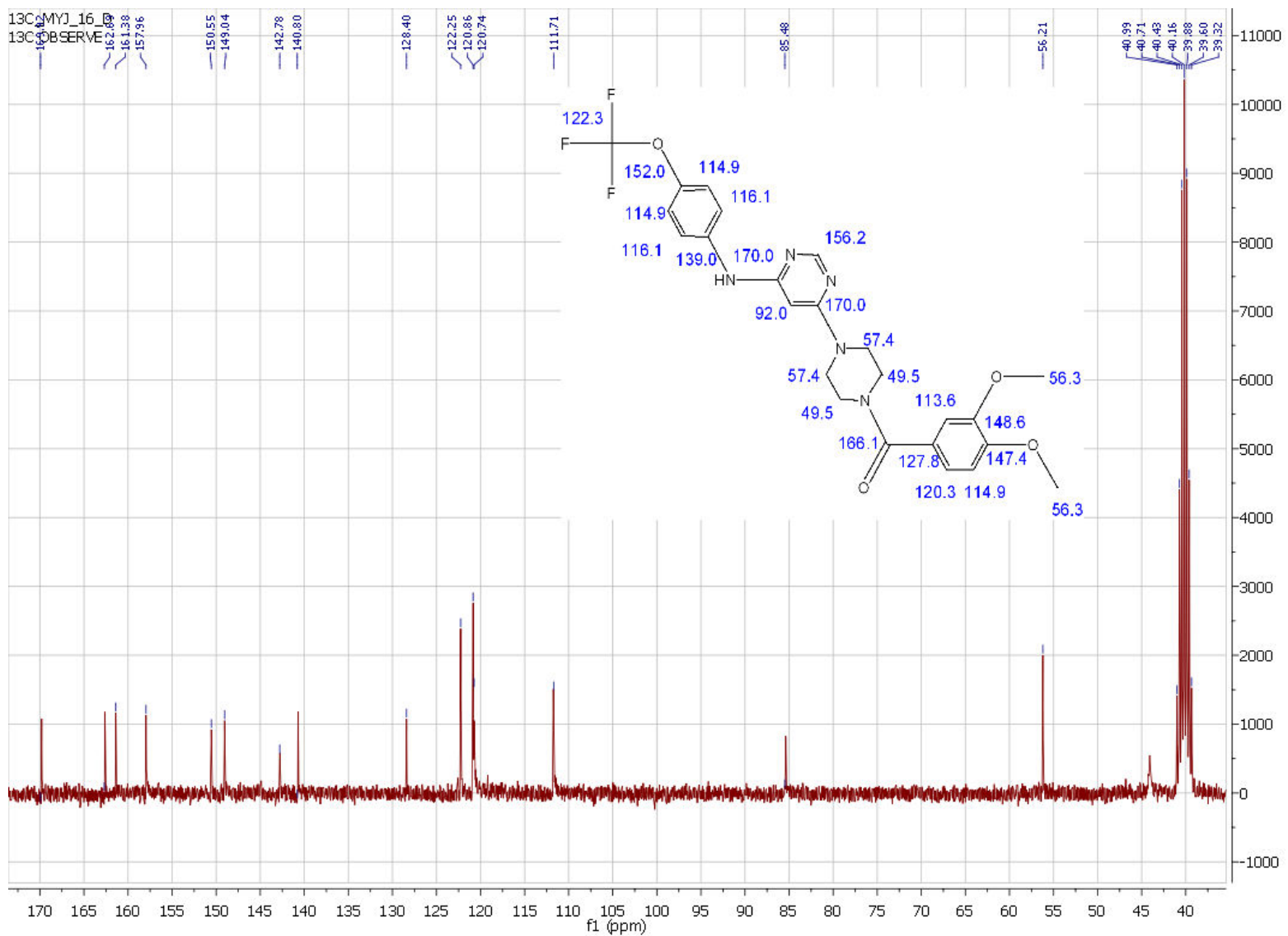
82. Hantschel, O., *Allosteric BCR-ABL inhibitors in Philadelphia chromosome-positive acute lymphoblastic leukemia: novel opportunities for drug combinations to overcome resistance*. *Haematologica*. 2012. **97**(2): p. 157-9.
83. Deng, X., et al., *Expanding the diversity of allosteric bcr-abl inhibitors*. *J Med Chem*. 2010. **53**(19): p. 6934-46.
84. Zhang, J., et al., *Targeting Bcr-Abl by combining allosteric with ATP-binding-site inhibitors*. *Nature*. 2010. **463**(7280): p. 501-6.
85. Khateb, M., et al., *Overcoming Bcr-Abl T315I mutation by combination of GNF-2 and ATP competitors in an Abl-independent mechanism*. *BMC Cancer*. 2012. **12**: p. 563.
86. Mian, A.A., et al., *Allosteric inhibition enhances the efficacy of ABL kinase inhibitors to target unmutated BCR-ABL and BCR-ABL-T315I*. *BMC Cancer*. 2012. **12**: p. 411.
87. Woessner, D.W., C.S. Lim, and M.W. Deininger, *Development of an effective therapy for chronic myelogenous leukemia*. *Cancer J*, 2011. **17**(6): p. 477-86.
88. Weisberg, E., et al., *Beneficial effects of combining a type II ATP competitive inhibitor with an allosteric competitive inhibitor of BCR-ABL for the treatment of imatinib-sensitive and imatinib-resistant CML*. *Leukemia*. 2010. **24**(7): p. 1375-8.
89. Iacob, R.E., et al., *Allosteric interactions between the myristate- and ATP-site of the Abl kinase*. *PLoS One*. 2011. **6**(1): p. e15929.
90. Hantschel, O., F. Grebien, and G. Superti-Furga, *The growing arsenal of ATP-competitive and allosteric inhibitors of BCR-ABL*. *Cancer Res*. 2012. **72**(19): p. 4890-5.
91. Hanahan, D. and R.A. Weinberg, *The hallmarks of cancer*. *Cell*, 2000. **100**(1): p. 57-70.

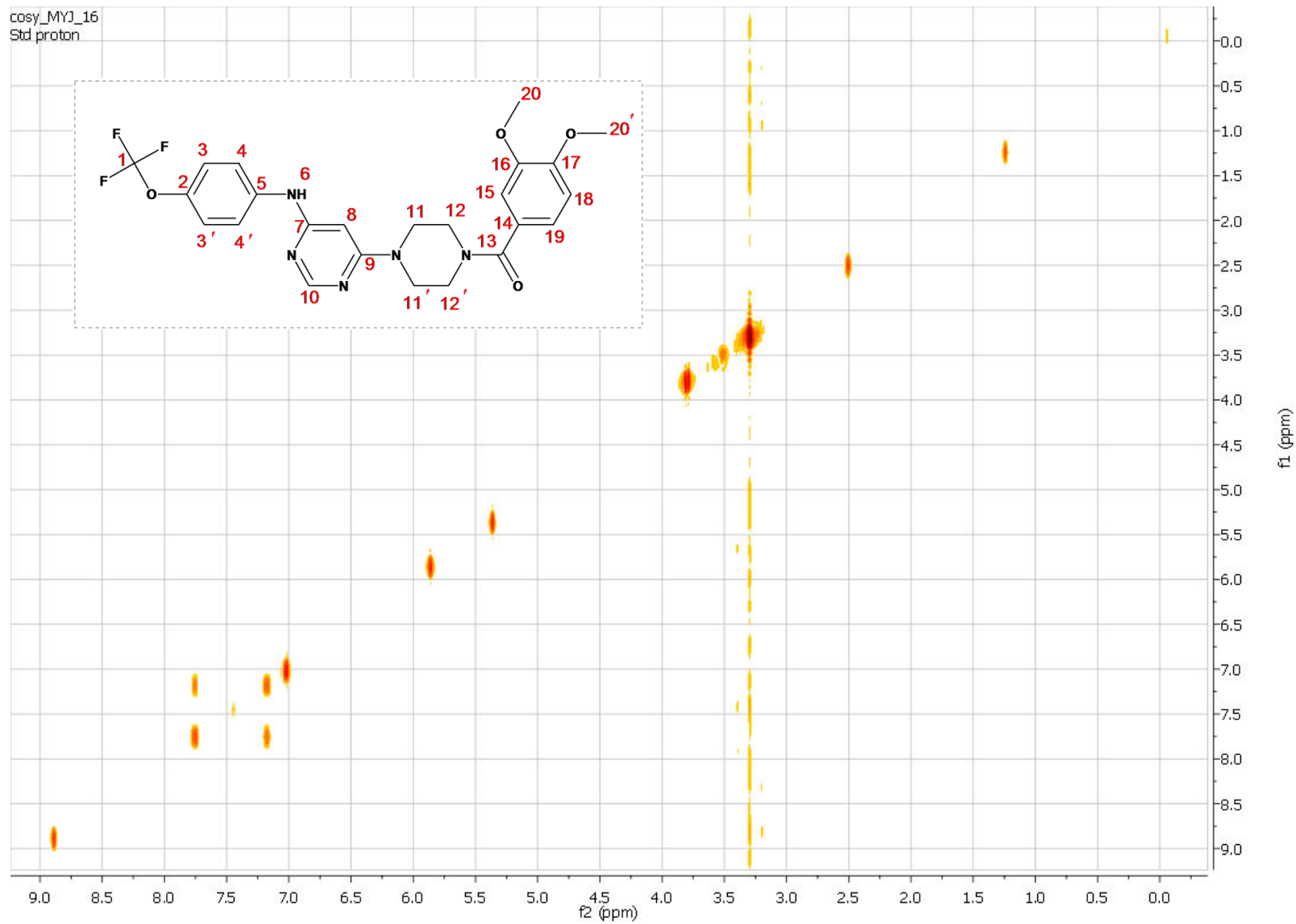
Chapter six

Appendices

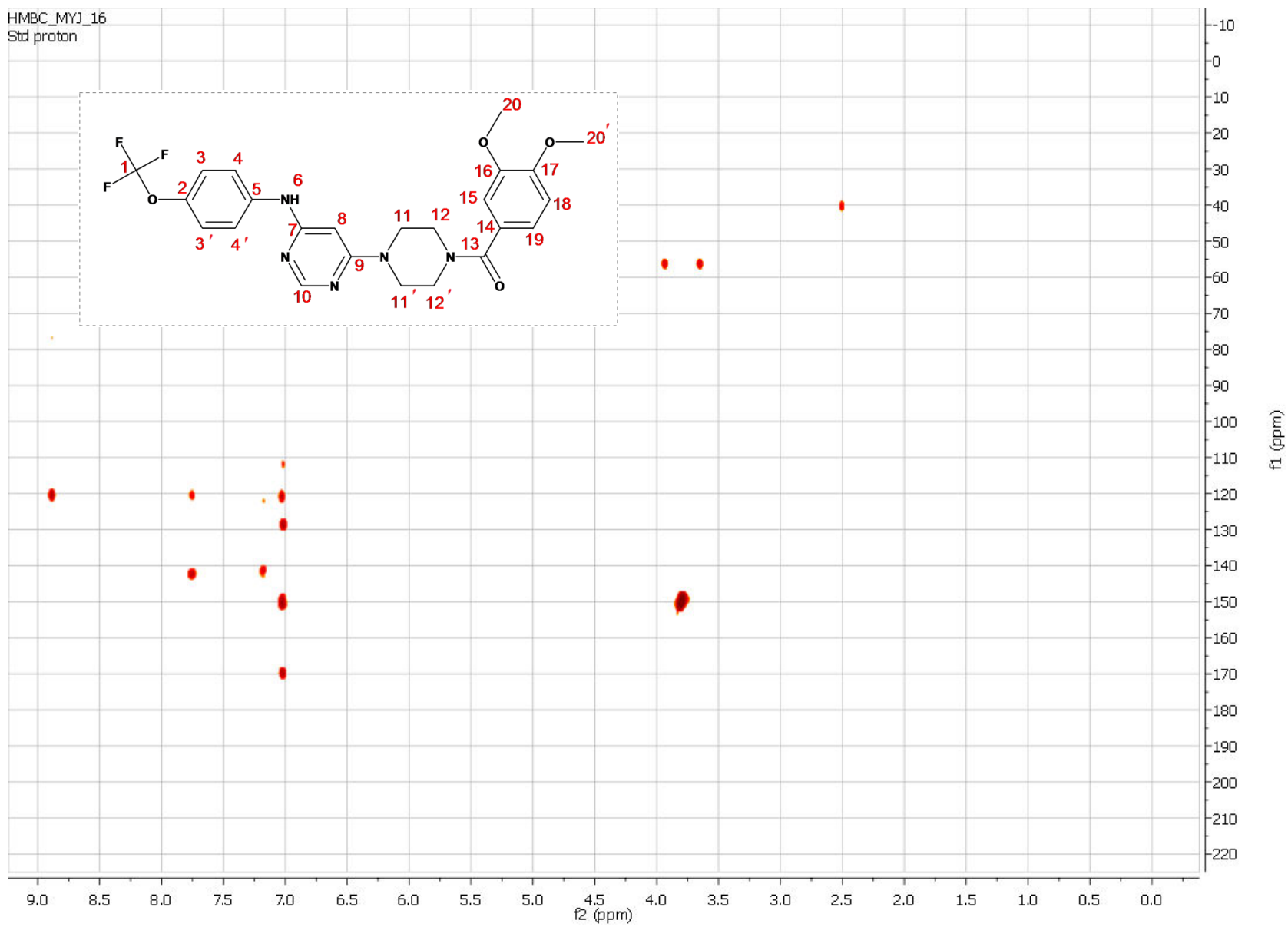
Appendix 6.1: Nuclear magnetic resonance (^1H -, ^{13}C -, COSY & HMBC NMR) of compound MYJ-16 (**28**)



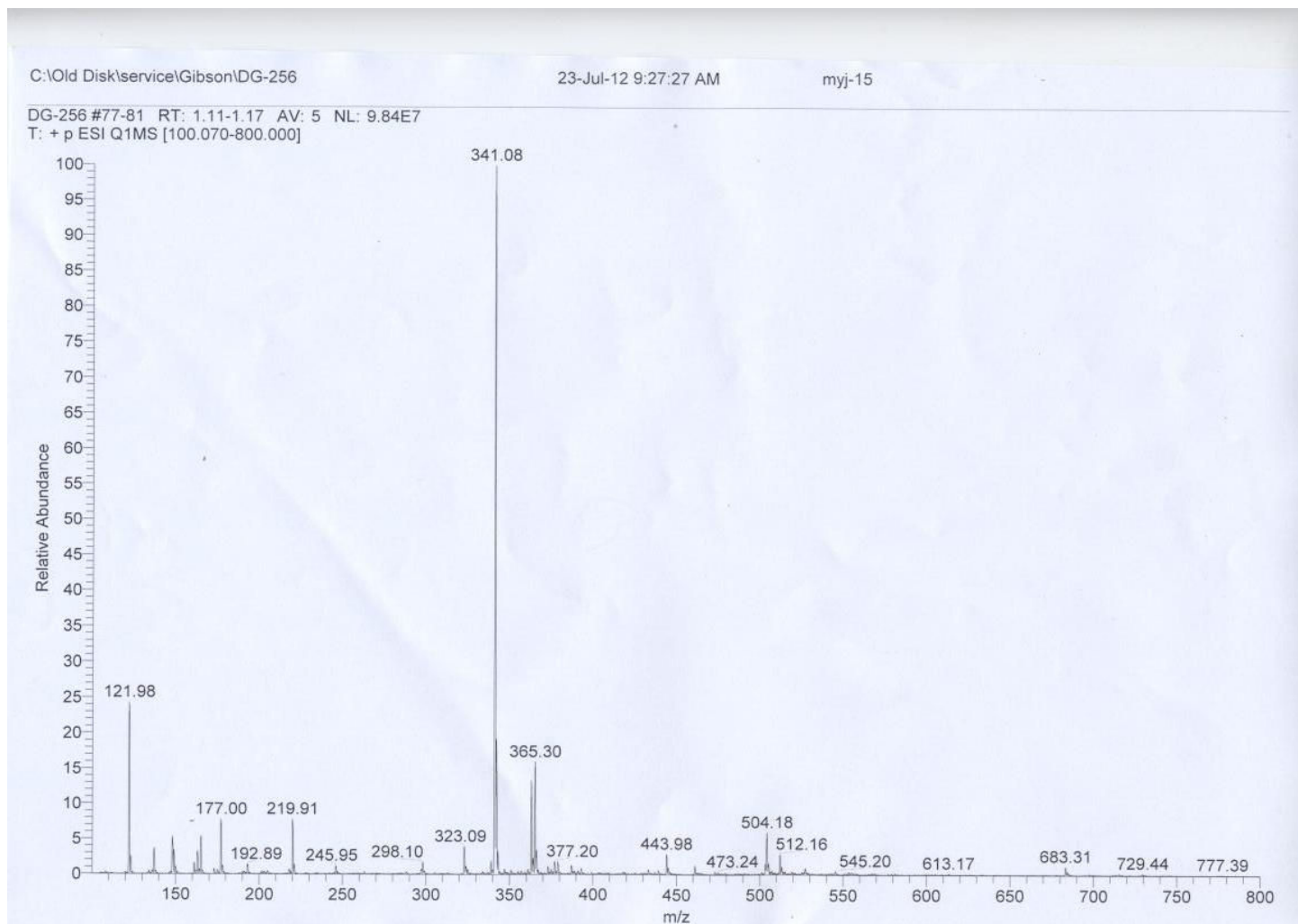




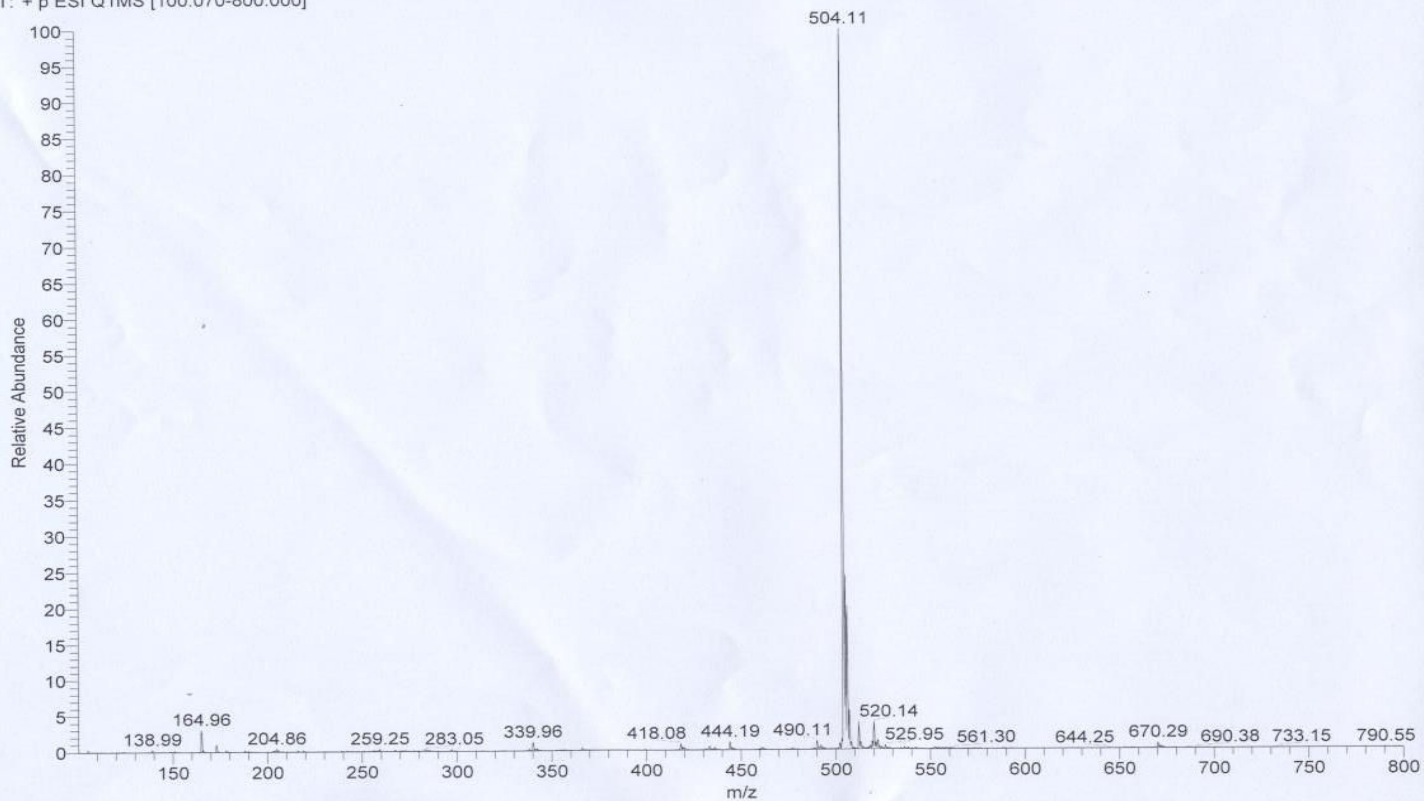
HMBC_MY1_16
Std proton



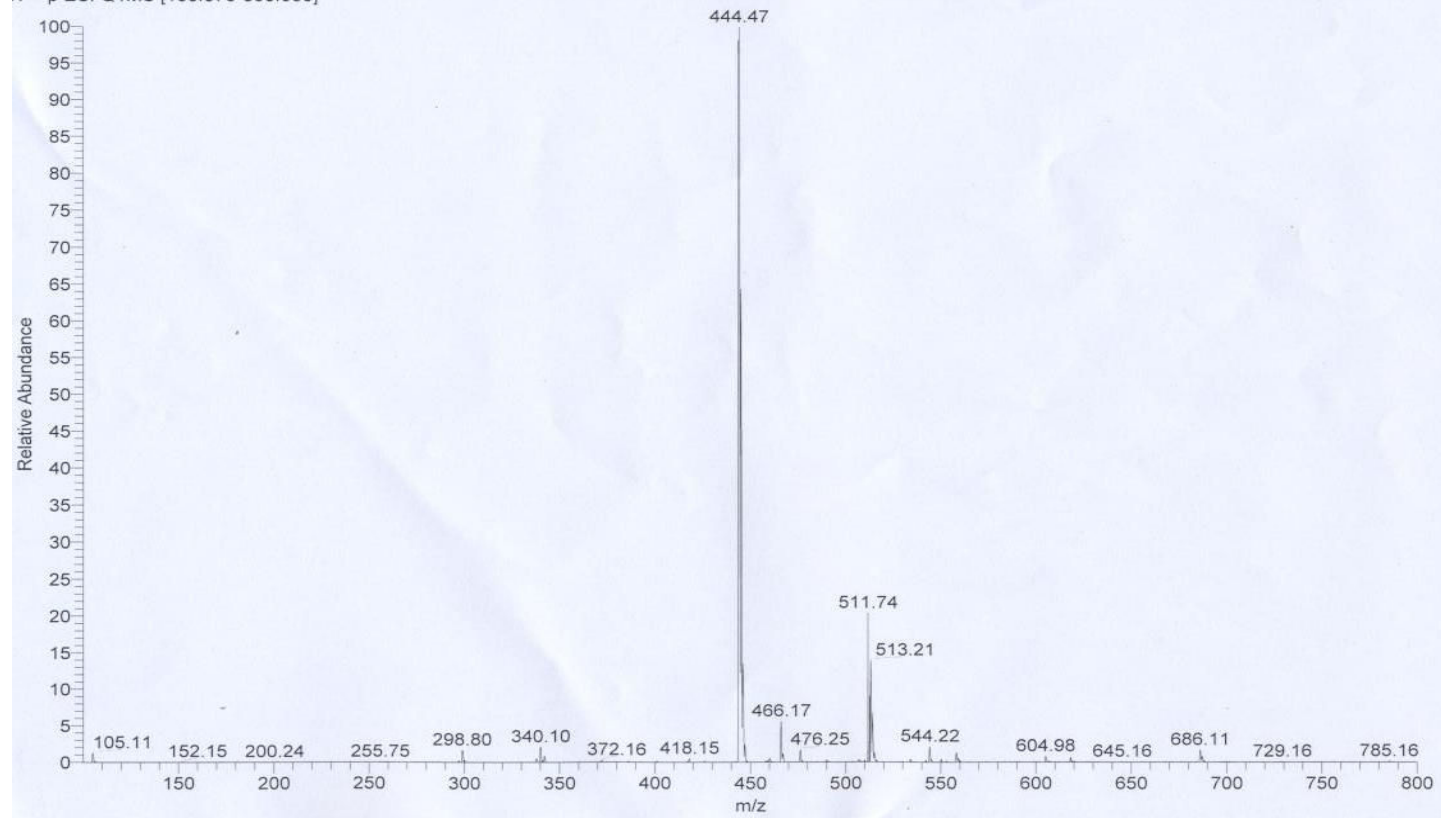
Appendix 6.2: Electrospray ionization mass spectrometry (ESIMS) of compounds MYJ-15 (**53**), MYJ-16 (**28**), MYJ-18 (**30**), MYJ-19 (**31**) and MYJ-20 (**32**)



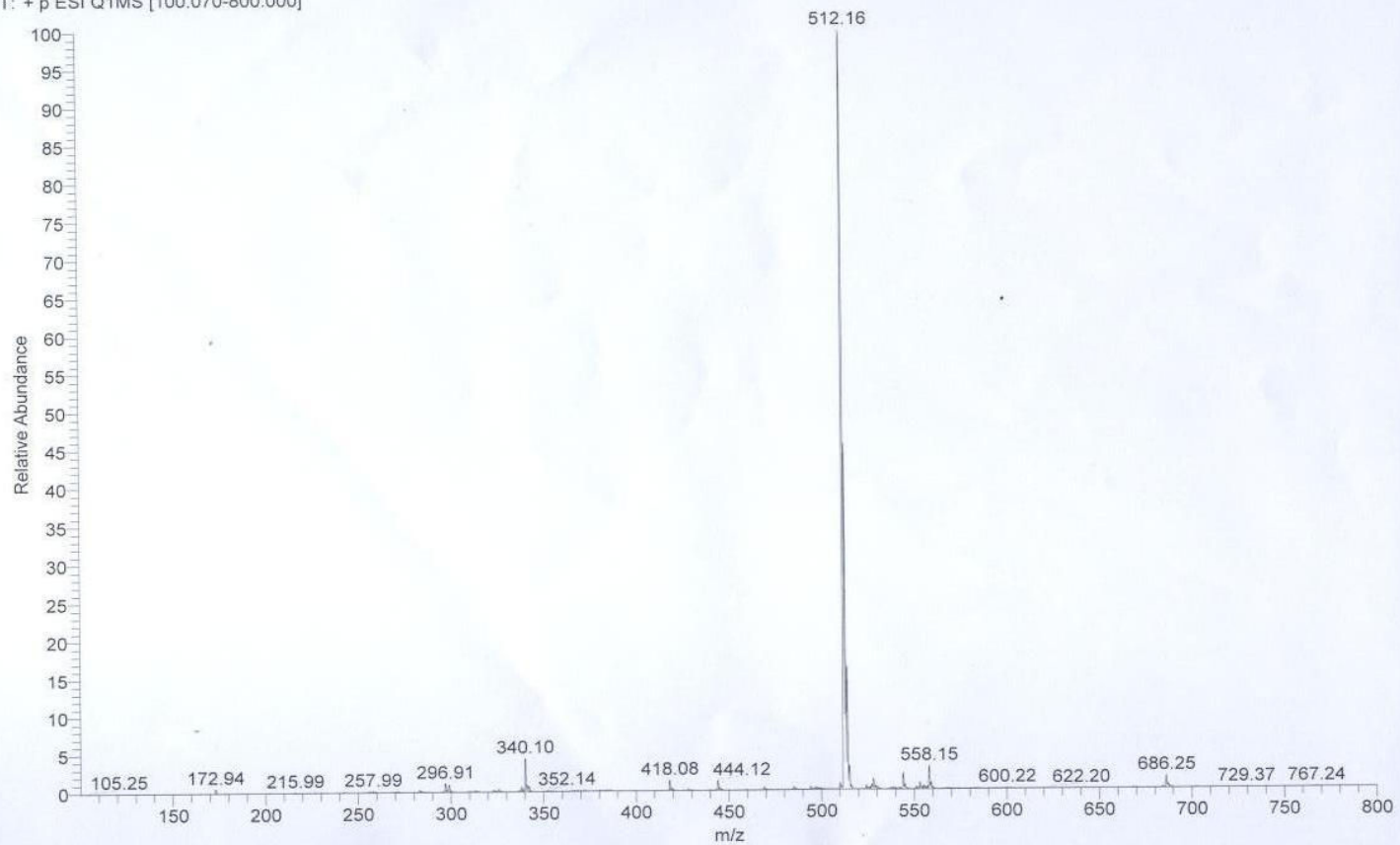
DG-255 #71-74 RT: 1.03-1.07 AV: 4 NL: 1.17E8
T: + p ESI Q1MS [100.070-800.000]

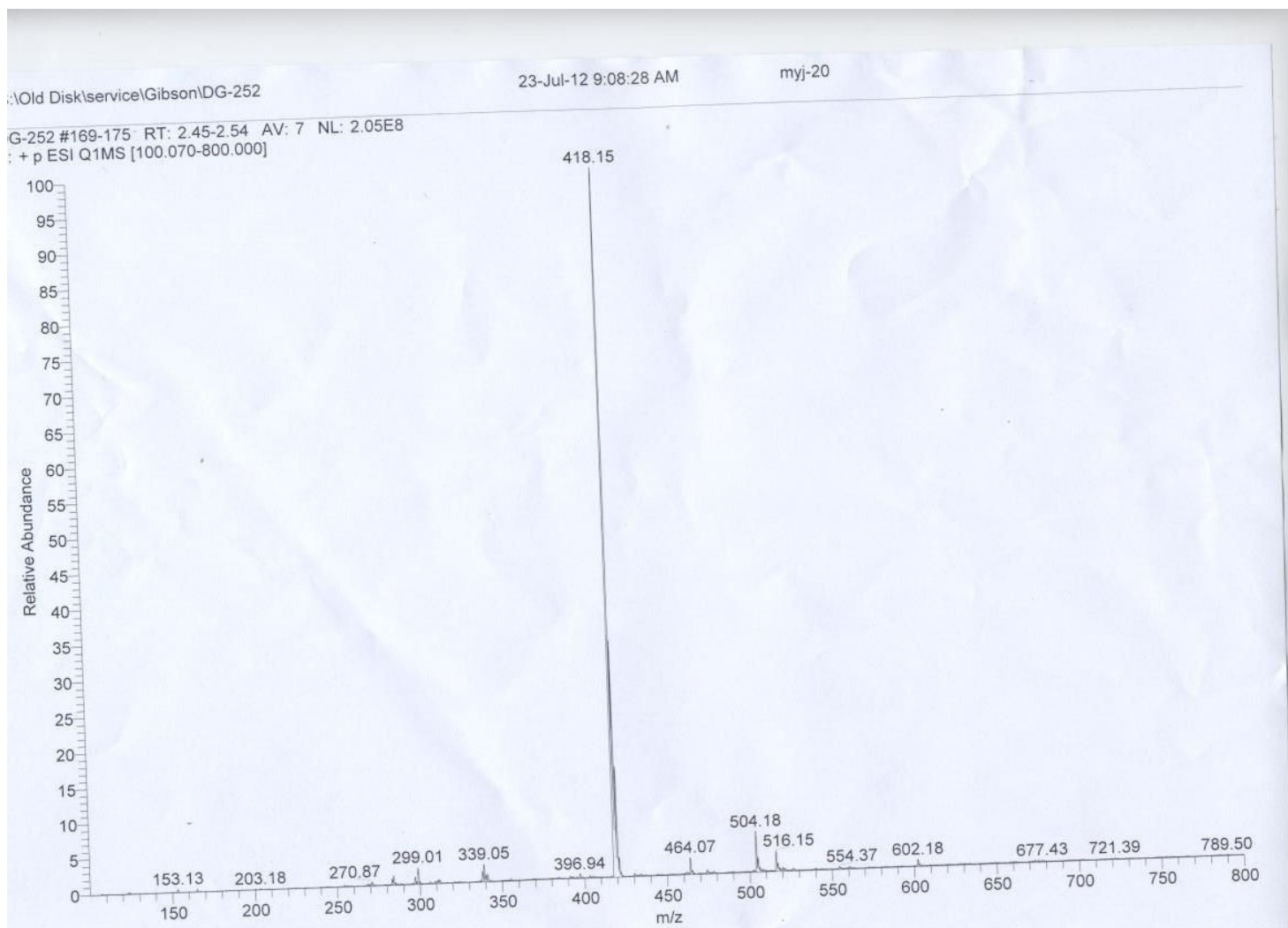


DG-254 #58-62 RT: 0.83-0.89 AV: 5 SB: 3 0.13-0.16 NL: 1.54E8
[+ p ESI Q1MS [100.070-800.000]]

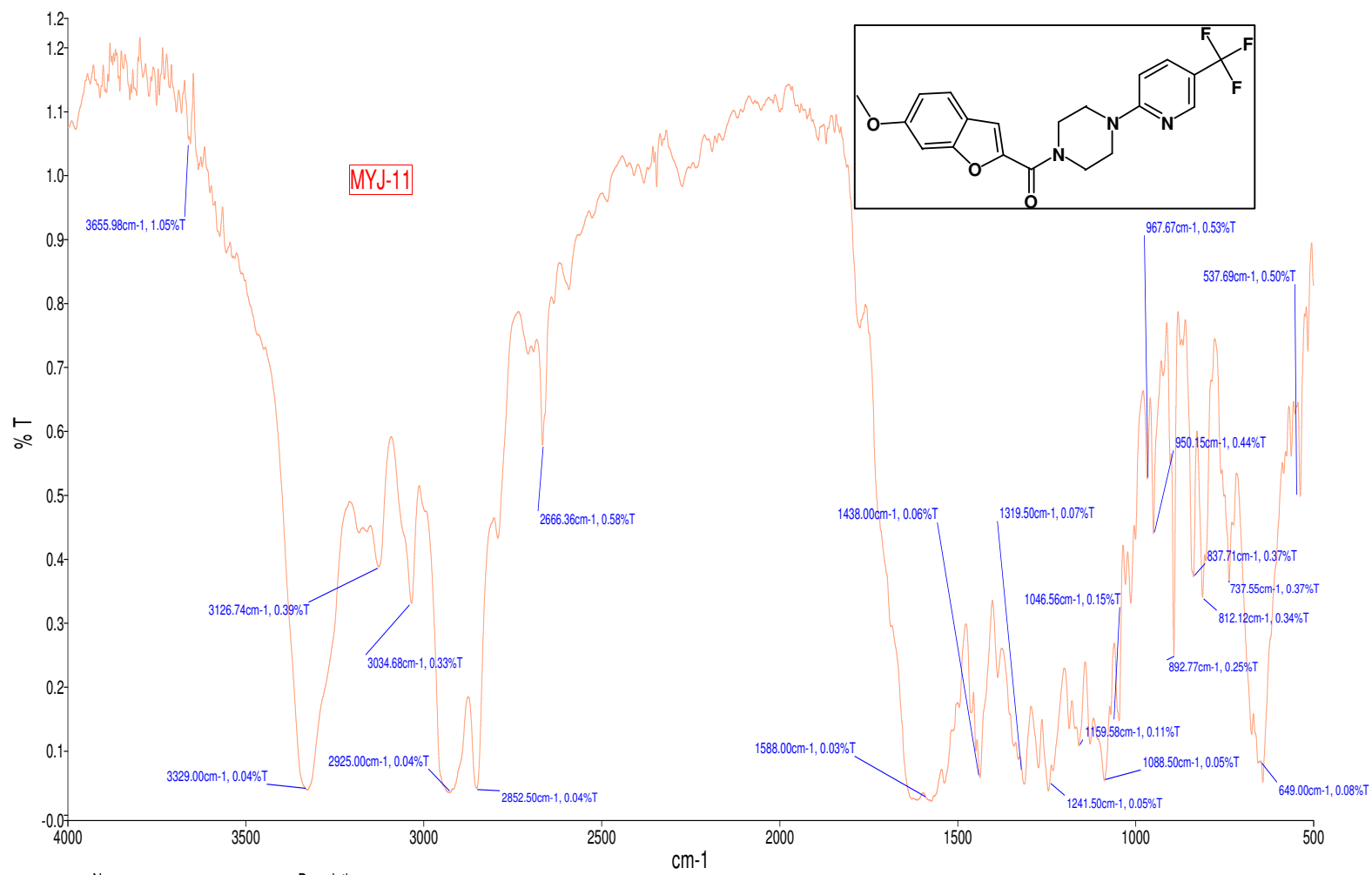


DG-253 #264-289 RT: 3.82-4.18 AV: 26 NL: 2.43E8
T: + p ESI Q1MS [100.070-800.000]

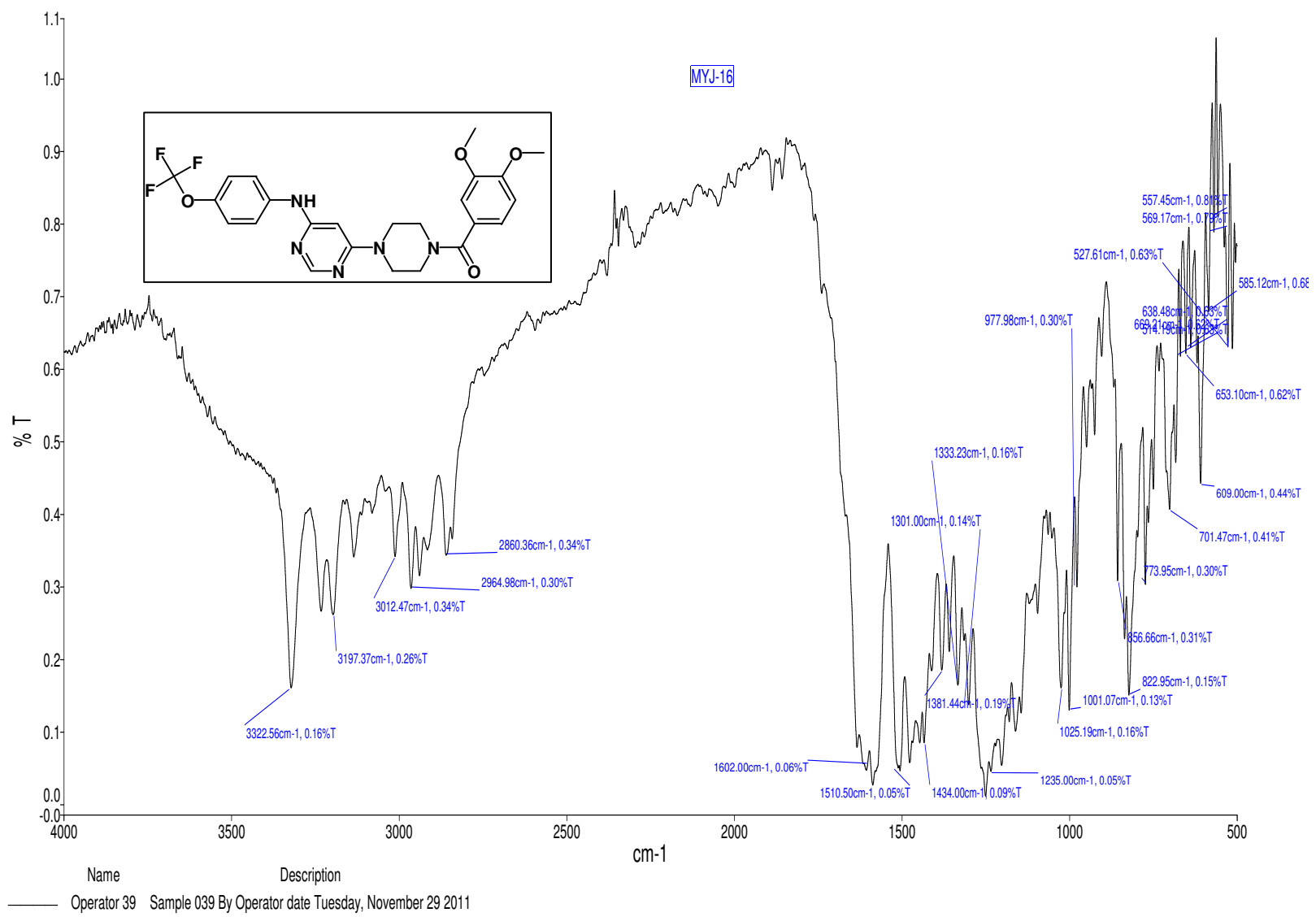


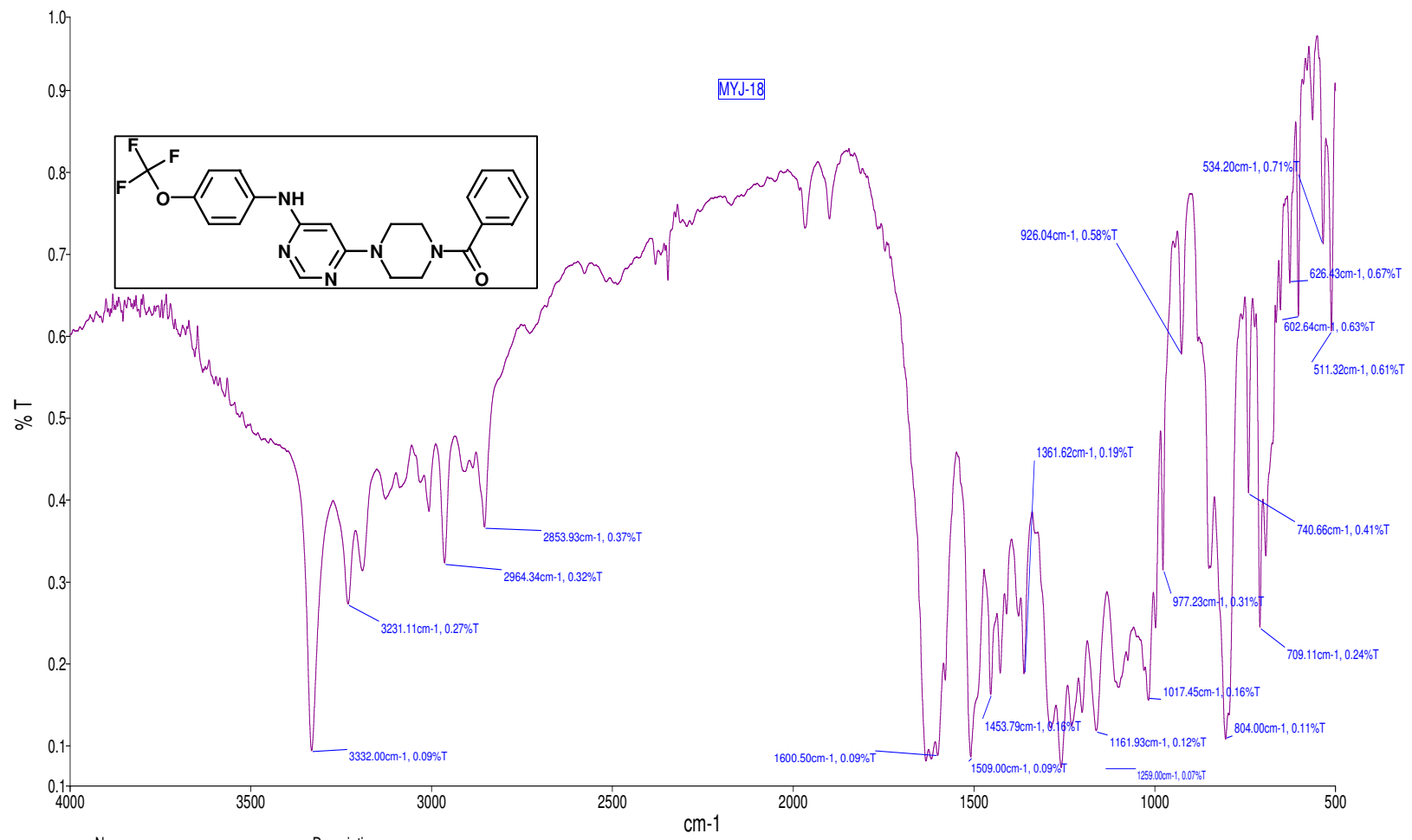


Appendix 6.3: Fourier transform infrared spectroscopy (FTIR) of compounds MYJ-11 (**49**), MYJ-16 (**28**), MYJ-18 (**30**), MYJ-20 (**32**), MYJ-22 (**34**) and MYJ-24 (**38**)

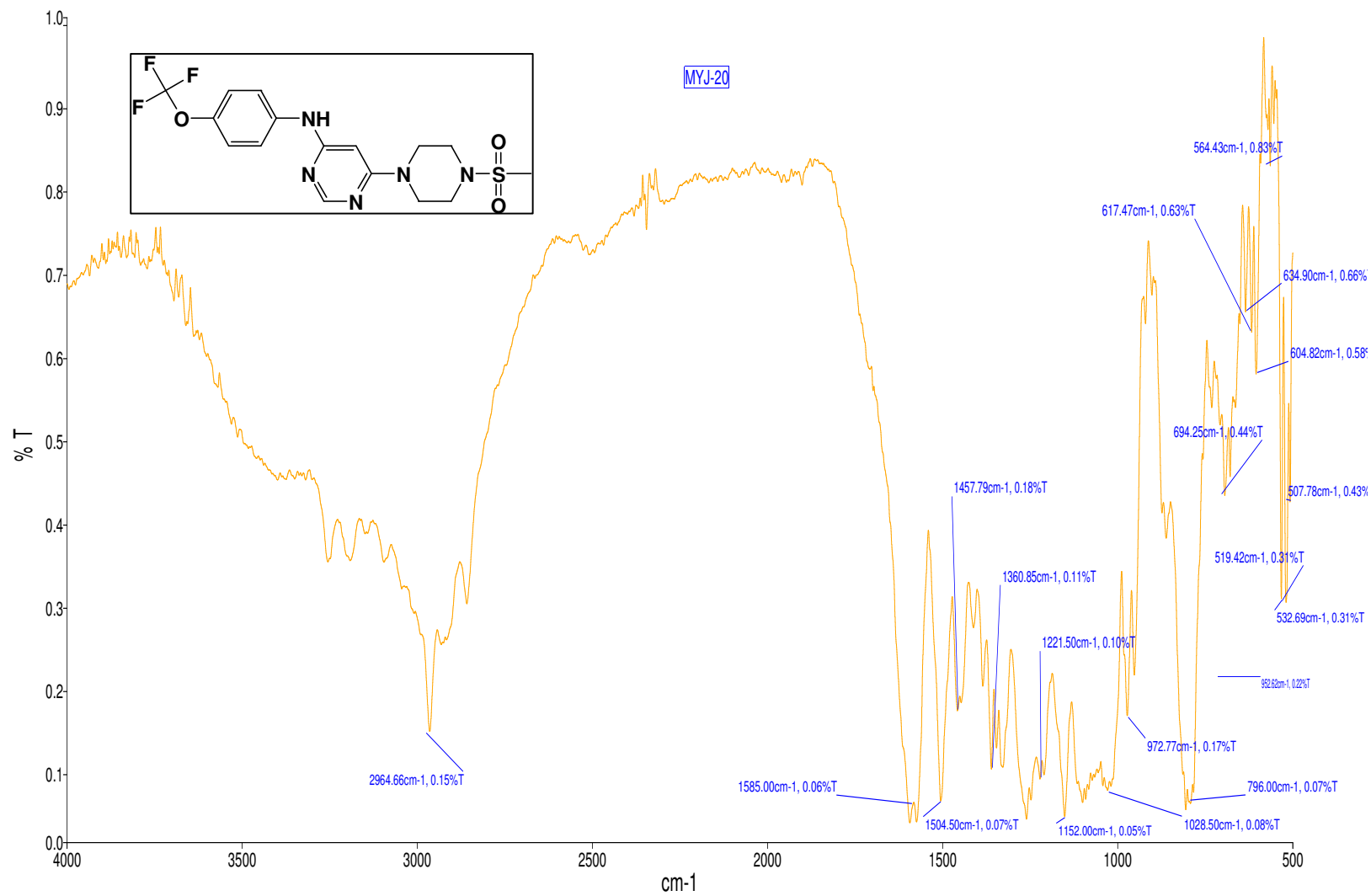


Name Description
 Operator 73 Sample 073 By Operator date Saturday, December 03 2011

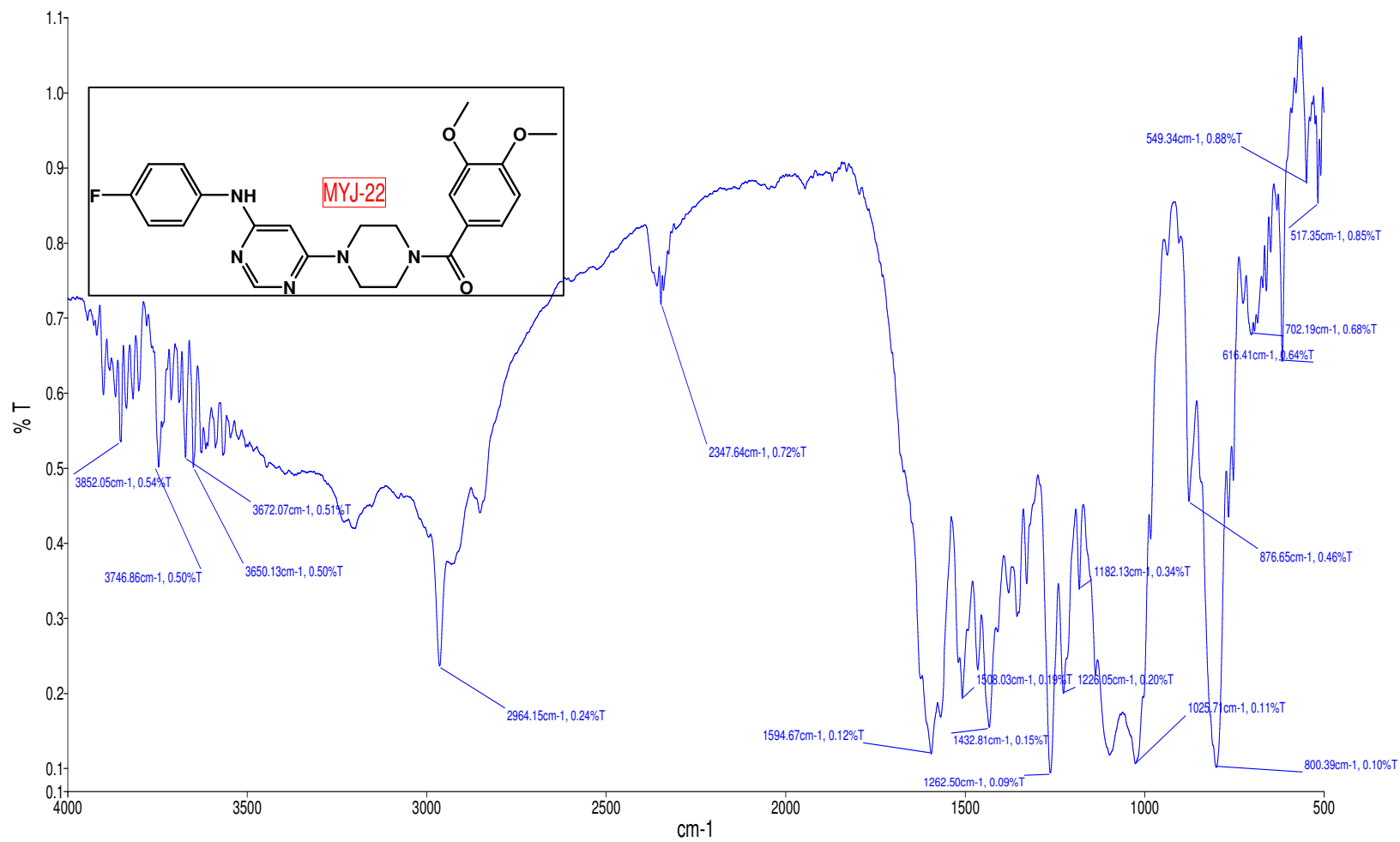




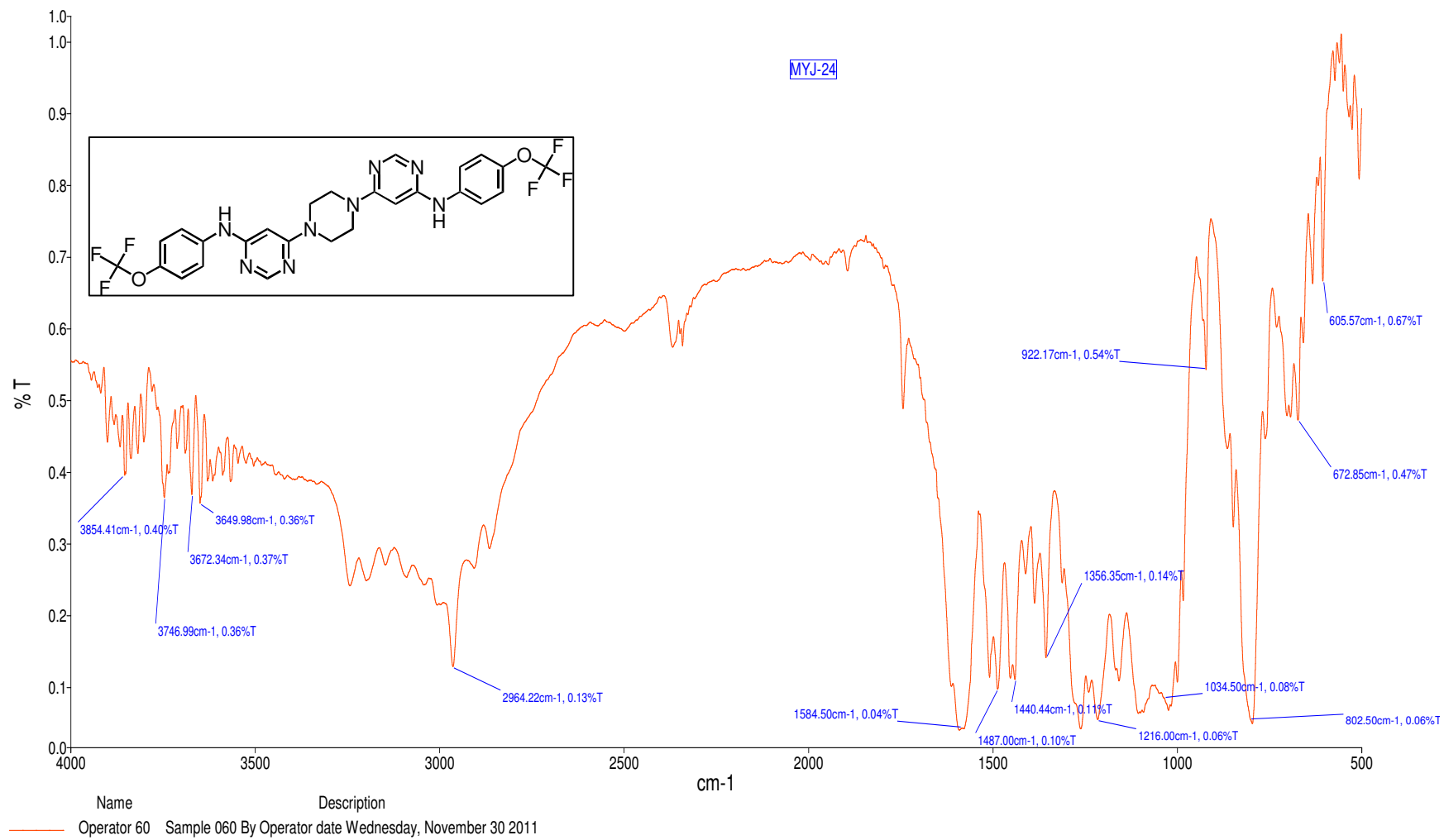
Name Description
 Operator 57 Sample 057 By Operator date Wednesday, November 30 2011



Name Description
 Operator 56 Sample 056 By Operator date Wednesday, November 30 2011



Name Description
 Operator 62 Sample 062 By Operator date Saturday, December 03 2011



تصميم و تحضير مثبطات أنزيم Bcr-Abl لعلاج سرطان الدم باستخدام مشتقات البيريبيدين

اعداد: مها نصري عواد- خوري

اشراف: د. يوسف ناجرة

ملخص:

ينتج مرض سرطان الدم اللوكيميا بنوعيه سرطان الدم النخاعي المزمن (النقوي) (CML) و سرطان الدم الليمفاوي الحاد (ALL) عن تبادل و التحام أجزاء من الكروموسومين ٩ و ٢٢، t(9:22) حيث ينتج كروموسوم جديد يسمى كروموسوم فيلادلفيا، والذي بدوره يولد الجين Bcr-Abl المسبب للمرض. بعد اكتشاف هذا الجين والتأكد بأنه المؤشر والعامل الرئيسي للإصابة باللوكيميا في ٨٠% من حالات سرطان الدم النخاعي المزمن و ٢٠% من حالات سرطان الدم الليمفاوي الحاد بدأت العديد من التجارب لتطوير مثبطات انتقائية له كوسيلة لعلاج مرض سرطان الدم. تعمل غالبية مثبطات انزيم Bcr-Abl على استهداف منطقة ATP binding pocket وهي منطقة ارتباط ATP في البروتين حيث تتم عملية الفسفرة، لكن وعلى الرغم من نجاح هذه المثبطات كعوامل مضادة لخلايا اللوكيميا السرطانية فان مقاومة الخلايا لهذه العقاقير نتيجة ظهور طفرات أوجدت قيودا "كبيرة" على استخدامها في العلاج الكيماوي. من بين عشرات الطفرات التي ظهرت خلال مراحل العلاج باستخدام هذه المثبطات فان الطفرة 'T315I' التي تدعى البواب كانت الأقوى حيث تعمل مقاومة كاملة لمثبطات انزيم Abl.

مؤخرا" تم اكتشاف مركبين هما GNF-2, GNF-5 وثبت أنهما يعملان بانتقائية كمثبطات لجين Bcr-Abl، مما يشكل نهج جديد لعلاج CML، وقد أثبتت هذه المركبات امتلاكها النشاط الخلوي ضد خلايا Bcr-Abl المتحولة من خلال استهداف منطقة خارج موقع ATP binding pocket والتي تعرف ب (MBP) myristate binding pocket، وكما ثبت بأن هذه المركبات يمكن أن تعمل بالتعاون مع المثبطات التي تستهدف ATP binding pocket لقمع العديد من الطفرات في مجال انزيم Bcr-Abl وخاصة الطفرة 'T315I'.

في هذا البحث تم التركيز على هذين المركبين GNF-2, GNF-5 اللذين يرتبطان في منطقة myristate binding pocket، وتبعاً لذلك تم تصميم ثلاث مجموعات من المركبات، وتصنيعها، وتنقيتها باستخدام

تقنيات الفصل الكروماتوغرافي، والتعرف عليها بواسطة: ($^{13}\text{C-NMR}$ ، $^1\text{H-NMR}$ و FTIR و ESIMS) واختبارها للنشاط البيولوجي ضد خلايا Ba/F3 التي تحتوي على أنزيم Bcr-Abl وحده أو الذي يحمل الطفرة 'T315I'.

أظهرت نتائج اختبار فعالية هذه المركبات على خلايا سرطانية تحمل البروتين Ba/F3 P185، أن المركبات MYJ-1 (20)، MYJ-2 (16) و MYJ-17 (29) أعطت فعالية محدودة في كبح نشاط البروتين Ba/F3 P185، وأن المركب MYJ-16 (28) أظهر فعالية أكثر باستخدام تراكيز مختلفة مقارنة مع المركب GNF-2 (8). المركب 28 أظهر وجود نشاط مماثل تقريبا عند فحص clonogenicity of Ba/F3 لخلايا Bcr-Abl المتحولة وخلايا Bcr-Abl التي تحمل الطفرة 'T315I' باستخدام تركيز ٢٥ ميكرومولار. كما أظهر المركب 28 أيضا نشاطا في تثبيط انتشار وتكاثر خلايا سرطان الدم اللينفاوي الحاد Sup-B15 بتراكيز أقل مقارنة مع المركبين MYJ-18 (30) و MYJ-19 (31) التي أظهرت وجود نشاط باستخدام تراكيز أعلى.

توضح الدراسة بأن هذه المجموعة المتنوعة من المركبات يمكن أن تستهدف على نحو فعال الجين Bcr-Abl في منطقة myristate binding pocket، مما قد يشكل نهج جديد لتطوير عقاقير لقمع Bcr-Abl وعلاج مرض سرطان الدم اللوكيميا.